

Implementation and evaluation of surge flow border irrigation
by Samir Mohamed Ismail

A thesis submitted in partial fulfillment of the requirements for the degree of Doctor of Philosophy in Civil Engineering
Montana State University
© Copyright by Samir Mohamed Ismail (1984)

Abstract:
Surge flow border irrigation can be accomplished by accumulating, then releasing water and letting it flow down the field. To apply this concept to border irrigation a dosing siphon and automatic drop gate were designed and tested. The dosing siphon holds back the water because of trapped air, and has a maximum practical flow of 22 L/s. The drop gate can be built for virtually any head and flow rate. The gate opens automatically when the water level on the upstream side of the gate rises to a predetermined level and remains open until the water surface drops to a lower predetermined level. The gate then returns automatically to its closed position by action of a counter balance weight. The automatic drop gate was tested in the laboratory and a discharge equation developed.

A mathematical model based on the differential storage equation was developed to simulate field conditions. The model was verified with laboratory tests. Field experiments were also conducted to evaluate surge flow border irrigation systems using the automatic drop gate. Surge flow and conventional continuous flow were compared. The surge flow treatments showed a higher uniformity of water penetration. Surge flow also showed a higher potential application efficiency than continuous irrigation under the same inflow. The higher efficiency of surge flow can be attributed to the rapid advance of the water front which is due to the accumulation of the small inflow, reduction in infiltration, and reduction in surface hydraulic roughness. Both the dosing siphon and automatic drop gate have practical application under appropriate field conditions.

D378
I55
cop.2

APPROVAL

of a thesis submitted by

Samir Mohamed Ismail

This thesis has been read by each member of the thesis committee and has been found to be satisfactory regarding content, English usage, format, bibliographic style, and consistency, and is ready for submission to the College of Graduate Studies.

Feb. 2, 1984
Date

Gerald Westeen
Chairperson, Graduate Committee

Approved for the Major Department

Feb. 2, 1984
Date

Fred F. Wilson
Head, Major Department

Approved for the College of Graduate Studies

Feb. 3, 1984
Date

Henry L. Parsons
Graduate Dean

IMPLEMENTATION AND EVALUATION OF SURGE FLOW BORDER IRRIGATION

by

Samir Mohamed Ismail

A thesis submitted in partial fulfillment
of the requirements for the degree

of

Doctor of Philosophy

in

Civil Engineering

MONTANA STATE UNIVERSITY
Bozeman, Montana

March 1984

STATEMENT OF PERMISSION TO USE

In presenting this thesis in partial fulfillment of the requirements for a doctoral degree at Montana State University, I agree that the Library shall make it available to borrowers under rules of the library. I further agree that copying of this thesis is allowable only for scholarly purposes, consistent with " fair use " as prescribed in the U.S. Copyright Law. Requests for extensive copying or reproduction of this thesis should be referred to University Microfilms International, 300 North Zeeb Road, Ann Arbor, Michigan 48106, to whom I have granted "the exclusive right to reproduce and distribute copies of the dissertation in and from microfilm and the right to reproduce and distribute by abstract in any format."

Signature Janice M. Smail

Date Feb. 2, 1984

ACKNOWLEDGMENTS

The author would like to thank the Agricultural Engineering Department and the Montana Agricultural Experiment Station for their financial support of this project.

The writer is greatly indebted to Dr. G. L. Westesen, for his supervision, valuable guidance, suggestions, and assistance in revising the manuscript. Particular appreciation is extended to Dr. W. E. Larsen for his sincere advice and valuable guidance in the development of automatic equipment for surge flow. Thanks to Drs. T. L. Hanson and R. L. Brustkern for their assistance and scientific advice. A special thanks to Professor T. T. Williams who helped to set up a joint program between the Civil Engineering Department and the Agricultural Engineering Department for this Ph. D. program.

The author wishes to express his appreciation and thanks to the secretary of the Agricultural Engineering Department, Darlene Ritchey, for her valuable guidance on the use of word processor during preparation of this dissertation.

Finally, the author's gratitude is to his wife, Mervat, for her help, patience, and encouragement.

TABLE OF CONTENTS

	Page
APPROVAL	ii
STATEMENT OF PERMISSION TO USE	iii
ACKNOWLEDGMENTS	vi
TABLE OF CONTENTS	v
LIST OF TABLES	viii
LIST OF FIGURES	x
ABSTRACT	xiii
1. INTRODUCTION	1
2. SURFACE IRRIGATION THEORY	7
General	7
Advance Phase	7
Storage Phase	9
Depletion Phase	9
Recession Phase	9
Infiltration	10
Infiltration Equations	11
Border Irrigation Hydraulics	13
Saint-Venant Equations	13
Kinematic-Wave Equations	15
Zero-Inertia Equations	16
Volume-Balance Equations	16
Surface Irrigation Automation	20
Automatic Structures	20
Automatic Discharge Control	21
Surge Flow Irrigation	23
3. SURGE FLOW IMPLEMENTATION	27
Dosing Siphon	27
Theory of Operation	27
Dosing Siphon Design	31

TABLE OF CONTENTS—Continued

	Page
Automatic Drop Gate	33
Theory of Operation	33
Force Analysis	37
Critical Design Criteria-Gate Opening and Closing	39
Critical Considerations for Design	40
4. LABORATORY TESTS	41
Equipment	41
Drop Gate Tests	42
Error Analysis	48
Dosing Siphon Tests	51
Error Analysis	55
Dosing Siphon Performance	56
5. MATHEMATICAL MODEL OF SURGE FLOW OPERATION	58
Model Development	59
Storage Outflow Function	59
Outflow Rating Curve	59
Inflow Hydrograph	60
Storage Function	60
Trapezoidal cross-Section	60
Parabolic Cross-Section	64
Refill Time	66
Release Time	67
Numerical Solution	67
Analytical Solution	69
Summary of Runs Made with the Model	70
Model Verification	70
Model Validation	72
6. FIELD EVALUATION AND ANALYSIS	74
Materials and Field Operation	74
Utilization of Field Data	78
Infiltration Characteristics	78
Analysis	84
Cumulative Intake Curves	84
Adjusted cumulative Intake	85
Performance Parameters	98
Distribution Uniformity	98
Potential Application Efficiency	99
Advance Rate	101
Formula validation	107

TABLE OF CONTENTS--Continued

		Page
7.	SUMMARY AND CONCLUSIONS	114
8.	BIBLIOGRAPHY	118
9.	APPENDICES	123
	Appendix A - Least Squares Method Calculations	124
	Appendix B - Print-Out of the Computer Program	127
	Appendix C - Computer Output	134
	Appendix D - Typical and Adjusted Intake	138

LIST OF TABLES

Tables		Page
1.	Head on the drop gate versus discharge obtained from several tests	45
2.	Summary of least squares method calculations	47
3.	Probable error calculations for the drop gate empirical equation	49
4.	Head on the dosing siphon versus discharge	53
5.	Discharge coefficient calculations for dosing siphon	55
6.	Trapezoidal rule method of computation	68
7.	Soil physical properties	74
8.	Irrigation treatments applied	77
9.	Sample data of cylinder infiltrometer (Test 1)	81
10.	Depth infiltrated based on opportunity times for continuous flow treatment	88
11.	Depth infiltrated based on opportunity times for surge flow treatment	90
12.	Probable error calculation for using the broad-crested weir equation	125
13.	Least squares method calculations for dosing siphon empirical discharge equation	125
14.	Probable error calculations for the dosing siphon empirical equation	126
15.	Probable error calculations for the dosing siphon using the orifice equation	126
16.	Typical and adjusted intake for continuous flow treatment for a pilot field test	139

LIST OF TABLES--Continued

Tables		Page
17.	Typical and adjusted intake for surge flow for a pilot field test.....	139
18.	Typical and adjusted intake for continuous flow treatment for field test No. 2.....	140
19.	Typical and adjusted intake for surge flow treatment for field test No. 2.....	140
20.	Typical and adjusted intake for continuous flow treatment for field test No. 3.....	141
21.	Typical and adjusted intake for surge flow treatment for field test No. 3.....	141
22.	Typical and adjusted intake for continuous flow treatment for field test No. 4.....	142
23.	Typical and adjusted intake for surge flow treatment for field test No. 4.....	142
24.	Typical and adjusted intake for continuous flow treatment for field test No. 5.....	143
25.	Typical and adjusted intake for surge flow treatment for field test No. 5.....	143
26.	Typical and adjusted intake for continuous flow treatment for field test No. 6.....	144
27.	Typical and adjusted intake for surge flow treatment for field test No. 6.....	144

LIST OF FIGURES

Figures		Page
1.	Definition sketch showing certain border irrigation terms	8
2.	Definition sketch for Saint-Venant Equations	14
3.	Schematic diagram illustrating the infiltration-advance problem	17
4.	Dosing siphon	28
5.	Sequence of events that occur during a dosing siphon operating cycle	29
6.	Schematic drawing of drop gate	35
7.	Automatic drop gate mechanism	36
8.	Water forces acting on the gate in both open and closed positions	37
9.	Depth changes during one cycle using the 30 cm drop gate and inflow of 11.5 L/s	43
10.	Depth changes during one cycle using the 30 cm drop gate and inflow of 3.6 L/s	43
11.	The control volume for applying the continuity equation to the drop gate system	44
12.	Drop gate discharge as a function of head	46
13.	Depth changes during one cycle using two different inflow rates	52
14.	Depth changes during three sequential cycles using the same inflow	52
15.	The control volume for applying the continuity equation to the dosing siphon system	53
16.	Dosing siphon discharge as a function of head	54

LIST OF FIGURES--Continued

Figures		Page
17.	Schematic representation of the trapezoidal cross-section characteristics along the reservoir.....	61
18.	Definition sketch for (a) dosing siphon, (b) drop gate.....	63
19.	Definition sketch for using parabolic cross-section.....	64
20.	Field layout for border irrigation systems using three drop gate sizes.....	75
21.	Plots of accumulated infiltration and average infiltration rate vs. elapsed time.....	79
22.	Cumulative cylinder infiltration curves from a bare silty loam soil.....	80
23.	Cumulative cylinder infiltration curves with typical and adjusted intake.....	86
24.	Advance-recession curves for surge flow and continuous flow for field test No. 1.....	87
25.	Adjusted depth infiltrated along the irrigated border-strip.....	89
26.	A pilot field test for one surge using a 30 cm gate compared to continuous flow.....	92
27.	Advance-recession curves for surge flow and continuous flow for field test No. 2.....	93
28.	Advance-recession curves for surge and continuous flow for field test No. 3.....	94
29.	Advance-recession curves for surge flow using a 15 cm gate and continuous flow for field test No. 4.....	95
30.	Advance-recession curves for surge flow using a 60 cm gate and continuous flow for field test No. 5.....	96
31.	Advance-recession curves for surge flow using a 30 cm gate and continuous flow for field test No. 6.....	97

LIST OF FIGURES—Continued

Figures		Page
32.	Comparison of the calculated position of the water front to the observed position for the continuous flow irrigation using different stream size.....	103
33.	The effect of off-time on the advance rate.....	111
34.	The effect of gate size on the advance rate of the first surge.....	112
35.	The effect of gate size on the advance rate of the second surge.....	112
36.	Computed cycle time for the dosing siphon using 4.8 L/s inflow rate.....	135
37.	Computed cycle time for the automatic drop gate using 3.6 L/s inflow rate.....	136
38.	Computed cycle time for the dosing siphon using 5.1 L/s inflow rate.....	137

ABSTRACT

Surge flow border irrigation can be accomplished by accumulating, then releasing water and letting it flow down the field. To apply this concept to border irrigation a dosing siphon and automatic drop gate were designed and tested. The dosing siphon holds back the water because of trapped air, and has a maximum practical flow of 22 L/s. The drop gate can be built for virtually any head and flow rate. The gate opens automatically when the water level on the upstream side of the gate rises to a predetermined level and remains open until the water surface drops to a lower predetermined level. The gate then returns automatically to its closed position by action of a counter balance weight. The automatic drop gate was tested in the laboratory and a discharge equation developed.

A mathematical model based on the differential storage equation was developed to simulate field conditions. The model was verified with laboratory tests. Field experiments were also conducted to evaluate surge flow border irrigation systems using the automatic drop gate. Surge flow and conventional continuous flow were compared. The surge flow treatments showed a higher uniformity of water penetration. Surge flow also showed a higher potential application efficiency than continuous irrigation under the same inflow. The higher efficiency of surge flow can be attributed to the rapid advance of the water front which is due to the accumulation of the small inflow, reduction in infiltration, and reduction in surface hydraulic roughness. Both the dosing siphon and automatic drop gate have practical application under appropriate field conditions.

CHAPTER 1

INTRODUCTION

Field irrigation is concerned with transference of water from a conveyance system to the plant root zone. The logical possibilities for irrigation are:

(a) to run the water over the surface so that it infiltrates the soil;

(b) to pass water into the soil at depth so capillary action raises it to the root zone, or;

(c) to cause water to fall to the ground in such a way that neither crop nor soil is damaged.

These are the basic categories of water application practice known as surface irrigation, sub-irrigation, and overhead irrigation. Each has inherent advantages and hazards which affect its value for a particular situation. The demands on water supplies are steadily increasing and in many areas the ground water supplies are being depleted. Irrigation is the largest consumer of water in many parts of the world and, hence, has received a great deal of attention during the past decade and will be receiving greater attention in the future.

In some areas surface irrigation has earned a reputation for being inefficient and wasteful. About two-thirds of the 25 million hectares (61 million acres) of irrigated land in the U.S. is now served by surface means (Irrigation Journal, 1979). The percentage is even higher

in many other parts of the world. Anticipated shortages of water and the high cost of energy to drive alternative systems, such as sprinklers, suggest that surface irrigation will remain popular, especially if abuses can be avoided. High runoff and deep percolation losses are cited as prime problems. However, there is nothing inherent about surface irrigation that causes inefficiencies. These inefficiencies are commonly the result of improper management and the irrigator's inability to completely control the water because of inadequate equipment.

Surface irrigation uses open channel flow to spread water over a field. The driving force in such systems is gravity, so surface irrigation is also called gravity flooding. Surface irrigation systems generally require a smaller investment than do other types of irrigation systems. However, this is not always the case, especially if extensive land forming is needed for an efficient system. In fact, the need for extensive land forming for surface irrigation is one of the main reasons other types of irrigation systems have been developed. In addition, some soils that are shallow, erosive, or on steep slope simply cannot be surface irrigated.

Surface irrigation can be accomplished by several application methods. These include border, furrow, check, and basin. In each case water moves over the land surface in an open channel flow. The water may be contained in small earth channels called furrows or corrugations or it may move as shallow overland flow over a carefully smoothed soil surface as in border irrigation. Aside from differences in channel

geometry and boundary conditions, the basic flow characteristics are much the same in all of the surface methods.

In border irrigation, water moves over the soil surface as shallow overland flow. The soil surface is permeable to water. The length of the border strip parallel to the flow is usually great with respect to the width. The surface may have a zero to small slope longitudinally and is preferably level in the transverse direction. Surface water depth is usually very small with respect to border width. The land surface may or may not be vegetated.

In the operation of border irrigation systems a relatively large stream of water is turned into the strip at the upper end. The water ponds at the upper end to an appreciable depth and also moves down the strip as a wave. The stream is generally turned off before it reaches the lower end which is then irrigated by water which flows down from the upper portion. In order to adequately irrigate the lower portion some runoff or ponding is usually required. The border strip method of irrigation is complicated. However, when adequately designed and properly used it is probably the most efficient and requires the least labor of all methods.

In the basin method the field to be irrigated is divided into level areas bounded by dikes or ridges. Water is turned in at one or more points until the desired gross volume has been applied to the area. The flow rate must be large enough to cover the entire basin in approximately 75 percent of the time required for the soil to absorb the desired amount of water. Water is ponded until it infiltrates. This

irrigation method is best suited to soils of moderate to low intake rates. Basin irrigation can also be applied to soils that have a moderately high to high intake rate but basin areas need to be small.

In some situations the farmer receives a small stream of water under a continuous delivery system. This continuous delivery system is often inefficient and excessive water use contributes to drainage problems. Attention has therefore been given to the advance phase of surface irrigation, which is primarily controlled by stream size, because of its bearing on intake opportunity time. Surface irrigation design and management objectives are generally to complete the advance phase of the irrigation as quickly as possible so that differences in intake opportunity time are minimized. Large stream sizes are required for the water to advance quickly. Cutback streams or runoff recovery systems can be used to minimize the runoff and deep percolation losses during the intake phase.

Automatic surface irrigation systems reduce labor, energy, and water inputs and maintain or increase farm irrigation efficiency. Automation is the use of mechanically or electrically actuated gates, structures, controllers, and other devices and systems to automatically control the amount of water diverted and applied.

The ideal irrigation system would have a low energy requirement, be automated, provide nearly instantaneous advance, and prevent runoff during the intake phase.

Stringham and Keller (1979) suggested surge flow as a method of automating cutback furrow irrigation. Surge flow is in essence an

operational practice in which irrigation is accomplished by cycling inflow to the field to produce a series of short pulses of water flowing over the field surface. These pulses are termed hydraulic surges, and thus lead to the name surge flow. The pulses are independent water applications whose sum is designed to satisfy the antecedent soil moisture deficit. These intermittent water applications lead to a discontinuity in the infiltration process, the result of which is often a reduction in surface layer permeability. However, this effect is widely variable depending on soil compaction and prior wetting history, surface water velocities, and duration of on-off periods. The exact mechanisms of surge flow irrigation are not completely known. However, the surge flow irrigation should in general yield the following results:

1. The alternating on-off system of controlling water delivery should achieve nearly uniform water penetration over the entire field.
2. Surges should provide water application efficiencies comparable to sprinkling without the high energy costs required to operate the sprinklers.
3. Surge systems should be partially or fully automated to reduce labor requirements and enable irrigation timing to best suit the crop and soil conditions.

The objectives of this study are:

1. To develop automated equipment for the practical application of surge irrigation to borders and basins. The automated equipment should be capable of collecting small inflows for a

period of time in a head ditch or a reservoir and discharging the water when the water surface rises to a certain level.

2. To develop a mathematical model which embodies the characteristics of the head ditch, the automatic device and required flow rates and which will yield the cycle time required for surge flow border irrigation.

3. To conduct field evaluations of surge flow border irrigation devices and systems and compare the surge flow systems with conventional continuous flow systems.

CHAPTER 2

SURFACE IRRIGATION THEORY

General

The border-strip method of surface irrigation utilizes a strip of land sloping longitudinally and level or nearly so laterally across the strip. The water is bounded by borders (ridges) to restrain the lateral flow of the water. In operation, a stream of water is turned into the strip at the upper end. It ponds there to an appreciable depth and also moves down the strip as a wave. The stream is turned off before the wave reaches the lower end which is then irrigated by water which was ponded on the upper portion.

Phases of a typical irrigation are shown in Fig. 1 and described in the following manner.

Advance Phase

The rate of advance down a border will be affected by five major factors. The first is the unit inflow. This may vary throughout the irrigation or remain constant.

The slope of the border determines the rate at which energy is added to the flowing water. Only a single average slope of the entire irrigation run is normally considered.

The forces restraining flow are those due to resistance--both from the soil surface and vegetation. The soil surface changes during an irrigation and between irrigations. The vegetative roughness is a function of the vegetation involved. Vegetation factors considered are stem rigidity, stem length, stem diameter and stem density, and the presence of leaves. These factors must be considered in combination and make the roughness representation difficult. Nevertheless, most analyses to date consider only a single roughness parameter, such as Manning's n.

Another factor affecting advance rate is the infiltration characteristic of the soil. Infiltration varies with time (during and between irrigations) and space (location within the field). Again, approximations are necessary. It is common in the field of irrigation to use a two-parameter infiltration representation. The most popular are the Kostiakov-Lewis (original or modified), the Philip, or the Soil Conservation Service representations.

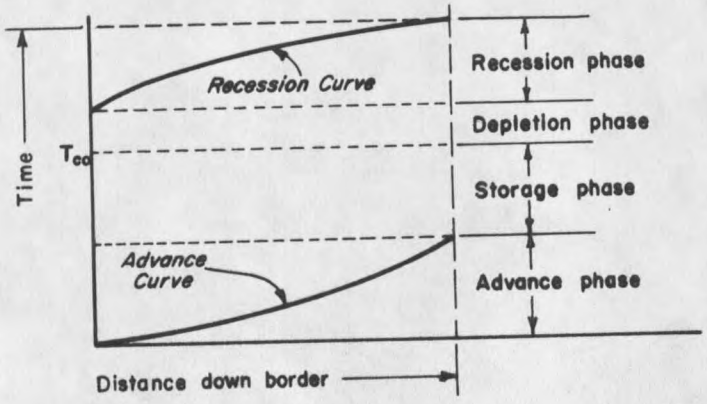


Figure 1. Definition sketch showing certain border irrigation terms.

Channel shape is the final variable affecting advance. Borders are considered a wide shallow rectangular channels. Therefore, the hydraulic radius is considered equal to the depth of flow.

Storage Phase

When water first reaches any point on the soil surface, the infiltration is generally high. The infiltration rate rapidly declines, however, often to some relatively constant value. Thus, when the water reaches the end of the border, the infiltration rate is constant or decreasing at every point within the border. The tail end of the border may have a dam over which the water cannot pass, and thus water begins to accumulate on the soil, as well as within the profile. Even if no dam exists, the soil is absorbing water. This phase, during which water covers the entire soil surface, is known as the storage phase. The storage phase ends when the inflow ceases (time T_{co}).

Depletion Phase

At some appreciable time after turning the water off the ponded water at the upper end will disappear by infiltration and movement on down the strip. This interval of time between turn off and disappearance is known as the depletion phase or as the recession lag time.

Recession Phase

The water that once covered the surface has either entered the soil or flowed to a lower portion of the field. This is known as the recession phase. Ideally this recession of water from the surface

begins at the head end and progress down the field until the water has either entered the soil or runoff. When the ponded water has been absorbed by the soil (or runoff at the end), the irrigation is complete.

Infiltration

Infiltration is the term applied to the process of water entry into the soil, generally by downward flow through all or part of the soil surface. The rate of this process determines how much water will enter the root zone, and how much if any, will runoff.

The infiltration rate is defined as the volume flux of water flowing into the profile per unit of soil surface area. This flux, with units of velocity, has also been referred to as infiltration velocity. For the condition wherein the water supply exceeds the ability of the soil to absorb water, infiltration proceeds at a maximal rate, which Horton (1940) called the soil's infiltration capacity. The infiltration rate generally decreases with time. Thus, the cumulative infiltration, which is the time integral of the infiltration rate, has a curvilinear time dependence with a gradually decreasing slope. As time elapses the infiltration rate asymptotically approaches a constant rate. This rate is termed the final infiltration capacity, or basic intake rate.

The time of irrigation is fixed by the quantity of water required to replenish the soil-moisture supply and the rate of infiltration. The length of time during which water is held on the soil surface also helps determine the length of run for border-strips or irrigation furrows and the size of the irrigation stream.

Infiltration Equations

The historical order of appearance of some widely applied infiltration rate equations are presented as follows.

The earliest equation was introduced by Green and Ampt (1911),

$$f = f_c + (b/F) \tag{2.1}$$

where

f = infiltration rate

f_c = final constant infiltration rate

F = cumulative infiltration

b = characterizing constant

The next equation is that of Kostiakov (1932),

$$f = K_k \, t^{-\alpha} \tag{2.2}$$

where

t = time after infiltration starts

K_k, α = constants which depend on the soil and initial conditions. The parameters in these equations have no physical interpretation and must be evaluated from experimenal data.

In some irrigation studies an extended or modified Kostiakov equation is used as follows,

$$F = a \, t^b + c \, t \tag{2.3}$$

where a, b, and c are constants which must be determined experimentally.

The third equation was derived by Horton (1940),

$$f = f_c + (f_o - f_c)\, e^{-\beta t} \qquad (2.4)$$

where

f_o = infiltration capacity at $t = 0$

β = a soil parameter which controls the rate of decrease of infiltration rate.

The equation contains three constants which must be evaluated experimentally.

The fourth equation is that of Philip (1957),

$$f = f_c + (1/2)\, s\, t^{-1/2} \qquad (2.5)$$

where s is a parameter which Philip called sorptivity. Sorptivity has a physical meaning involving the geometry of the soil pore spaces, the surface tension and the viscosity of water.

The fifth equation was proposed by Holtan (1961):

$$f = f_c + a\, (S_t - F)^n \qquad (2.6)$$

where

S_t = water storage capacity of the soil's first impeding strata

a, n = constants dependent on soil type, surface and cropping conditions.

The USDA, Soil Conservation Service (1974), classified soils into intake families. The equation of these families takes the following form,

$$F = a\ t^b + c \qquad (2.7)$$

where

a, b, c = constants unique to each intake family

Border Irrigation Hydraulics

The phenomenon of surface irrigation is characterized by unsteady varied flow and is further complicated by the fact that boundaries are moving and that interfacial tension forces are in effect. As a natural phenomenon, the laws of mass, energy, and momentum conservation must be satisfied. It is known that surface water flow in irrigation can be described by the equations of Saint-Venant (Fig. 2). The following are the governing flow equations.

Saint-Venant Equations

The partial differential equations of Saint-Venant (Chow, 1959; Henderson, 1966; Strelkoff, 1969), governing the unsteady, nonuniform surface water flow in border irrigation consist of an equation of continuity comprising a volume balance and an equation of motion, representing an impulse-momentum balance. For surface irrigation hydraulics it can be assumed that the flow is essentially one dimensional, i.e, that it is effectively guided by the channel walls. The channel is assumed to be prismatic and it is also assumed that the flow is gradually varied, i.e, that the pressure distribution in all cross sections is hydrostatic. An additional assumption is that the velocity distribution in each cross section is virtually uniform, but drops to zero at the walls. A further assumption is that the resistance

to the flow introduced by soil surface roughness and plant stems and leaves, is dependent upon flow depth and velocity in the same way as if the flow were steady and uniform and without seepage. Finally, the bottom slope is assumed small so that the cosine of its angle with the horizontal is essentially unity. The effect of these assumptions was discussed at length by Strelkoff (1969).

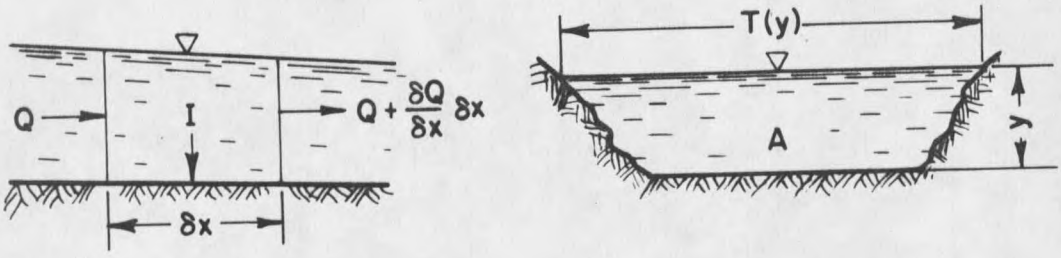


Figure 2. Definition sketch for Saint-Venant Eguations.

The continuity equation (Fig. 2) is

$$\frac{\partial A}{\partial t} + \frac{\partial Q}{\partial X} + I = 0 \qquad (2.8)$$

where

A = cross-sectional flow area taken at the middle of the element.

Q = discharge

I = volumetric rate of infiltration per unit length of channel

An impulse-momentum balance states that the sum of the net hydrostatic pressure force on the water instantaneously contained within a slice, plus the gravitational force, minus the resisting force of wall friction and plant retardance; equals the momentum net flux out of the

slice, plus the rate at which momentum builds within the slice. Stated mathematically, in the above order, this is

$$-\gamma A \frac{\partial y}{\partial X} \partial X + \gamma A S_o \partial X - F \partial X = \partial X \frac{\partial(\rho Q V)}{\partial X} + \frac{\partial(\rho V A \partial X)}{\partial t}$$

In the above equation, γ is the unit weight of water, $y(X,t)$ is the depth of flow, S_o is the bottom slope, F is the total resisting force per unit length of channel, $V(X,t) = Q(X,t)/A(y)$ is the average velocity of flow and ρ is the mass density of water. Considering zero-velocity components for the flow that is drawn off in soil infiltration, there is no loss of momentum by the water within the slice from this source. Division of the equation by the weight of the slice and passage to the limit $\partial X \longrightarrow 0$ yields the equation of motion

$$\frac{1}{g}\frac{\partial V}{\partial t} + \frac{V}{g}\frac{\partial V}{\partial X} + \frac{\partial y}{\partial X} = S_o - S_f + \frac{IV}{Ag} \qquad (2.9)$$

The complete solution of Eqs.(2.9) and (2.8) either by finite difference techniques or the method of characteristics is commonly known as a full hydrodynamic model (Bassett and Fitzsimmons, 1976; Katapodes and Strelkoff, 1977).

Kinematic-Wave Equations

The kinematic-wave approximation can be obtained by setting the right-hand side only of Eq. (2.9) equal to zero. The method fails for any stage of an irrigation where the bottom slope approaches the horizontal anywhere in the flow. In a kinematic wave the surface flow

at all points is considered to be at normal depth. The application of kinematic-wave theory to border-irrigation flow was studied by Smith (1972).

Zero-Inertia Equations

In the case of border irrigation, the depths and velocities are typically so small as to suggest that the acceleration or inertial terms which are the first two terms of Eq. (2.9) are small compared to the remaining terms and could be safely neglected. The first operational zero-inertia model of the complete irrigation process reported by Strelkoff and Katapodes (1977) neglected these terms.

Along with Eq. (2.8) the governing equation becomes,

$$\frac{\partial y}{\partial X} = S_o - S_f \qquad (2.10)$$

Volume-Balance Equations

Equation (2.9) can be entirely supplanted by two assumptions regarding the flow of water on the soil surface. The first assumption is that the depth of flow at the upstream end of the field equals normal depth for the given inflow. The second is that the average depth of surface flow is a given constant fraction, r_y, of the normal depth typically $0.7 < r_y < 1.0$. Computations for the advance phase of an irrigation (prior to cutting off the water), based on this volume-balance approach have been executed numerically (Hall, 1956). The solution of the volume balance equation has been expressed in series form by Philip and Farrell (1964) for infiltration equations of the

Kostaikov type or Philip type. Michael (1968) added a solution for an infiltration equation of the Soil Conservation Service type.

At any given time after the start of an irrigation, the stream has advanced to some point X in the field and surface and sub-surface profiles appear as in Fig. 3.

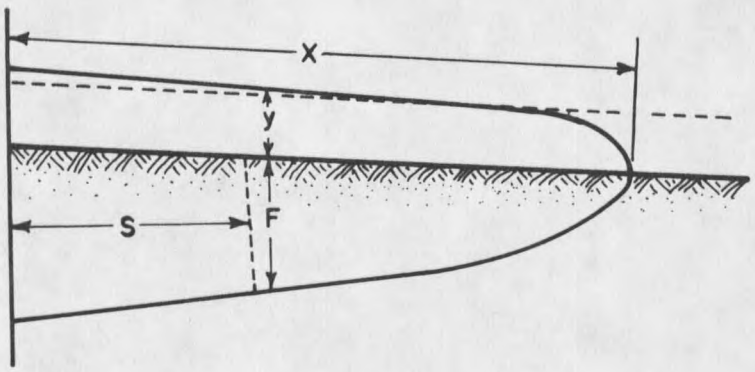


Figure 3. Schematic diagram illustrating the infiltration-advance problem.

The infiltration rate I, is related to the depth of infiltration F, by the formula,

$$I = T \frac{\partial F(X,t)}{\partial t}$$

in which T is the top width of the flow. The depth of infiltration is dependent primarily upon the infiltration opportunity time, i.e, the time the water has been in contact with the soil.

In order to prove that the working equation of Lewis and Milne (1938) can be derived from the general continuity equation the following analysis is proposed.

Integrating Eq. (2.8) with respect to X from 0 to X yields the result

$$Q = \frac{d}{dt} \int_0^X A \, dX + T \frac{d}{dt} \int_o^X F \, dX$$

Integrating this equation with respect to time and dividing the equation by T or the width of border, yields

$$\int_0^t q \, dt = \int_0^X (A/T) \, dX + \int_0^X F \, dX$$

where q is the flow per unit width of border.

If y is defined as the average depth of water on the soil surface, then the cross sectional area of the flow along the soil surface is y X where:

$$y \, X = \int_0^X (A/T) \, dX$$

where, F is a function of $(t - t_s)$, and X is a function of t_s.
The following can be written:

$$F \, dX = F \, (dX/dt_s) \, dt_s$$

$$\int_0^X F \, dX = \int_0^t F_{(t-ts)} \; X'(ts) \; dt_s$$

$$q \, t = y \, X + \int_0^t F_{(t-ts)} \; X'(ts) \; dt_s \qquad (2.11)$$

where

t_s = value of t at which X(t) = s

$F_{(t-ts)}$ = accumulated infiltration at the point X = s at time t_s

s = value of X at $t = t_s$, and

$X'_{(ts)}$ = value of dX/dt at $t = t_s$

Equation (2.11) was originally proposed by Lewis and Milne (1938). Philip and Farrel (1964) analysed the physical restrictions on X and F in Eq. (2.11). The equation is valid if X is a monotonic increasing function of t. This condition on X(t) places a restriction on the form of F(t) for which the analysis is valid. Sufficient conditions are

$$F > 0 \quad , \frac{dF}{dt} > 0 \qquad \text{and} \qquad \frac{d^2F}{dt^2} < 0$$

Generally, the physical restrictions on F are such that these conditions are realized and Eq. (2.11) is valid. Philip and Farrel (1964), using the Faltung or convolution theorem of Laplace transformation, obtained the general solution of Eq. (2.11) as follows.

$$\frac{X}{q} = L^{-1} \frac{1}{s^3 \, L\{F\} + y \, s^2} \qquad (2.12)$$

Equation (2.12) represents the general solution of Eq. (2.11) in terms of Laplace transformation. It can be applied to different forms of F(t), depending on whether the appropriate transformations and inverse transforms can be evaluated readily.

Michael (1968) obtained the following particular solutions of the Soil Conservation Service infiltration equation (Eq. (2.7)):

For a small value of t, i.e., $\frac{Bt^b}{\Gamma(2+b)} < 1$

$$X = \frac{q\ t}{c+y}\left[\frac{1}{\Gamma(2)} - \frac{Bt^b}{\Gamma(2+b)} + \frac{B^2\ t^{2b}}{\Gamma(2+2b)} - \frac{B^3\ t^{3b}}{\Gamma(2+3b)} + \frac{B^4\ t^{4b}}{\Gamma(2+4b)} - \ldots\ldots\right] \quad (2.13)$$

where, $B = \frac{a\ \Gamma(b+1)}{c + y}$

For large value of t, i.e., $\frac{B\ t^b}{\Gamma\ (2+b)} > 1$

$$X = \frac{q\ t}{c+y}\left[\frac{1}{Bt^b\ \Gamma(2-b)} - \frac{1}{(Bt^b)^2\ \Gamma(2-2b)} + \frac{1}{(Bt^b)^3\ \Gamma(2-3b)} - \frac{1}{(Bt^b)^4\ \Gamma(2-4b)} + \ldots\ldots\ldots\right] \quad (2.14)$$

Surface Irrigation Automation

Automatic Structures

A structure can be classified as fully automatic or semiautomatic. Fully automatic structures usually use sensing devices located in the field or programmed timers to trigger their operation. A fully automatic gate will reset itself after the completion of one irrigation and be ready for the next. A semiautomatic gate will require manual resetting between irrigations. These gates are usually triggered by a mechanical timer.

Boundurant and Humpherys (1962) described some automatic structures of the check type which control the water level in farm distribution ditches. After checking the water level to a raised position for a predetermined time, the automatic gate releases, allowing the water to flow to the next set. Individual furrows or border strips receiving the water must be well graded so they may be irrigated without the farmer's attention. A timing or sensing device is required to trigger these automatic structures. The energy required to operate the structure itself is usually obtained from the flowing water. Automatic controls vary from simple alarm-clock-timer released checks to elaborate radio and electronically controlled structures with programmable timers or moisture-sensing devices.

Cutback streams from lined ditches can be obtained by constructing the ditch in a series of level bays with spile outlets at equal elevation along the side of the ditch. Water is released sequentially downstream from one bay to the next by timed check gates. As the water advances to the next check, the water level in the upper bay is lowered and flow from the upper bay outlets is reduced (Garton, 1966; Humpherys, 1971; Nicolaescu and Kruse, 1971; Hart and Borrelli, 1972; Evans, 1977).

Automatic Discharge Control

Higher water application efficiency may theoretically be obtained if the flow in a furrow is reduced or cutback after the water has reached the end of the field. This technique is difficult to employ in practice because of the time required to readjust the individual furrow

streams and the difficulty in managing the surplus water. Structures and systems were developed to automatically reduce the flow of water to the furrow after a prescribed time interval (Garton, 1966).

Pneumatically operated and radio controlled valves were also developed to control the discharge from turnout structures (Haise et al., 1965). These valves control the discharge from alfalfa-type valves, an underground pipeline system or from turnouts in the farm ditches. The pneumatic valve for pipeline distribution systems is essentially an inflatable O-ring which when inflated forms an annular seal between the alfalfa valve seat and valve lid. The lay-flat pneumatic valve for ditch systems is a flat, rectangular tube that inflates to form a closure within the underground portion of the turnout pipe. Inflation and exhaustion of air from the valves is remotely controlled by a signal transmitted by wire or by radio from a centrally located timing device.

The most common gates for automatic control of open channel systems are the drop closed and drop open types. The drop closed gate is used to divert water directly onto irrigated fields or from one ditch into another. In the open position, it is suspended over a flow opening and, when tripped, falls by its own weight to stop the flow of water. Semiautomatic drop closed gates and dams tripped by mechanical timers are extensively used in New Zealand (Taylor,1965 ; Stoker, 1978).

The drop open gate is hinged so that when tripped, it either falls or swings open to allow water to flow downstream. Gates may be tripped by different actuating devices such as mechanical timers, solenoids, floats, or pneumatic and hydraulic cylinders. Gates of various

configurations and design have been used by different investigators (Calder and Weston, 1966; Kinberlin, 1966; Humpherys, 1969; Hart and Borrelli, 1970; Lorimor, 1973; Evans, 1977; Haise et al., 1980).

Surge Flow Irrigation

Chow (1959) referred to a moving hydraulic jump due to an abrupt decrease or increase in flow, such as that caused by sudden closing or opening of a gate, as a surge.

Stringham and Keller (1979) first introduced the concept of surge flow furrow irrigation. The system they described used an automated gated pipe with a microprocessor control unit. The cutback capability was accomplished by reducing the time instead of the instantaneous flow rate into the furrow. Stringham and Keller concluded that most simple irrigation valves could be operated in an on-off mode quite effectively, but not in the fully-on, partially-off mode needed for cutback systems. In order to achieve the needed cutback flow they cycled the valves on and off in a manner that achieved a time averaged cutback flow without changing the instantaneous discharge of the valves. When the valves are open half the time and closed half the time the same average stream size is achieved as if half the flow runs full time. The cycle time can be variable. Three banks of four furrows, each 660 ft long were studied. Each bank supplied two wheel rows and two non-wheel rows (wheel rows refer to furrows compacted by tractor tires). The surge valves for all three banks were set to give a discharge of 13 gpm. The first bank had a constant rate until the water reached the end of the furrow. The second bank was cycled at a steady rate of 8 seconds on and 8 seconds

off giving an average flow rate of 6.5 gpm. The third bank was cycled at a steady rate of 16 seconds on and 8 seconds off giving an average flow rate of 8.6 gpm. They reported that the advance time for the 16 sec on, 8 sec off, furrows was faster than the advance time for the steady flow in spite of the fact that the average stream flow was only about 67 percent as large. Furthermore, for the first 300 ft of furrow, the advance rate in all three operational modes was nearly the same even though the 8 sec on, 8 sec off flow regime had an average stream size of only 50 percent of the steady flow.

There have been two approaches to conducting surge flow experiments. The first approach was to use different instantaneous streams with different cycle ratios to give an equal quantity of water applied to each furrow over a given cycle time. The second approach was to use a constant stream with different cycle times and constant cycle ratios to give a time average stream equal to the continuous flow. The second approach eliminates the effects of using variable instantaneous flow rates on the advance rate.

Bishop et al. (1981) conducted field tests to study the effect of cycling furrow inflows on advance rates. They reported that the effects of surge flow irrigation were most apparent during the first irrigation. In the second irrigation the advantages of surge flow were substantially reduced. The difference between the continuous and surge flow treatments was significant and the differences among the surge flow treatments were not. In the second irrigation when infiltration differences were less noticeable in the field or when tractor wheel

compaction reduces these differences mechanically, the advance under surge flow was much closer to the advance under continuous flow.

Walker et al. (1982) developed a flowing infiltrometer that measures furrow intake under conditions representative of actual field conditions. The extended Kostiakov equation was used to fit the field measurements. These investigators noticed a significant reduction in the opportunity time exponent and uncertain reduction in the basic intake rate. The number of tests run was too small to determine the specific differences between surged and continuous waterings. The effect of soil type on infiltration in surge flow was dependent on the stability of soil aggregates.

Podmore and Duke (1982) conducted a study of surge flow in furrow irrigated corn. Surge irrigation in furrows was achieved by equipping gated pipe with a pneumatically activated pillow valve for each furrow. The ratio of average steady state infiltration rates, derived from inflow and outflow measurements, for surge irrigation to that of continuous flow was approximately 0.5, indicating that surge irrigation had a significant impact on the infiltration process. A constant furrow inflow and cycle ratio of 50% duty and a variable cycle time was used. This procedure resulted in a more rapid advance for the continuous flow treatment since, in a given time, twice as much water was applied to the continuous flow treatment as compared to the surge treatments. In another experiment the continuous flow rate was reduced by 50% so that all treatments had the same average flow rate. In this case the surge flow treatments advanced slightly more rapidly than the continuous flow treatments. The reported irrigation efficiency for surge flow was lower

or equal to that for continuous flow. The same gross application was used for all treatments. Since the surge treatments produced lower steady state infiltration rates, more runoff was produced when compared to continuous flow irrigation. Consequently, lower irrigation efficiencies resulted. No significant difference was reported for the surge flow and continuous flow treatments.

Podmore et al. (1983) switched surge irrigation applications to continuous flow at half the instantaneous inflow rate after about 75% of the furrows had completed advance. They concluded that surge irrigation with cutback after advance gave higher application efficiencies than either continuous flow or fully surged conditions. They suggested that the optimum surge system might begin an irrigation with short cycle times and increase the cycle times as the advance progressed.

A compelete analysis of border irrigation would require information on the effect of land slope, infiltration, roughness of soil surface, vegetation, and depth of water on the advance rate.

CHAPTER 3

SURGE FLOW IMPLEMENTATION

Surge flow requires turning the water on and off. When small, continuous flows are available these flows can be accumulated, then released. Two methods of water accumulation were considered, the dosing siphon and the automatic drop gate.

Dosing Siphon

The dosing siphon was developed by Hazen (1974,1975 A,B) for the hydraulic transport of livestock and poultry wastes. More recently, Markel (1981) analyzed the dosing siphon operation. The dosing siphon starts to release water when the level rises to a predetermined level, then stops releasing water when the level drops to a lower predetermined level.

The plan for the dosing siphon which was constructed and used in laboratory tests is shown in Fig. 4. The siphon consists of a water reservoir with a bell compartment. The bell compartment has a closed upper portion and an open lower portion which is spaced above the bottom of the reservoir.

Theory of Operation

The sequence of events that occur during a dosing siphon operating cycle are shown in Fig. 5. In step (a), if a siphon has just been

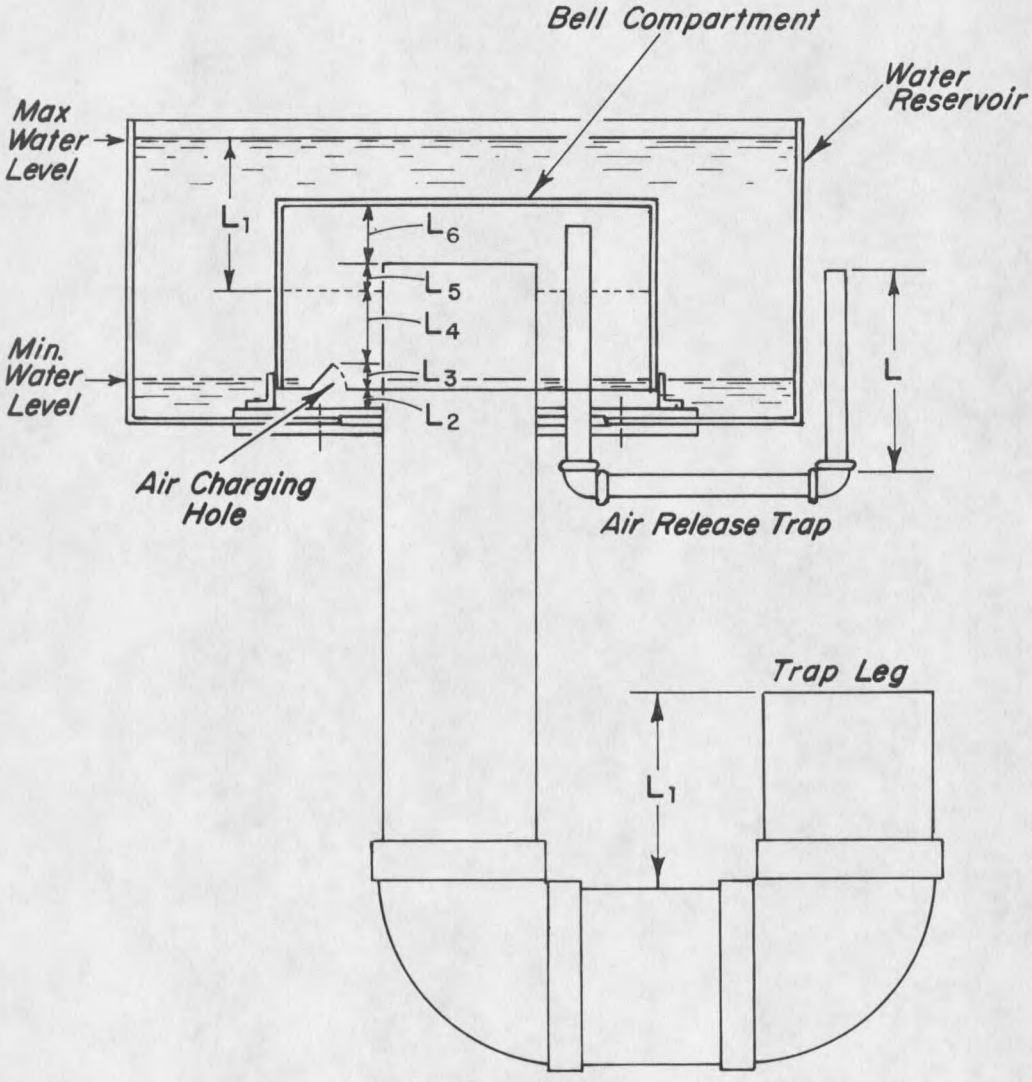


Figure 4. Dosing siphon. The water reservoir will continue to fill until head L_1, is equal to the air release trap leg L. Further filling forces an air bubble through the trap to release the air and start the flow.

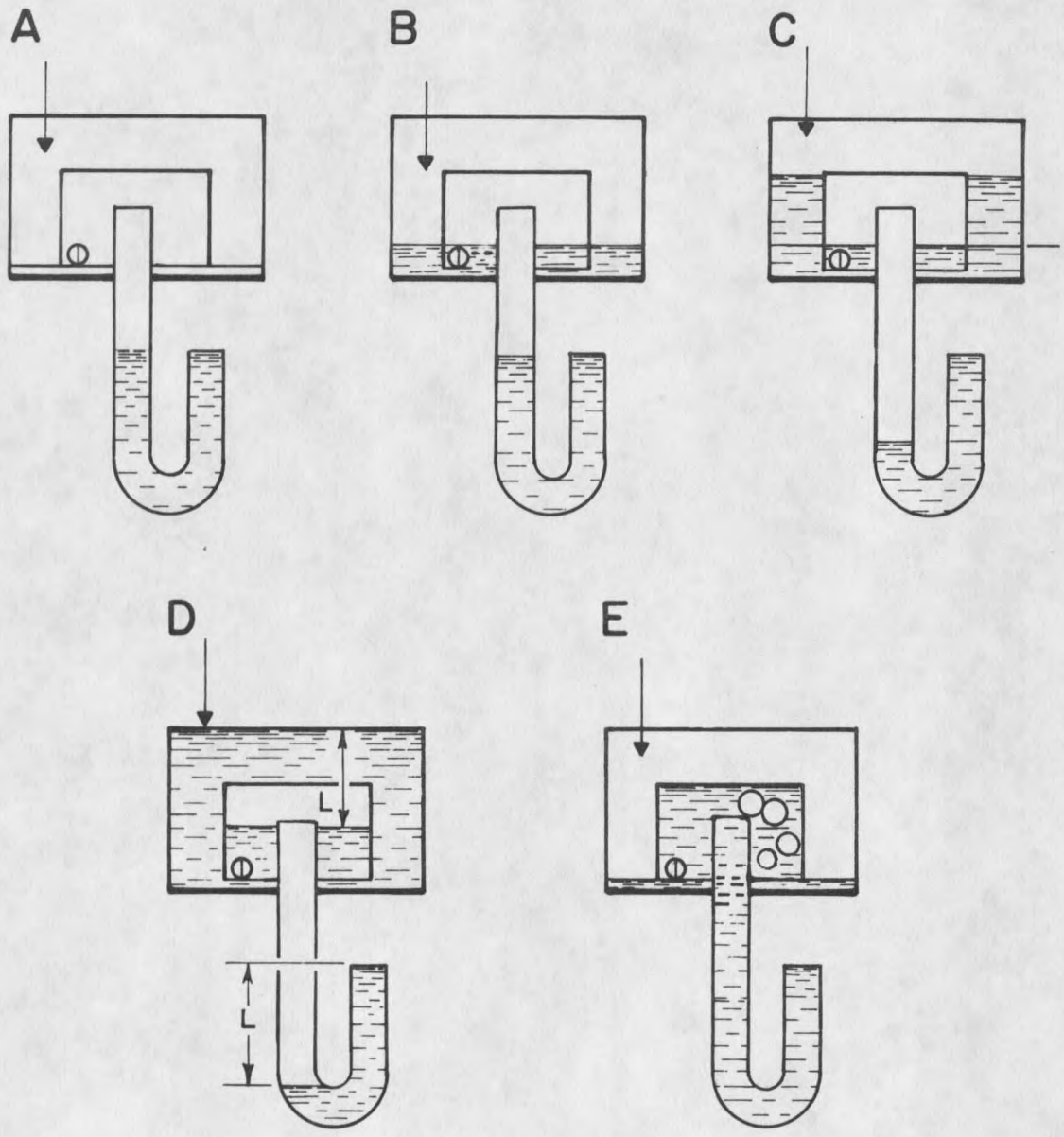


Figure 5. Sequence of events that occur during a dosing siphon operating cycle (after Markel, 1981).

constructed, the trap must be filled with water before the unit can function. In step (b), the water level will rise equally in both the reservoir and inside the bell until the air-charging hole in the bell is covered. At this time, the air within the bell is sealed off by water at the bottom of the bell and by water in the first leg of the trap. In step (c), as more water flows into the reservoir, the level of water in the reservoir will rise, but the level of water in the bell rises only enough to displace water in the siphon tube. The pressure in the trapped air increases as the water level in the reservoir increases. The water levels in the two arms of the trap become unbalanced to counter the air pressure. In step (d), the water level in the first trap leg reaches its lowest possible level. Further water added to the reservoir forces a bubble of air through the second leg of the trap. In step (e), during discharge, the water level in the reservoir drops to the level of the bottom of the bell. At this juncture, large quantities of air will flow under the bell, interrupting flow and the cycle begins again.

In Fig. 4 a supplementary trap, called the air-release trap, is provided to enhance the release of the air from the bell at the beginning of the discharge phase. This trap height is slightly less than the main trap height, so the water in the small trap is swept out very rapidly after the first bubble of air passes upward through this small trap. The down leg of this trap leads up into the top of the bell so that air is scavenged from the bell by this trap while water is flowing down the main discharge pipe. Once all the air from the bell has been removed, water also flows through this trap to recharge it.

Dosing Siphon Design

Siphon configuration is shown in Fig. 4. An initial assumption is that the air in the bell is incompressible. The design parameters are outlined in the following order.

1. Choose the distance, L_1, and the cross-sectional area of the discharge pipe, A_p.
2. Determine the bell compartment cross-sectional area, A_1 (6 to 8 times A_p).
3. Calculate L_4 using the following equation,

$$L_1 A_p = L_4 (A_1 - A_p)$$

The preceding equation states that the volume of water displaced from the first trap leg, L_1 must equal the water occupying the vertical interval in the bell, L_4.

4. The distance L_5 is equal to 25 to 50 mm to compensate for air compressibility.
5. The height of the air charging hole, L_3, is equal to 10 -15 mm.
6. The clearance under the bell, L_2, should be chosen to give a perimeter flow area of at least twice the cross-sectional area of the discharge pipe so that this area will not restrict flow during discharge,

$$L_2 \pi D_B = 2(\pi/4) D_p^2$$

Where D_B is the bell diameter.

and D_p is the pipe diameter.

7. The distance, L_6 is governed by the same considerations as L_2, according to the following equation,

$$L_6 \pi D_p = 2 (\pi/4) D_p^2$$

Therefore: $$L_6 = D_p/2$$

8. The vertical distance from the discharge end of the pipe to the maximum water level in the reservoir should be at least five times the pipe diameter, as stated by Hazen (1975 B).

Hazen (1974, 1975 A, B) indicated that the position of the bottom of the bell compartment determines the level of the water at the end of the discharge cycle. The position of the bottom of the bell compartment should be as close to the bottom of the reservoir as possible without restricting flow into the bell compartment to give maximum reservoir capacity. The minimum vertical distance from the discharge end of the conduit to the water level in the reservoir of five tube diameters is needed to insure that the discharge pipe flows full. The position of the upper end of the conduit with respect to the bell compartment is also quite important. Insufficient intrusion of the conduit into the compartment will result in premature discharge and lack of complete siphoning. Inadequate clearance between the top of the conduit and the top of the bell compartment will restrict flow into the conduit thereby reducing the rate of discharge. The bell compartment air charging opening must be above the low water level and it can be circular, an inverted U, rectangle, square, or an inverted V. Hazen (1975 A, B) also claimed that the natural rotational movement of the water as it enters the upper end of the conduit can be substantially eliminated if the upper end of the conduit is beveled rather than horizontal. The bevel can vary from 30° to about 60°, but 45° is preferred. A beveled upper

end will reduce entrance losses and provide up to a 50% increase in the throughput of the dosing siphon.

Automatic Drop Gate

Some irrigation projects have continuous inflow without adequate head for proper operation of the dosing siphon. The need for an automatic device that functions under any head available to the farmer led to the development of the automatic drop gate. The gate opens automatically when the water level on the upstream side of the gate rises to a predetermined level and remains open until the water surface drops to a lower predetermined level. The gate then returns automatically to its normally closed position by action of a counter balance weight. This gate has the following advantages:

1. Opens and closes automatically.
2. Can be designed for any head available between the water surface in the basin and the irrigated land.
3. Can be designed with head ditch characteristics incorporated so the required cycle ratio for surge flow irrigation can be achieved.
4. Needs no electronic system or timer to cycle.
5. Needs minimal management.
6. Easily designed and economically fabricated.

Theory of Operation

The automatic drop gate mechanism is shown in Figs. 6 and 7. The equilibrium conditions for the gate occur at the closing position and at the opening position when the moments due to the counter weight equal

the moments resulting from the water acting on the gate. When the water level on the upstream side of the gate rises to a height such that the moments due to the resultant force from the water pressure exceed the moments due to the counter weight the gate opens automatically. The gate remains open as long as the moments due to the water acting on the gate exceed the moments due to the counter balance. When the water level drops to a lower predetermined level, the gate automatically returns to its normally closed position. Points A, B, C, and D which include the floating link A-C should follow the same line of action in both open and closed positions to give the most uniform torque over the operating range. The linear displacement A-B made by the link OO-A is equal to the displacement C-D of the top of the gate due to movement from the closed to the open position. Equation development follows:

$$AB = CD \qquad \text{or}$$

$$2\ R_L \sin(\beta/2) = 2\ R_g \sin(\theta/2)$$

The angle θ made by moving the gate from the closed position to the open position is always 90^0, so

$$R_L = (0.7071/\sin(\beta/2))\ R_g \tag{3.1}$$

From the geometry the distance Y between the two pivots OO and O is,

$$Y = R_g + R_L\ (\sin\alpha + \cos\alpha) \tag{3.2}$$

Where, $\alpha = (90^0 - \beta)/2$

Also from the geometry the length of floating link Z can be determined as follows:

$$Z \cos 45 = R_L \sin\alpha + R_L \cos\alpha - R_L \sin\alpha$$

$$Z = 1.4142\ R_L \cos\alpha \tag{3.3}$$

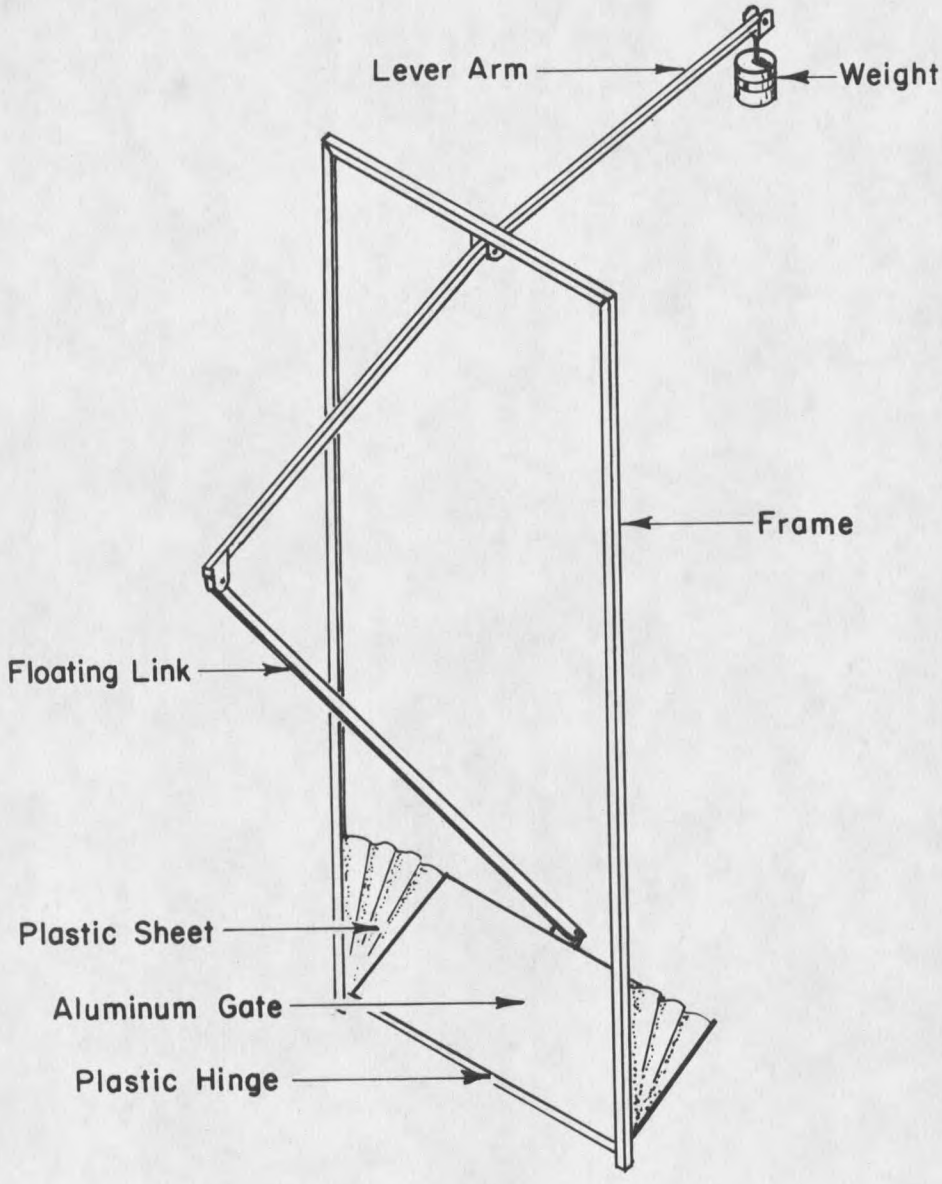


Figure 6. Schematic drawing of drop gate.

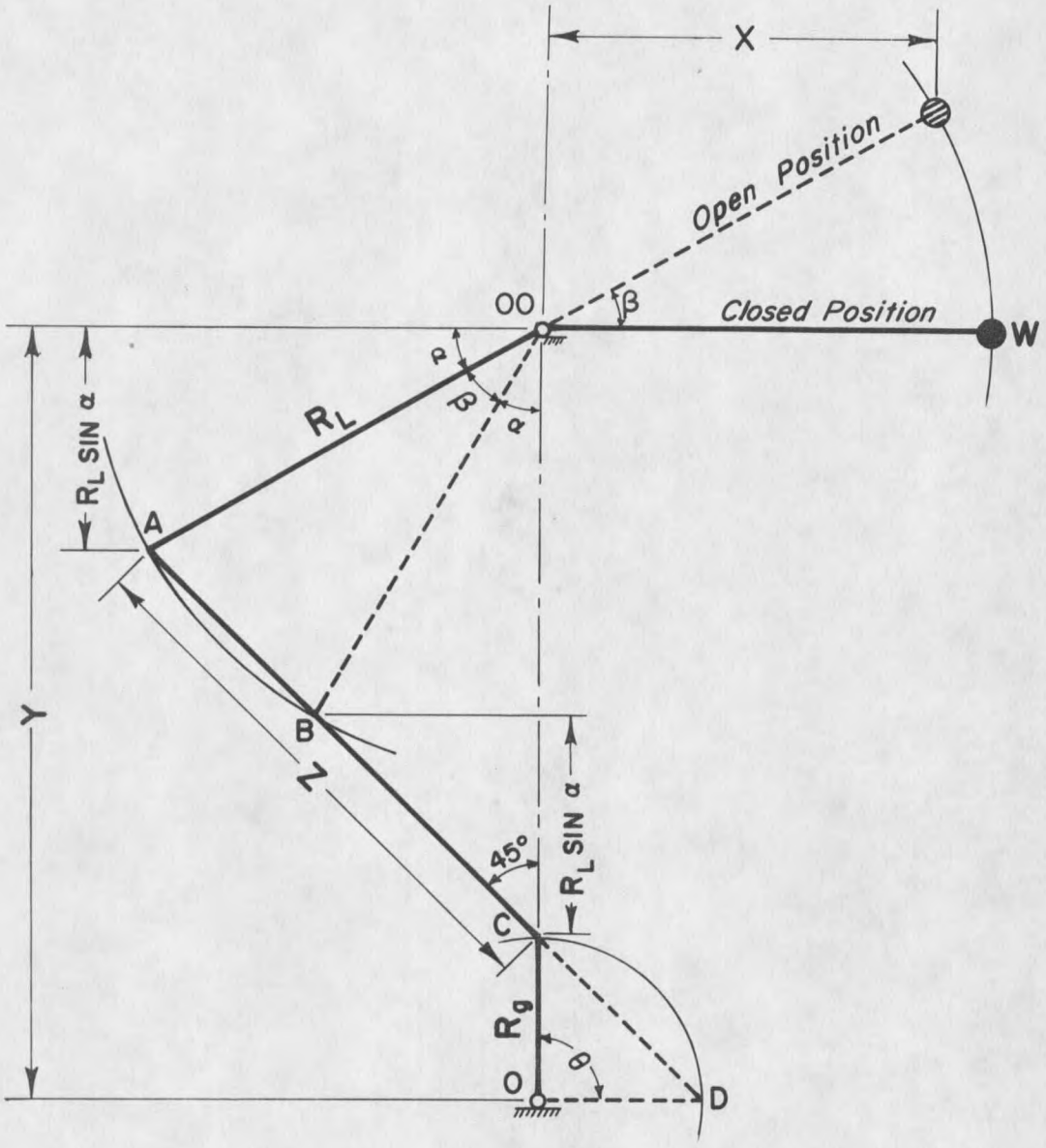


Figure 7. Automatic drop gate mechanism.

Force Analysis

Referring to Fig. 8 the moment T_1 about the pivot O due to the force exerted by the water acting on the gate while the gate is closed and ready to open is:

$$T_1 = \gamma\, h_{cg}\, A\, (1/3)(h)$$

$$T_1 = 1(gm/cm^3)((1/2)h)\,(h)(L)(h/3)$$

$$T_1 = (1/6)(L)\, h^3 \qquad (3.4)$$

Where,

L = the effective width of the gate (cm).

γ = the specific weight of water (gm/cm^3)

h = the height of the water behind the gate at opening (cm).

h_{cg} = the depth of water above the centroid of the plane area, A.

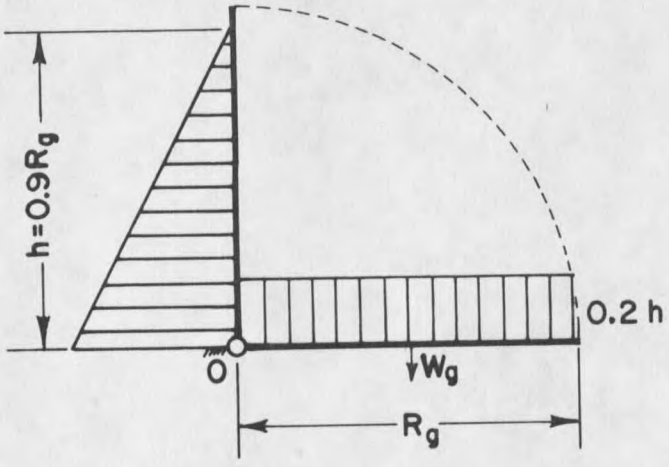


Figure 8. Water forces acting on the gate in both open and closed positions.

In order for the gate to close and prevent water flow when the water surface drops to o.2h the counter weight must overcome the following forces:

1. The weight of the gate.

2. The weight of the water over the gate.

When the gate is just ready to close, the moment about the pivot O, T_2 is,

$$T_2 = (1\ gm/cm^3)\ .2h\ Rg\ \ L\ 0.5Rg + Wg\ 0.5Rg$$

The gate should open before the water gets to the top of the gate. Thus

$$h = 0.9\ Rg$$

where 0.9 was used for the opening conditions as a factor of safety to insure that the gate will open before any overflow can occur,

$$T_2 = 0.09\ Rg^3\ L + 0.5\ Rg\ Wg \qquad (3.5)$$

This equation implies that the gate is ready to close when the depth of water over it is equal to 0.2h of water.

The second important consideration in designing the gate is to keep the lever OO-W horizontal when the gate is closed. This gives maximum torque from the counter balance W(gm).

The ratio of the torque at the closing and opening positions due to the water acting on the gate must be equal to the ratio of the torque due to the counter balance weight,

$$T_2 = T \text{ open position} = W \times \cos\beta$$

$$T_1 = T \text{ closed position} = W \times \cos 0 = W \times$$

$$T_2/T_1 = \cos\beta \qquad (3.6)$$

To determine the counter weight magnitude let X equal the torque lever length for the counter weight at any instant. This means $X = R_L$ at the closing position, and $X = R_L \cos\beta$ at the opening position. Taking the moment of the counter balance weight at any instant about the pivot OO gives,

$$W X = G R_L \cos(\beta/2) \tag{3.7}$$

Where G is the transmitting force to the floating link AC and is in the direction of the link and again taking the moment about the pivot OO gives,

$$T = G R_g \cos(\theta/2) \tag{3.8}$$

Where T is the torque about the pivot OO at any instant. Eliminating G between Eqs. (3.7) and (3.8) gives

$$W \cdot X/T = (R_L/R_g)(\cos\beta/2)/(\cos\theta/2) \tag{3.9}$$

Substituting $T = T_1$, and $X = R_L$,

$$W = T_1 (\cos\beta/2)/(R_g \cos\theta/2) \tag{3.10}$$

It can also be seen that substituting $T = T_2$ and $X = R_L\cos\beta$ yields the same answer for determining W by knowing that $T_2 = T_1 \cos\beta$.

Critical Design Criteria-Gate Opening and Closing

When the head on the closed gate reaches the design opening head the change occurs rapidly due to decreased resisting torque of the upward moving weight and increased opening torque due to water on the gate. This rapid change in torque is not as noticeable during the closing cycle and ceases to exist when the inflow rate approaches the outflow rate at a head equal to or greater than the design closing head.

The critical relationships for gate closing using the weir formula requires that:

$$Q_{in} < a(.2h)^r$$

As the gate starts to close the closing torque of the weight arm increases slowly while the weight of the water on the gate decreases slowly. At the same time the momemtum of the water in the direction of flow starts to act upon the gate. This momentum component is small compared to the weight of the water. However, the combined effect is significant and it may be necessary for the head to drop below the design closing head for rapid gate closing.

Critical Considerations for Design

The preceding analysis has shown that gate closure occurs when the water surface drops below 0.2h. Thus the inflow to a reservoir area must be less than the outflow corresponding to the head of 0.2h over the gate. If the inflow rate exceeds an amount which has a corresponding head of o.2h the gate will stay open because the water surface over it will not drop enough.

It can be seen that there is a compromise in designing the gate between the closing head and the weight of the gate material itself. The lighter the gate, the larger the closing head, and the consequent accommodation of adequate inflow. For lightness the gate material selected is Aluminum 6061-T6, 2.5 mm. thick. A plastic hinge is used to join the gate with the frame. Plastic sheeting is used as sides for the gate to prevent leakage around the gate when it is in the closed position.

CHAPTER 4

LABORATORY TESTS

Equipment

An automatic drop gate and a dosing siphon were designed and constructed, then tested in the laboratory to check performance and determine head discharge relationships. A rectangular plywood flume 240x120x66 cm was used as a reservoir. A strain gauge pressure transducer was used to measure the water depth in the flume. Depth measurements were recorded on a strip-chart recorder as a function of time. A 30x30 cm drop gate was tested with variable inflow rates. Tests with a 15 cm siphon used three variables: inflow rate, the length of the downpipe trap leg, and the minimum head or the distance between the top of the discharge pipe and the lowest head in the reservoir.

The changes of the water depth in the flume during one cycle were obtained directly from the strip-chart. One cycle is defined as the period required for a complete opening and closing, i.e, the time between the first opening to the next opening. The data gathered from each test include:

1. Inflow rate.
2. Highest water level.
3. Lowest water level.
4. Total time the gate is open, on-time.

5. Total time the gate is closed, off-time.

6. Outflow rate.

All the preceding data were obtained from the strip-chart record as described later.

Drop Gate Tests

Typical strip chart records that show the depth of water as a function of elapsed time during the drop gate operation with different inflow rates are presented in Figs. 9 and 10. These figures show that the inflow function is linear and the outflow is curvilinear. A continuity equation was developed to describe the discharge function of the drop gate shown by these figures. The continuity equation was applied to the control volume as shown in Fig. 4.3.

The continuity equation is,

$$\sum \rho\, Q = \frac{ds}{dt} \tag{4.1}$$

Since the density is constant,

$$Q_{in} - Q_{out} = A_t \frac{dH}{dt} \tag{4.2}$$

When the gate is closed (called off-time) the outflow is equal to zero and

$$Q_{in} = A_t \ (dH/dt)$$

Q_{in} can be measured by knowing the water surface area, A_t, which is constant, and the rate of water rise. This is the slope of a straight line as shown in Figs. 9 and 10.

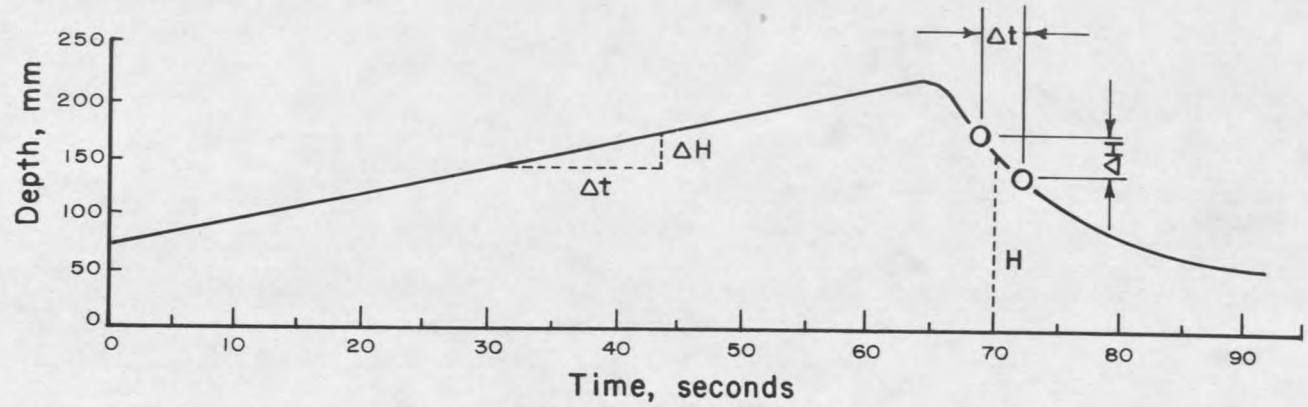


Figure 9. Depth changes during one cycle using the 30 cm drop gate and inflow of 11.5 L/s.

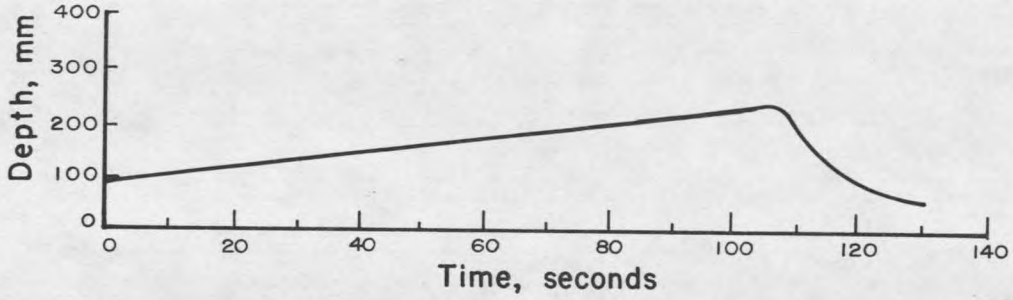


Figure 10. Depth changes during one cycle using the 30 cm drop gate and inflow of 3.6 L/s.

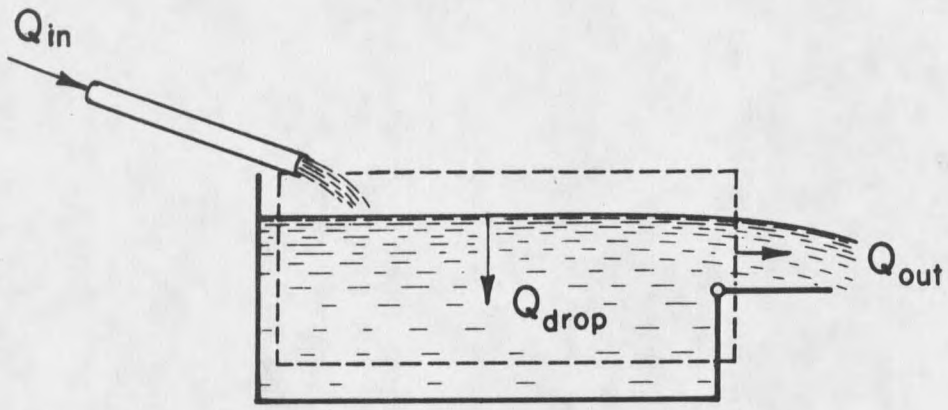


Figure 11. The control volume for applying the continuity equation to the drop gate system.

When the gate is open (called on-time) the outflow is variable and the slope of Fig. 9 is not constant. The rate of change of this slope (dH/dt) is negative. The outflow (Q_{out}) can be written as:

$$Q_{out} = Q_{in} - A_t\ (dH/dt)_{on} \qquad \text{(dH/dt when gate is open)}$$

and

$$Q_{in} = A_t\ (dH/dt)_{off} \qquad \text{(dH/dt when gate is closed)}$$

therefore,

$$Q_{out} = A_t(dH/dt)_{off} - A_t(dH/dt)_{on} \tag{4.3}$$

Where Q_{out} could be expressed in the weir type equation,

$$Q_{out} = a\ H^r \tag{4.4}$$

The slope of a curvilinear function at any given point of H is equal to the slope of a line drawn tangent to the curve at that point. The terminology of the derivative is,

$$\frac{dH}{dt} = \underset{\Delta t \longrightarrow 0}{\text{limit}}\ \frac{\Delta H}{\Delta t}$$

The slope or tangent to the curve can be determined by using two points, a small distance apart, to define the tangent. The chord between these two points approximates the actual slope. The average head was taken at the midpoint of these chord sections. Table 1 represents the discharge versus head relationship obtained from different strip charts as described and shown in Fig. 9. This procedure was developed to determine the discharge equation for the gate because it was not possible to obtain adequate inflow for constant head tests.

Table 1. Head on the drop gate versus discharge obtained from several tests as shown in Fig. 10.

H(m)	Q(L/s)
0.1539	36.420
0.1319	24.384
0.0862	16.284
0.1207	20.759
0.1777	44.236
0.0863	16.511
0.1319	25.970
0.1893	46.020
0.0835	15.350
0.1377	31.860
0.2005	54.516

The data presented in Table 1 were plotted on log-log paper (Fig. 12) and used to determine the value of the constants in the empirical relationship between the discharge and the head on the drop gate as shown by Eq. (4.4) modified to logarithmic form as:

$$\log Q = \log a + r \log H$$

A least squares method was used to determine these constants. The method is summarized in Table 2.

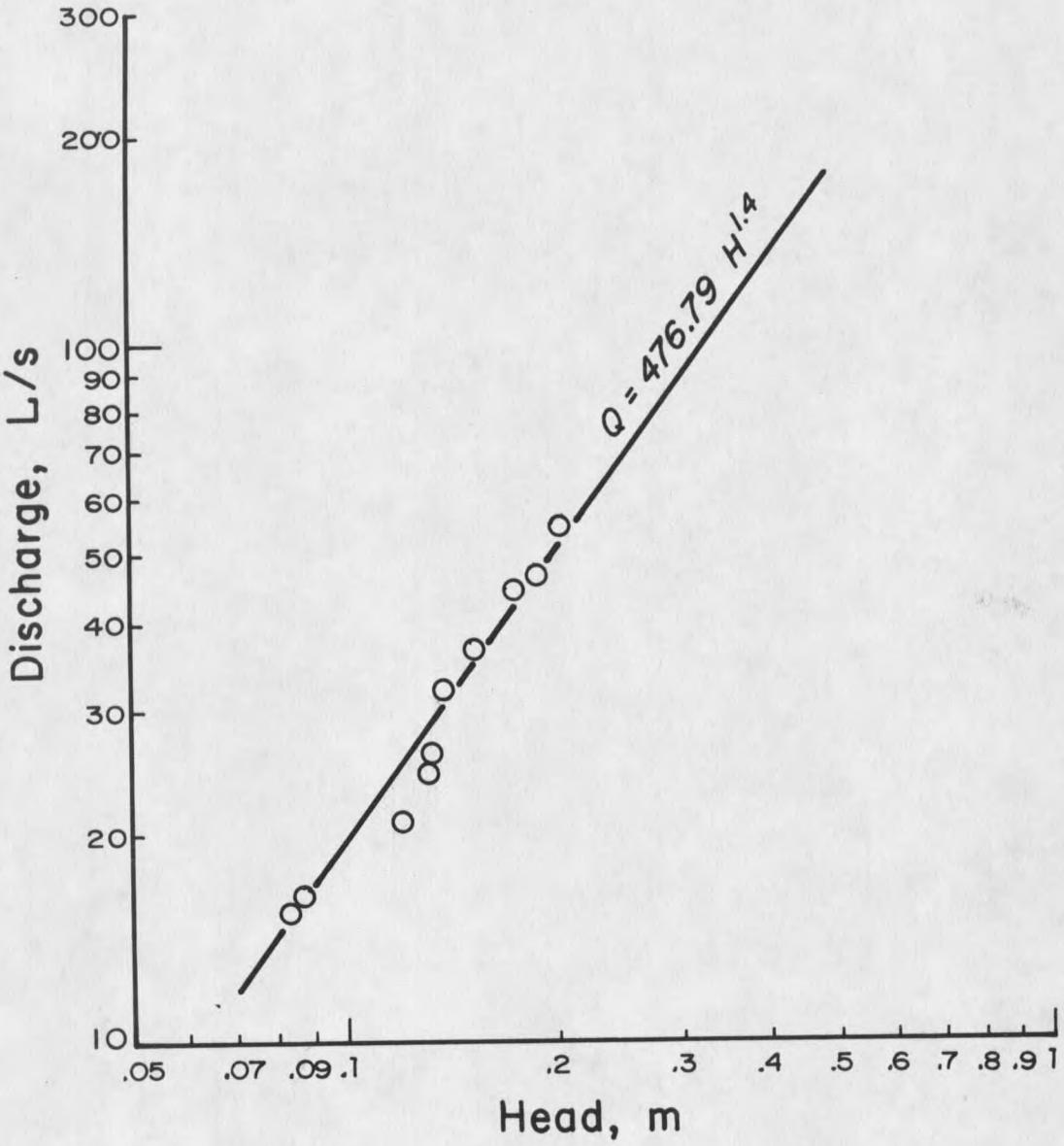


Figure 12. Drop gate discharge as a function of head.

Table 2. Summary of least squares method calculations.

No.	Q(L/s)	log Q	H(m)	log H	log Q log H	$(\log H)^2$
1	36.420	1.561	.1539	-0.81276	-1.26872	o.66058
2	24.384	1.387	.1319	-0.87975	-1.22021	0.77397
3	16.284	1.212	.0862	-1.06449	-1.29016	1.13314
4	20.759	1.317	.1207	-0.91829	-1.20938	0.84326
5	44.236	1.646	.1777	-0.75031	-1.23501	0.56297
6	16.511	1.218	.0863	-1.06399	-1.29594	1.13207
7	25.970	1.415	.1319	-0.87975	-1.24484	0.77396
8	46.020	1.663	.1893	-0.72285	-1.20210	0.52251
9	15.350	1.186	.0835	-1.07831	-1.27887	1.16276
10	31.860	1.503	.1377	-0.86107	-1.29419	0.74143
11	54.516	1.737	.2005	-0.69788	-1.21222	0.48704
Total		15.845		-9.7294	-13.7516	8.7937

The least squares method is described as follows:

$$\log a = \frac{\sum(\log H)^2 \quad \log Q - \sum \log H \quad \sum(\log Q \log H)}{n \sum(\log H)^2 - (\sum \log H)^2} \tag{4.5}$$

Substituting the corresponding values from Table 4.2 into the preceding equation gives:

$$\log a = \frac{(8.7937)\ (15.845) - (-9.7294)\ (-13.7516)}{11\ (8.7937) - (-9.7294)^2}$$

$$a = 476.79$$

The exponent r, can be determined from the following equation,

$$r = \frac{n \sum(\log H \log Q) - \sum \log Q \sum \log H}{n \sum(\log H)^2 - (\sum \log H)^2} \tag{4.6}$$

Substituting the corresponding values in the preceding equation,

$$r = \frac{11\ (-13.78516) - (-9.7294)\ (15.845)}{11\ (8.7936) - (-9.7294)^2}$$

$$r = 1.3995$$

The general form for the drop gate empirical equation then becomes:

$$Q = 476.79\ H^{1.4} \qquad (4.7)$$

The constant a is the product of discharge coefficient and the gate width as:

$$a = c\ L = 476.79$$

where $L = 0.292$ m

therefore: $c = 1632.28$

The discharge equation becomes:

$$Q = 1632.28\ L\ H^{1.4} \quad \text{L/s} \qquad (4.8)$$

The equivalent equation in English units would be:

$$Q = 3.33\ L\ H^{1.4} \quad \text{cfs}$$

Error Analysis

The probable error, E(%) of the value of the calculated flow (Q_c) from the measured flow (Q) was calculated from least squares fit equation as,

$$E(\%) = (10^s - 1) \times 100 \qquad (4.9)$$

Where s is the logarthmic standard deviation.

The variance is a measure of the goodness of fit of the empirical equation to the actual observed values. The variance for the linear equation is defined as s^2 and is calculated from:

$$s^2 = \frac{\sum e_i^2}{n - 2} \qquad (4.10)$$

Where,

$$e_i = \log Q - (\log a + r \log H) \qquad (4.11)$$

Q, H = the observed values

n = the number of data points

s = the standard deviation and is a measure of the accuracy of fit

Q_c = the calculated value of the discharge using the empirical equation.

The numbers used in determining the probable error are tabulated in Table 3.

Table 3. Probable error calculations for the drop gate empirical equation.

No.	Q (L/s)	log Q	H (m)	log H	e_i	e_i^2
1	36.420	1.561	o.1539	-0.8127	0.0205	0.00042
2	24.384	1.387	0.1319	-0.8797	0.0596	0.00356
3	16.284	1.212	0.0862	-1.0645	0.0239	0.00057
4	20.759	1.317	0.1207	-0.9183	-0.0757	0.00573
5	44.236	1.646	0.1777	-0.7503	0.0181	0.00033
6	16.510	1.218	0.0863	-1.0640	0.0293	0.00086
7	25.970	1.415	0.1319	-0.8797	-0.0316	0.00100
8	46.020	1.663	0.1893	-0.7228	-0.0033	0.00001
9	15.350	1.186	0.0835	-1.0783	0.0173	0.00030
10	31.860	1.503	0.1377	-0.8611	0.0302	0.00091
11	54.516	1.737	0.2005	-0.6978	0.0357	0.00127
					Total	0.01497

$$s^2 = \frac{0.01497}{11 - 2}$$

$$s = 0.04079$$

$$E(\%) = (10^{0.04079} - 1) \times 100 = 9.8\ \%$$

Using Eq.(4.8) to predict the discharge under a certain head on the drop gate yields a probable error of 9.8 %.

The equation for a broad-crested weir is:

$$Q = 1877\ L\ H^{1.5} \quad L/s \qquad (Q = 3.4\ L\ H^{1.5} \quad cfs) \qquad (4.12)$$

The probable error due to the use of the broad-crested weir equation, was found to be 13%, as calculated from Appendix A, Table 12.

The strip chart records gave the relationship between the head and time which were used to determine the discharge. If it is assumed that these two sources of error are caused by independent measurements, then the total probable error in results due to error in measurement techniques is the sum of the two,

$$\Delta Q/Q = (\Delta t/t) + r\ (\Delta H/H) \qquad (4.13)$$

Where r is the exponent in Eq.(4.8).

The minimum time increment, Δt, that could be measured on the chart, Δt was 1 second, and the minimum depth increment, ΔH, was 10 mm per line. The average time for one cycle was 100 seconds, and the total head was about 200 mm. The exponent of the empirical equation, r is 1.4. Substituting these values into Eq. 4.13 gives

$$\Delta Q/Q\ (\%) = [(1/100) + 1.4(10/200)] \times 100$$

$$= 8\%$$

The probable error in the discharge determined by the method of least squares was 9.8%, as compared to an 8% probable error in results due to errors in measurement techniques. These two error estimates agree quite closely.

Dosing Siphon Tests

A dosing siphon 150 mm in diameter similar to the one shown in Fig. 4 was used in laboratory tests. A typical depth change during one cycle of operation of the dosing siphon is shown in Fig. 13. Two inflow rates were used. Figure 14 shows a nearly linear relationship between head and time for the discharge as well as the fill portion of the cycle. The water depths obtained from the strip chart records were used to determine the discharge function for the dosing siphon. The continuity equation was applied to the control volume as shown in Fig. 15 to determine the outflow function.

The method used to apply the continuity equation to the dosing siphon for determining the discharge versus head relationship is the same as that described for the drop gate. The data from different strip charts are shown in Table 4. The data were plotted on log-log paper (Fig. 16) and used to develop the empirical discharge equation for the dosing siphon.

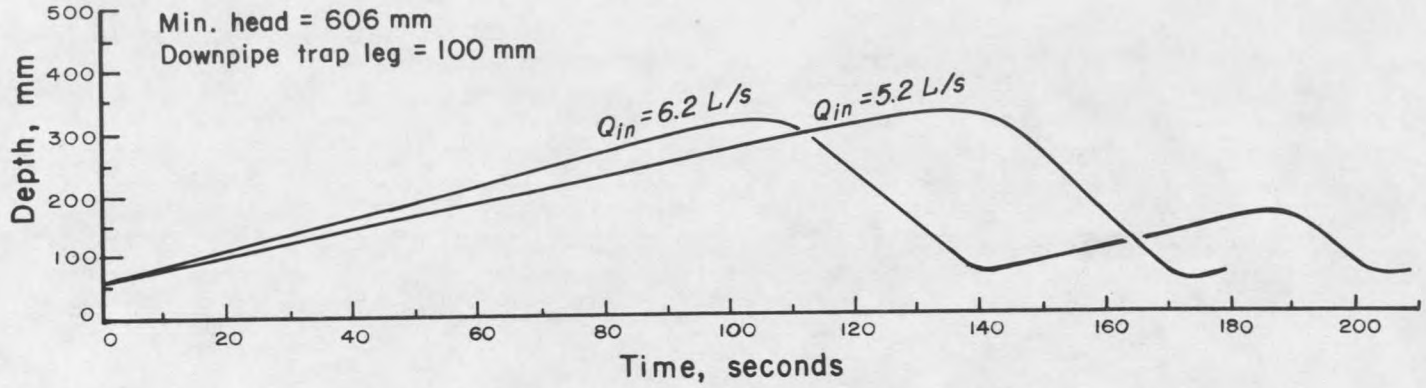


Figure 13. Depth changes during one cycle using two different inflow rates.

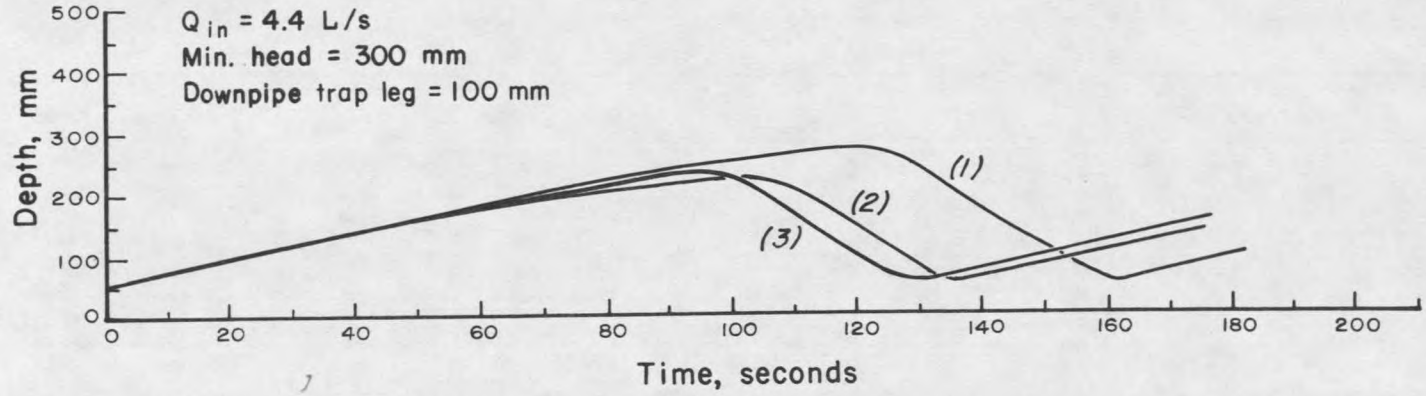


Figure 14. Depth changes during three sequential cycles using the same inflow.

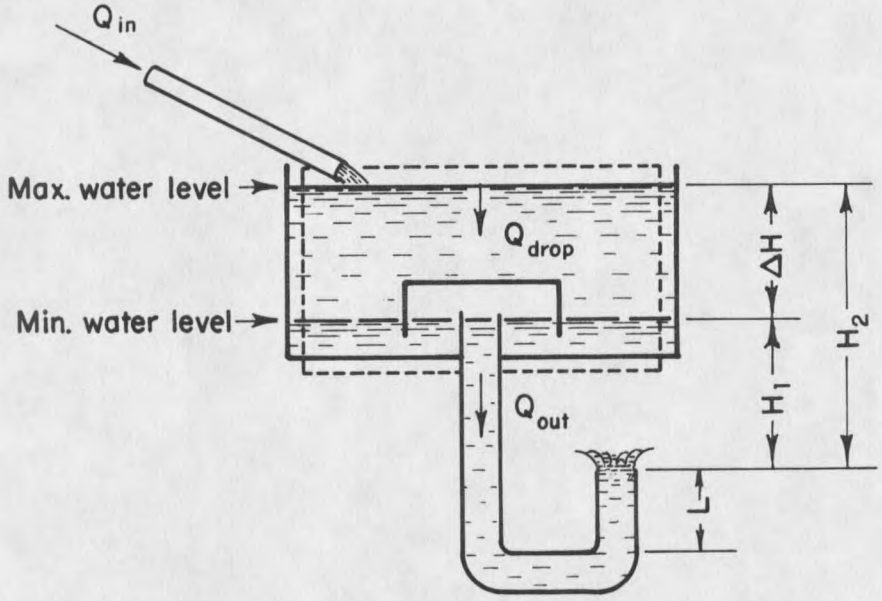


Figure 15. The control volume for applying the continuity equation to the dosing siphon system.

Table 4. Head on the dosing siphon versus discharge. Data obtained from several tests.

H(m)	Q(L/s)
0.4267	21.580
0.3706	20.645
0.2545	14.670
0.7684	28.094
0.6236	26.111
0.7303	30.303
0.3892	20.844
0.3283	18.748
0.1426	9.431
0.3810	17.813
0.4115	19.088

The calculations for the discharge equation are shown in Appendix A, Table 13. The following empirical equation was developed using the method of least squares.

$$Q = 36.35\ H^{.66} \qquad L/s \qquad (4.14)$$

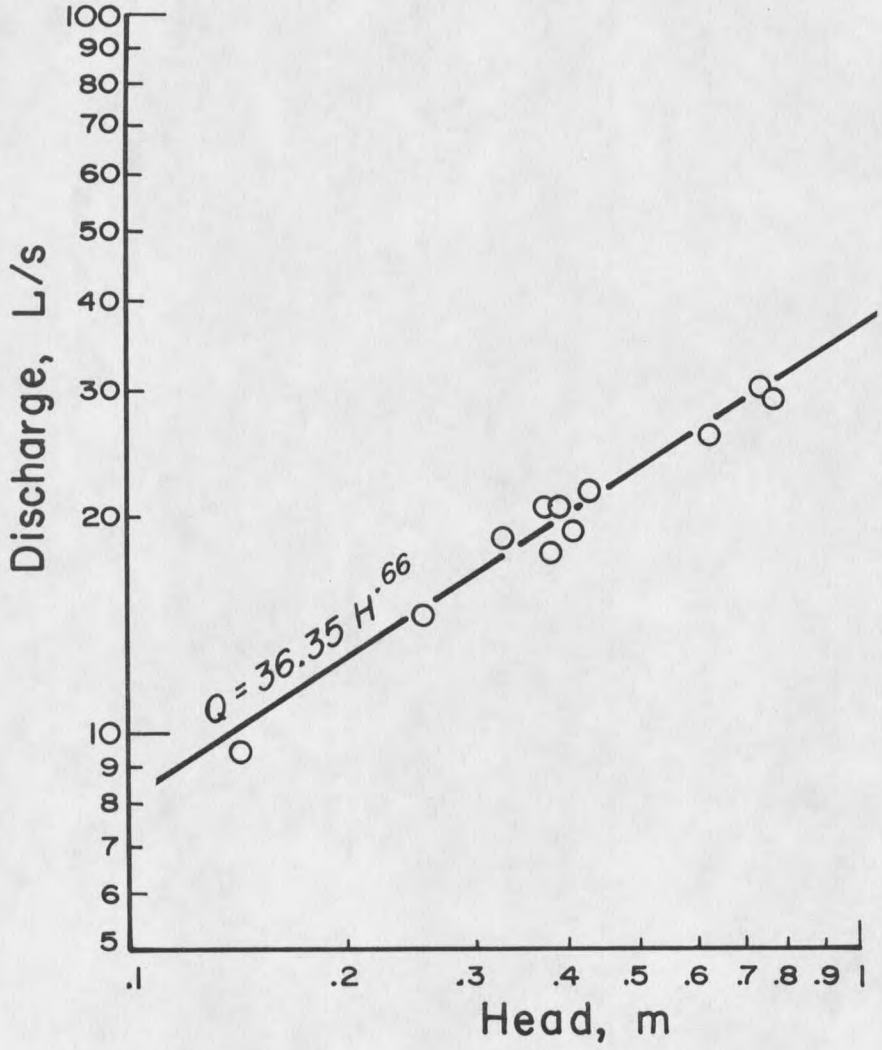


Figure 16. Dosing siphon discharge as a function of head for the experimental data shown in Table 4.

The dischage constant a of 36.35 is the product of the dischage coefficient, c, and the area of the discharge pipe, A_p. The area of the discharge pipe, $A_p = .01895\ m^2$

therefore:

$$Q = 1918.52\ A_p\ H^{.66} \quad L/s \qquad (Q = 2.87\ A_p\ H^{.66} \quad cfs) \qquad (4.15)$$

Error Analysis

The probable error in the discharge determined by the method of least squares is 6.9%. The calculations are shown in Appendix A, Table 14.

The general orifice equation for flow is:

$$Q = c\ A_p\ H^{.5}$$

The average discharge coefficient can be determined as shown in Table 5, and was found to be $c_{av.} = 1696.0$.

Table 5. Discharge coefficient calculations for dosing siphon.

$Q_{obs.}$ (L/s)	$H_{obs.}$ (m)	c
21.580	0.4267	1743.57
20.645	0.3706	1789.83
14.670	0.2545	1534.75
28.094	0.7684	1691.49
26.111	0.6236	1745.10
30.303	0.7303	1871.48
20.844	0.3892	1763.37
18.748	0.3283	1726.91
17.813	0.3810	1523.09
19.088	0.4115	1570.46

The orifice equation using the average discharge coefficient would be:

$$Q = 1696\ A_p\ H^{.5} \quad L/s \qquad (Q = 3.07\ A_p\ H^{.5} \quad cfs) \tag{4.16}$$

The probable error in the discharge determined by the orifice equation was found to be 7.6%. Calculations are shown in Appendix A, Table 15. The probable error as a result of error in measurement techniques, can be summarized as follows

The exponent in the empirical equation, $r = .66$

The minimum reading on time scale, $\Delta t = 1$ second

The average cycle time, $t = 100$ seconds

The minimum reading on depth scale, $\Delta H = 10$ mm

The average measured depth, $H = 200$ mm

Substituting the preceding values in Eq. 4.13,

$$\Delta Q/Q\ (\%) = [(1/100) + 0.66\ (10/200)] \times 100$$

$$= 4.3\%$$

It can be seen that the probable error in the discharge determined by the method of least squares is 6.9%, compared to 4.3% probable error in results due to error in measurement techniques.

Dosing Siphon Performance

The results of a test conducted to verify the effect of increasing the inflow under the same minimum head of 606 mm (H_1 in Fig. 15) and using a 100 mm downpipe trap leg are shown in Fig. 13. The siphon will reset with a 5.23 L/s inflow rate which corresponds to 2 mm/s rate of water rise in the reservoir. As soon as the inflow was increased to 6.17 L/s which corresponds to 2.45 mm/s rate of water rise,

the siphon did not reset. The rate of water rise is important because it affects the opportunity time for air to enter the bell and interrupt the flow so the siphon can reset.

Figure 14 shows the effect of changing the minimum head to 300 mm while using the same downpipe trap leg of 100 mm. With larger minimum head shown in Fig. 13 the siphon began releasing water at a depth of 320 mm, but with the lower minimum head shown in Fig. 14 the siphon started to release water at a depth of 270 mm. As the minimum head decreases the maximum head also decreases until it reaches a point at which the siphon does not reset. This minimum head was found to be about 260 mm which is close to twice the siphon diameter (150 mm). Hazen (1975 B) indicated that the minimum head must be about five times the siphon diameter. Figure 14 also shows that at the beginning of the dosing siphon continuous operation the first cycle time was longer than the consequent cycles. Under low head, the amount of air entering the bell decreases every cycle as the elapsed time increases.

CHAPTER 5

MATHEMATICAL MODEL OF SURGE FLOW OPERATION

A mathematical model was developed to simulate the emptying and refilling time for a head ditch and to give the required frequency ratio for surge flow irrigation. The discharge function for both the drop gate and the dosing siphon are incorporated in the model. The following assumptions were made.

1. The head ditch is large enough to function as a reservoir.
2. The effect of movement of a steep negative wave, created by sudden water release, on the outflow hydrograph can be neglected.
3. The positive wave traveling upstream due to the sudden closure of the device through which water is already flowing can be neglected because the flow discharge before the closure is usually limited.
4. The outflow hydrograph is independent of downstream conditions, or their effect can be neglected.
5. The resistance to flow along the ditch does not affect the shape of the free-outflow hydrograph.
6. The ditch can be considered a prismatic channel.

Model Development

The cycle ratio of a given ditch depends on these relations: ditch inflow hydrograph, cross sectional shape, the depth of water, the device opening characteristics (area, shape, position in relation to ditch and irrigated land), and type of flow (free-surface, flow under pressure).

Storage Outflow Function

The simple differential storage equation was considered.

$$p - Q = \frac{ds}{dt} \tag{5.1}$$

With p the inflow to the head ditch, Q the outflow from the ditch, and ds/dt the rate of change of the storage volume with time.

The solution of Eq. (5.1) is feasible if integrable mathematical expressions can be written for p, Q, and s.

Outflow Rating Curve

The outflow rating curve, a relation of the outflow discharge through the device to the water level in the head ditch, can be determined by,

$$Q = a\ h^r \tag{5.2}$$

Where h is the water level above the depth for which Q = 0, and a and r the coefficients which depend only on boundary conditions (outlet shape) and type of flow (closed or free outlets). The values of a and r were determined from the laboratory calibration tests for the drop gate and the dosing siphon.

Inflow Hydrograph

It is practically impossible to describe an entire natural inflow hydrograph by a simple mathematical expression however, it is feasible to determine some of their parts by simple mathematical expressions. The simplest forms of the function $p = f(t)$ to be used in this analysis are: (1) $p = 0$ (zero inflow, such as when the water is fully stored in the upstream ditch) (2) $p = p_o$ = constant or nearly constant (regulated constant inflow from upstream).

Storage Function

The storage function, which relates the volume in the ditch to its level can be written as follows,

$$ds = A_t \, dh \tag{5.3}$$

Where s is the storage volume, h is the depth of water above the level of zero outflow and A_t is the water surface area at depth h.

Ditch cross-sections considered in analyzing storage depth relationships were rectangular, trapezoidal, and parabolic.

Trapezoidal Cross-Section. Figure 17 shows the conditions that control water surface area in a ditch. The surface area is affected by changes in slope and reach length. The assumption of a prismatic channel (channel built with unvarying cross section and constant bottom slope) are necessary to make the solution of the problem feasible. Two conditions exist the first shown in Fig. 17 when the water surface is in

contact with the upstream check and the second when the water surface falls below the upstream check.

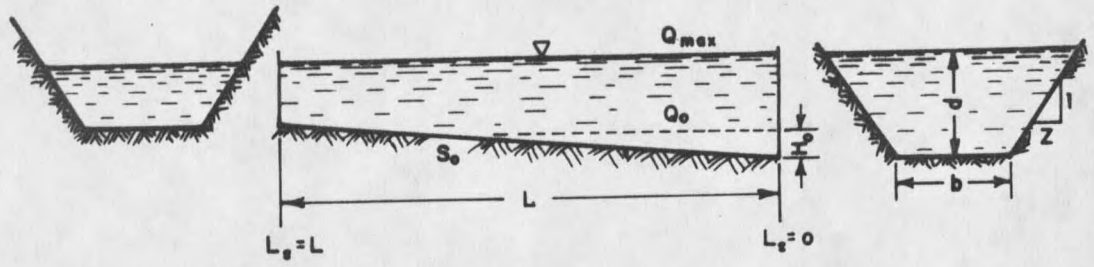


Figure 17. Schematic representation of the trapezoidal cross-section characteristics along the reservoir.

Under the first condition, $d > s_o L$

Where,

d = the water depth at the site of the flow device.

s_o = the ditch bottom slope.

L = the ditch reach length.

From Fig. 17 the following expression for the water surface area can be written,

$$A_t = \frac{(b + 2zd) + (b + 2z\,(d - s_o L))}{2} L$$

where:

A_t = the water surface area.

z = the side slope.

b = the bottom width.

Simplifying terms,

$$A_t = (b\ L - z\ s_o\ L^2) + 2\ z\ L\ d \qquad (5.4)$$

Under the second condition, $d < s_o\ L$

Again from Fig. 17 the following relationship can be written:

$$A_t = \frac{(b + 2\ z\ d) + b}{2} \quad \frac{d}{s_o}$$

where, $d/s_o = L_s$ of Fig. 17.

Simplifying,

$$A_t = b\ d/s_o + z\ d^2/s_o \qquad (5.5)$$

The depth of the water, d, can be related to the head on the existing flow device such as a dosing siphon or drop gate.

For the dosing siphon shown in Fig. 18, the following relationships exists:

$$d = h - Y$$

Where,

h = the effective head on the dosing siphon.

Y = the difference in elevation between zero storage and zero head.

For the drop gate shown in Fig. 18, the following relationship exists,

$$d = h + H_o$$

Where,

H_o = the difference in the level of zero outflow and the level of zero storage.

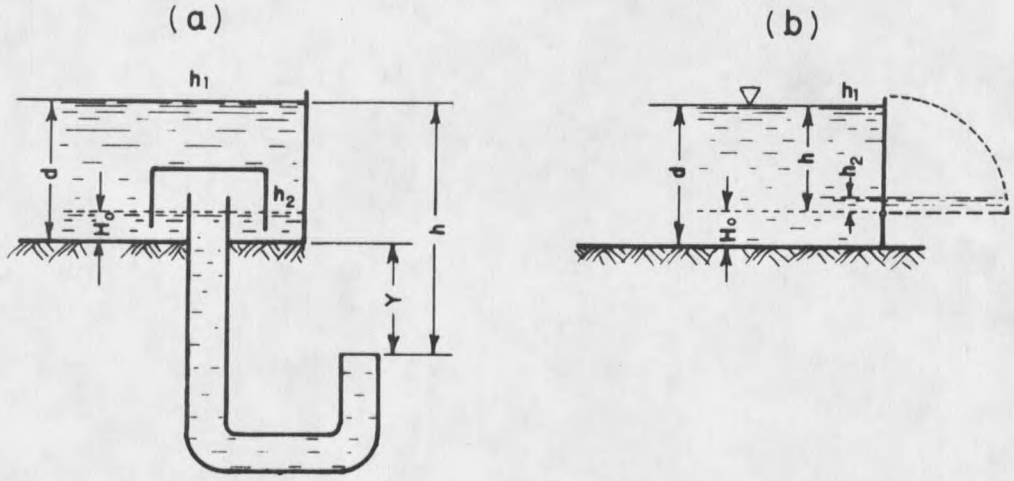


Figure 18. Definition sketch for (a) dosing siphon, (b) drop gate.

Generally, the depth equation can be written as follows,

$$d = h + c \tag{5.6}$$

Where,

$c = -Y$ for the dosing siphon

$c = H_o$ for the drop gate

Substituting Eq.(5.6) into Eq.(5.4) yields,

$$A_t = (b\,L - z\,s_o\,L^2) + 2\,z\,L(h + c)$$

or,

$$A_t = (b\,L - z\,s_o\,L^2 + 2\,z\,c\,L) + 2\,z\,L\,h \tag{5.7}$$

Substituting Eq.(5.6) into Eq.(5.5) yields,

$$A_t = (h + c)\,b/s_o + (h + c)^2\,z/s_o$$

or,

$$A_t = (b\,c/s_o + c\,z/s_o) + (b/s_o + 2\,c\,z/s_o)\,h + (z/s_o)\,h^2 \tag{5.8}$$

A general expression for A_t may be written as

$$A_t = A_o + A_1\,h + A_2\,h^2$$

where A_o, A_1, and A_2 are constants for a given prismatic trapezoidal channel.

The surface area for a rectangular cross-section ditch can be derived from the equation for the trapezoidal cross-section by substituting $z = 0$ in both Eq.(5.7) and Eq.(5.8).

Parabolic Cross-Section. Referring to Fig. 19 the following equation was used for the parabolic cross-section,

$$d = c_p X^2 \qquad \text{at } L_s = 0$$

At the first section ($L_s = 0$) the depth equals d, and in the next section, L_s upstream, from the first section, the depth is $(d - s_o L_s)$, so

$$d - s_o L_s = c_p X^2 \qquad \text{for all values of } L_s$$

or,

$$X = [(d - s_o L_s)/c_p]^{.5} \tag{5.9}$$

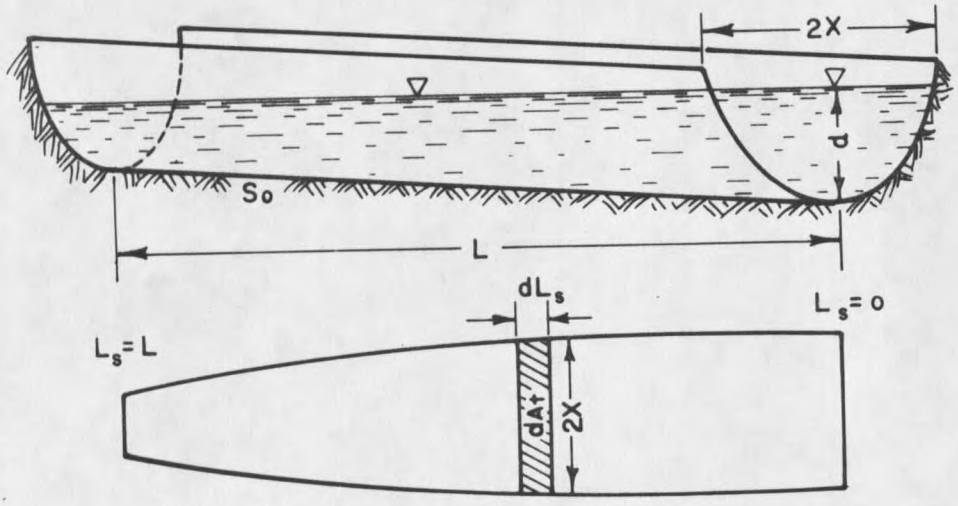


Figure 19. Definition sketch for using parabolic cross-section.

For a small element of surface area, which has a (2X) width and dL_s length increment,

$$dA_t = (2X)\, dL_s \tag{5.10}$$

Substituting Eq.(5.9) into Eq.(5.10), the integral is

$$A_t = \frac{2}{c_p{}^{.5}} \int_0^L (d - s_o L_s)^{.5}\, dL_s$$

which yields upon integration,

$$A_t = \frac{-4}{3\, s_o c_p{}^{.5}} \left[(d - s_o L_s)^{3/2} \right]_0^L \tag{5.11}$$

Considering the following two cases,

Condition 1, $d > s_o L$

The limits for this case are,

$$L_s = 0 \qquad\qquad L_s = L$$

Inserting the limits in Eq.(5.11) yields,

$$A_t = \frac{-4}{3\, s_o\, c_p{}^{.5}} \left[(d - s_o L)^{3/2} - d^{3/2} \right] \tag{5.12}$$

Substituting Eq.(5.6) into Eq.(5.12),

$$A_t = \frac{-4}{3\, s_o\, c_p{}^{.5}} \left[(h + c - s_o L)^{3/2} - (h + c)^{3/2} \right] \tag{5.13}$$

Condition 2, $d < s_o L$

The limits for this case are,

$$L_s = 0 \qquad L_s = d/s_o$$

Inserting the limits in Eq.(5.11) yields

$$A_t = \frac{4}{3\ s_o\ c_p^{.5}}\ d^{3/2} \tag{5.14}$$

Substituting Eq.(5.6) into Eq.(5.14),

$$A_t = \frac{4}{3\ s_o\ c_p^{.5}}\ (h + c)^{3/2} \tag{5.15}$$

Refill Time

Using a constant inflow, p_o, with zero outflow, Q_{out}, to refill the reservoir the following equation can be written,

$$p_o = A_t \frac{dh}{dt}$$

or,

$$dt = \frac{A_t}{p_o}\ dh$$

integrating,

$$\Delta t = \int_{h_1}^{h_2} \frac{A_t}{p_o}\ dh \tag{5.16}$$

Substituting the general expression for A_t, in the case of trapezoidal or rectangular cross-section.

$$\Delta t = \int_{h_1}^{h_2} \frac{A_o + A_1\ h + A_2\ h^2}{p_o}\ dh$$

$$\Delta t = \frac{A_o}{p_o}(h_2 - h_1) + \frac{A_1}{2p_o}(h_2^2 - h_1^2) + \frac{A_2}{3p_o}(h_2^3 - h_1^3) \qquad (5.17)$$

In the case of a parabolic cross-section

$$\Delta t = \int_{h_1}^{h_2} \frac{(h + c)^{3/2} - (h + c - s_o L)^{3/2}}{p_o} dh$$

$$\Delta t = \frac{2}{5p_o}[(h_2+c)^{5/2}-(h_1+c)^{5/2}] - \frac{2}{5p_o}[(h_2+c-s_o L)^{5/2}-(h_1+c-s_oL)^{5/2}] \qquad (5.18)$$

Release Time

Writing the simple storge equation,

$$Q - p = (ds/dt)$$

and inserting the value of $Q = a\ h^r$, the following may be developed,

$$a\ h^r - p_o = \frac{A_t}{dt}\ dh$$

Separating variables, and integrating the differential equation yields the following:

$$\Delta t = \int_{h_1}^{h_2} \frac{A_t}{a\ h^r - p_o} dh \qquad (5.19)$$

Numerical Solution. In many cases the water surface area, A_t in Eq.(5.19) cannot be described by an integrable expression as in the previous situation. In order to generalize the solution to handle any exponent in the outflow relationship, either integer or real, the numerical solution must be considered.

There are numerous formulas for numerical integration, but for many engineering applications the trapezoidal rule is quite adequate. To recall its derivation, the required integral may be put in the following form,

$$\int_a^b f(x)\,dx$$

Where by dividing the range of integration into n equal parts, the ordinates at the points of subdivision are.

$$f_o = f(a),\ f_1,\ f_2,\ldots\ldots,\ f_{n-1},\ f_n = f(b)$$

The definite integral above can be visualized as the area under the function f(x), and thus any method of approximating an area is essentially a method of approximating this definite integral form.

The trapezoidal rule can be written as follows

$$A = h\left(\frac{1}{2} f_o + f_1 + f_2 + \ldots\ldots + f_{n-1} + \frac{1}{2} f_n\right)$$

Table 6. shows the computational pattern in detail.

Table 6. Trapezoidal rule method of computation.

x	f(x)	Average	$\sum$	$h = \int_{x_o}^{x} f(x)\,dx$
$x_o=a$	f_o	....	$= 0$	$h = \int_{x_o}^{x_o} f(x)\,dx$
x_1	f_1	$(f_o + f_1)/2$	$= f_o/2 + f_1/2$	$h = \int_{x_o}^{x_1} f(x)\,dx$
x_2	f_2	$(f_1 + f_2)/2$	$= f_o/2 + f_1 + f_2/2$	$h = \int_{x_o}^{x_2} f(x)\,dx$

By more advanced methods it can be shown that the dominant part of the error made by using the trapezoidal rule to approximate an integral is

$$\frac{f_n - f_o}{12} \quad h^2$$

If this quantity is subtracted from the last integral, the improved value would be obtained.

A computer program written in BASIC is presented in Appendix B for determining the emptying and refilling time for specific ditch conditions.

Analytical Solution

The analytical solution for Eq.(5.19) is not feasible for most expressions of A_t and values of r, but it is useful to find an analytical solution for at least one case to verify the model. The following case was considered,

$$r = 1/2 \qquad A_t = A_o + A_1 h$$

Equation (5.19) can be mathematically divided into two parts after substituting the preceding values in order to be integrated as follows,

$$\Delta t = - \int_{h_1}^{h_2} \frac{A_o}{a\, h^{.5} - p_o}\, dh - \int_{h_1}^{h_2} \frac{A_1\, h}{a\, h^{.5} - p_o}\, dh$$

substituting,

$$X^2 = h \qquad 2\, X\, dX = dh$$

$$\Delta t = - \int_{X_1}^{X_2} \frac{2\, X\, A_o}{a\, X - p_o}\, dX - \int_{X_1}^{X_2} \frac{2\, A_1\, X^3}{a\, X - p_o}\, dX$$

substituting $B = -p_o/a$, and integrating

$$\Delta t = -\frac{2A_o + 3A_1B(2B-1)}{a}(X_1 - X_2) - \frac{2A_oB + 2A_1B^2}{a} \ln\frac{X_1 + B}{X_2 + B}$$

$$+ \frac{2A_1}{3a}[(X_1 + B)^3 - (X_2 + B)^3] - \frac{3A_1B}{a}(X_1 + X_2 + 2B) \qquad (5.20)$$

In case of the inflow discharge $p_o = 0$, Eq.(5.20) yields

$$\Delta t = \frac{2A_o}{a}(X_1 - X_2) + \frac{2A_1}{3a}(X_1^3 - X_2^3)$$

Summary of Runs Made with the Model

Model Verification

In order to determine whether the model was operating as intended, the following simplifying assumptions for which the model's true characteristics are known from the analytical solution was considered:

rectangular reservoir,

bottom width (b) = 1.015 m (3.33 ft)

maximum depth = 0.289 m (.95 ft)

bottom slope = 0.0

reservoir length (L) = 2.438 m (8 ft)

dosing siphon as a control device

siphon diameter (D_p) = o.155 m (6.115 in)

flow coefficient (c) = 1.696 (3.01)

minimum water depth = .076 m (.25 ft)

distance from bottom to siphon outlet = 0.228 m (.75 ft)

inflow rate = 4.79×10^{-3} m^3/s (.1693 cfs)

Substituting z=0 and $s_o = 0$ in Eq.(5.7) yields

$$A_t = A_o = b \cdot L$$

$$= (1.016)(2.438) = 2.477 \text{ m}^2$$

The discharge pipe cross-sectional area,

$$A_p = (\pi/4)(.155)^2 = 0.01887 \text{ m}^2$$

$$B = -(p_o/a) = -(.00479)/[(.01887)(1.696)]$$

$$= -0.15$$

$$X_1 = (0.289 + 0.228)^{.5} = 0.719$$

$$X_2 = (.076 + 0.228)^{.5} = 0.5514$$

substituting the preceding values in Eq.(5.20), the emptying time can be obtained,

$$\Delta t = \frac{2A_o}{a}(X_1 - X_2) - \frac{2A_oB}{a} \ln \frac{X_1 + B}{X_2 + B}$$

the preceding equation yields on substitution,

$$\Delta t = 34.06 \text{ seconds}$$

This compares to 34.78 sec. obtained from the computer program as shown in Appendix C, Fig. 36.

Substituting in Eq.(5.17) the refill time can be obtained,

$$\Delta t = (A_o/p_o)(h_2 - h_1)$$

$$= (2.4774/.00479)(.517 - 0.304)$$

$$= 110.16 \text{ seconds}$$

This compares to 110.24 sec. obtained from the computer program as shown in Appendix C, Fig. 36.

Model Validation

In order to determine whether the mathematical model is an accurate representation of the real system under study the results obtaind from the laboratory tests were compared to the results obtained from the mathematical model.

The following laboratory test was conducted:

rectangular reservoir

bottom width = 1.916 m (3.333 ft)

maximum depth = 0.537 m (1.763 ft)

bottom slope = 0.0

reservoir length = 2.438 m (8 ft)

drop gate as a control device

gate width = 0.292 m (0.958 ft)

gate coefficient of discharge = 1.877 (3.4)

Distance-gate bottom to reservoir bottom = 0.305 m (1 ft)

minimum water depth = 0.366 m (1.2 ft)

inflow rate = 0.0363 m^3/s (.1282 cfs)

Experimentally the emptying time was found to be 22 seconds and the refill time was found to be 117 seconds. The computer program gave an emptying time of 22.7 seconds and a refill time of 117 seconds as shown in Appendix C, Fig. 37.

Another lab test was conducted using the dosing siphon as follows:

rectangular reservoir

bottom width = 1.016 m (3.333 ft)

maximum depth = 0.732 m (1.55 ft)

bottom slope = 0.0

reservoir length = 2.438 m (8 ft)

siphon diameter = 0.155 m (6.115 in)

flow coefficient = 1.696 (3.01)

minimum water depth = .076 m (.25 ft)

distance from reservoir bottom to siphon outlet = .502 m (1.646 ft)

inflow rate = .0513 m^3/s (.18107 cfs)

Experimentally the following were found:

Emptying time = 45 seconds

Refill time = 190 seconds

From Appendix C, Fig. 38, the mathematical model gave:

Emptying time = 43.9 seconds

Refill time = 191.5 seconds

The maximum error was found to be about 2.5%, which is considered reasonable.

CHAPTER 6

FIELD EVALUATION AND ANALYSIS

Materials and Field Operation

Field experiments were conducted during the 1983 irrigation season at the Post Research Center near Bozeman, MT. The purposes of the experiments were to evaluate surge flow border irrigation systems using the automatic drop gate and compare the surge flow systems with conventional continuous flow systems.

The field was divided into eight border strips each 3 m by 102 m and separated by dikes 1 m wide and 0.3 m high. The slope in the direction of irrigation was 1.5 percent. There was nearly zero cross slope. Field layout is shown in Fig. 20. The soil was a silty clay loam. Physical properties of the soil are shown in Table 7.

Table 7. Soil physical properties.

Depth	%Sand	%Clay	%Silt	Available water* (cm/m)
0-30cm	8	33.2	58.8	22.1
30-60cm	6	39.2	54.8	20.8

*Moisture percentage at wilting point is 50 % of the field capacity and the bulk density is 1.3 gm/cm^3

For the surge flow experiments, basins 4.5 m by 3 m were constructed at the head of border strips No. 2, 5 and 7. The basins accumulated the inflow from the supply pipe for a period of time

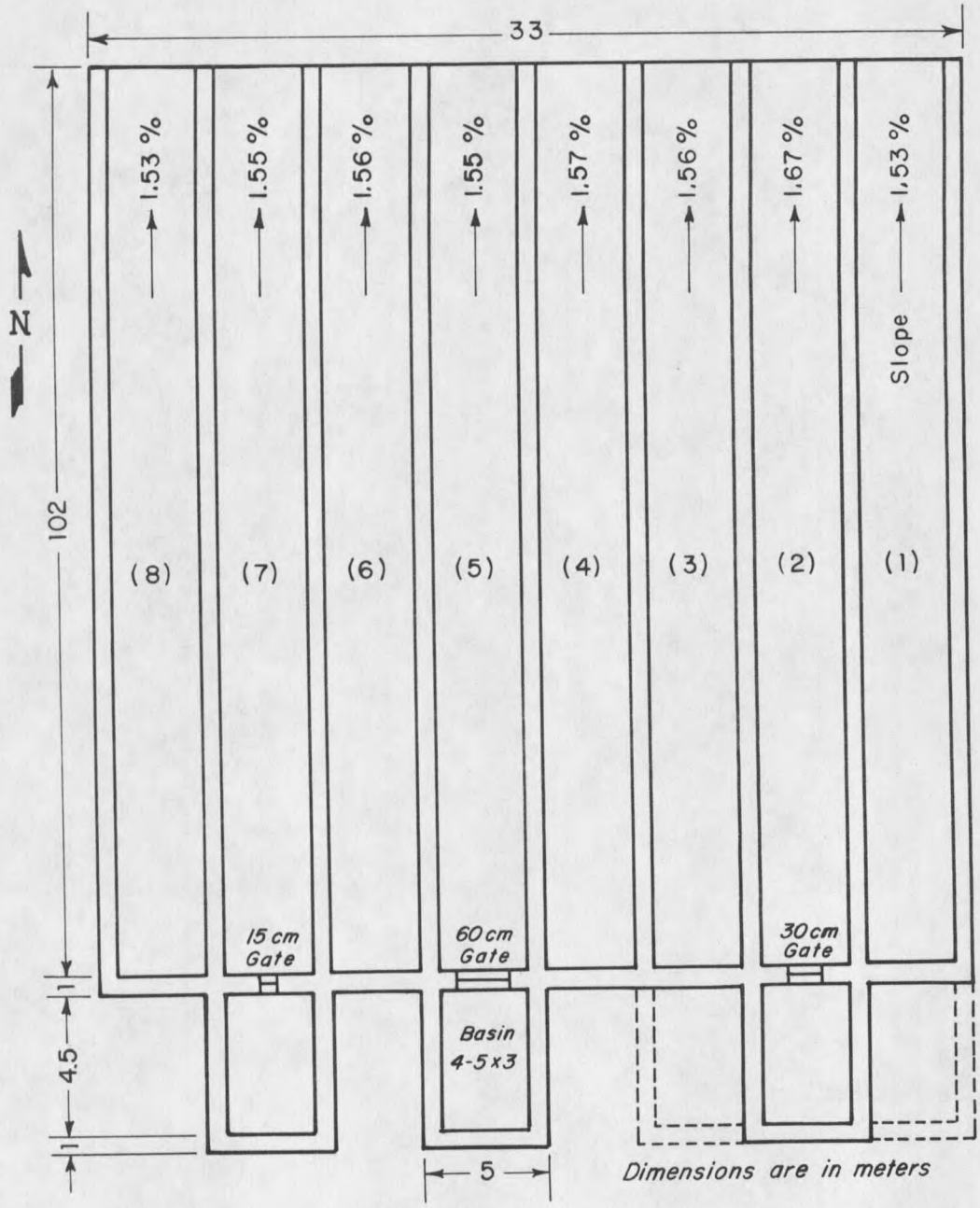


Figure 20. Field layout for border irrigation systems using three drop gate sizes.

(off-time) then released the accumulated water (on-time) using the automatic drop gate. The drop gate was built in three sizes 15, 30, and 60 cm and installed in borders No. 7, 2, and 5, respectively.

The developed mathematical model was used to calculate the cycle time produced by using a specific automatic drop gate size as shown in Table 8. The cycle time has been defined as the period required for a complete on/off cycle, i.e., the time between the beginning of one surge to the beginning of the next. The inflow to the basin was measured volumetrically and the same inflow was used for the continuous and surge treatment to evaluate various surge flow rates and cycle times as compared to conventional continuous flow border irrigation.

A full evaluation was performed for each treatment as follows:

1. The soil moisture deficiency was determined using a soil sampling tube and gravimetric samples.
2. The infiltration rate and cumulative infiltration were measured using a cylinder infiltrometer.
3. The advance and recession rates were measured using stakes placed at 10 m intervals.
4. The field slope was determined by measuring the elevation at each stake.
5. The time for water to reach each station was recorded.
6. The time when the water disappeared from the surface at each station was recorded.

The irrigation treatments applied are described in Table 8.

Table 8. Irrigation Treatments Applied.

Border No.	Date	Irrigation mode	Inflow rate(L/min) Basin	Border
2	7/26/83	One surge with 18 min on and 30 min off using 30cm gate and 4.5x9m basin.	300	
3	7/26/83	continuous		300
8	8/1/83	Four surges with 3 min on and 18 min off using 15cm gate and 4.5x3m basin.	66.7	
7	8/1/83	Continuous		66.7
6	8/2/83	Four surges with 3 min on and 12 min off using 15cm gate and 4.5x3m basin.	100	
5	8/2/83	Continuous		100
4	8/2/83	Four surges with 3 min on and 6 min off using 15cm gate and 4.5x3m basin.	200	
1	8/2/83	Continuous.		200
8	8/17/83	Two surges with 4 min on and 18 min off using 15cm gate and 4.5x3m basin.	200	
7	8/17/83	Continuous		200
5	8/17/83	Two surges with 1 min on and 18 min off using 60cm gate and 4.5x3m basin.	200	
3	8/17/83	Continuous		200
2	8/17/83	Two surges with 2 min on and 18 min off using 30cm gate and 4.5x3m basin.	200	

Utilization of Field Data

The procedures for preparing data for analysis are outlined below.

1. The advance and recession curves for each test were plotted. Surge flow is combined with the continuous flow for the same discharge on one sheet for comparison.
2. The advance and recession curves were extrapolated beyond the end of the measuring station until intersection to graphically portray the runoff.
3. All the individual cumulative infiltrated depth curves from the cylinder infiltrometer data were plotted on log-log paper. A general cumulative infiltrated depth equation was developed.
4. The infiltrated depth along the border-strip was calculated from the intake opportunity time at each station and plotted.

Infiltration Characteristics

The USDA, Soil Conservation Service, classifies soils into intake families. The equation for these families is as follows

$$F = a\ t^b + c \qquad (6.1)$$

Where F is the cumulative intake (mm), t is the time water is in contact with the soil (min), and a, b and c are constants unique to each intake family.

Field experimental data on accumulated infiltration versus time (Table 9), when plotted on a uniform co-ordinate paper (Fig. 21), gave a parabolic curve. When the data were plotted on log-log paper in Fig. 22 a linear relationship was indicated. Some data on the initial stage of

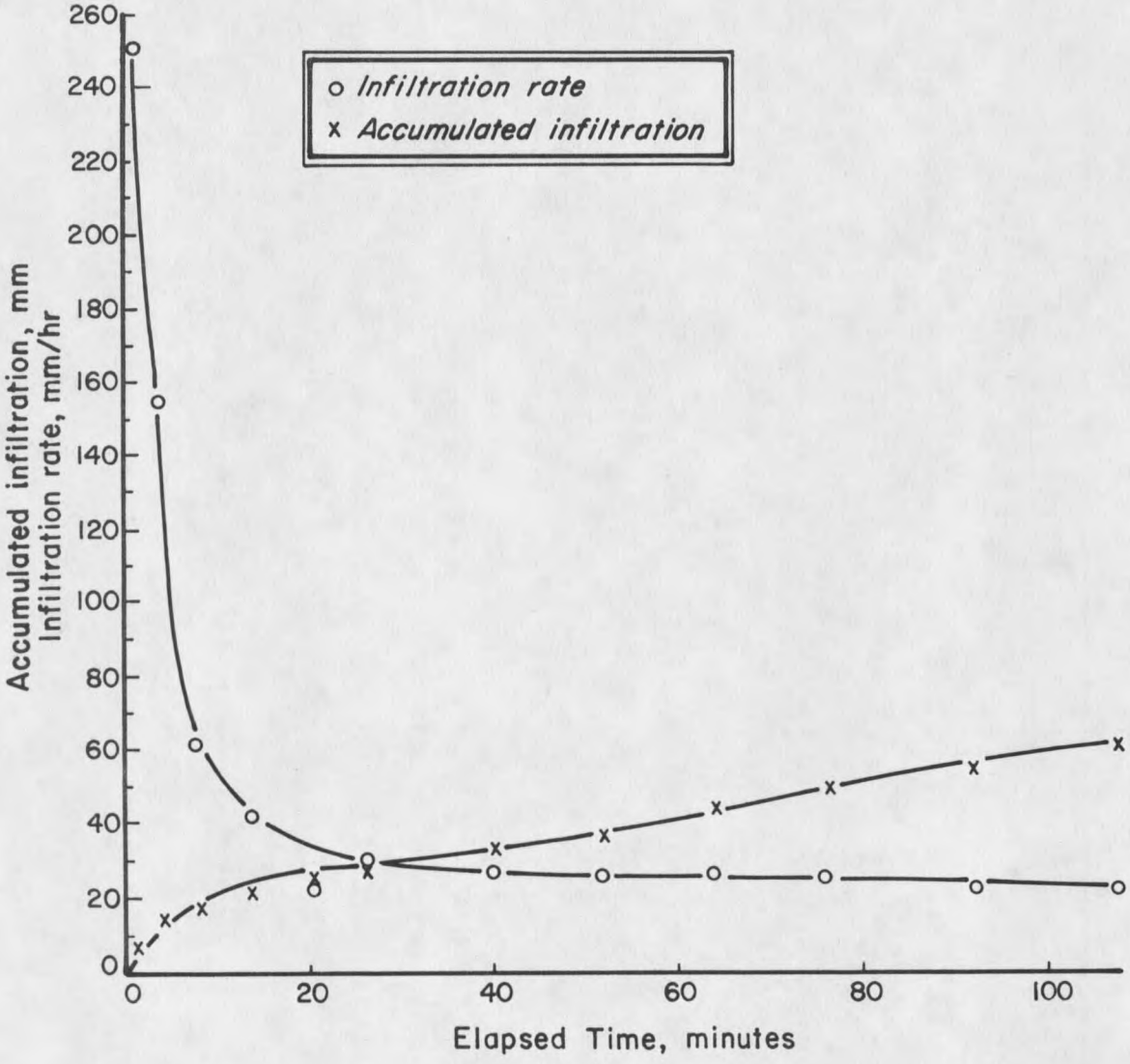


Figure 21. Plots of accumulated infiltration and average infiltration rate vs. elapsed time, based on the experimental data presented in Table 9.

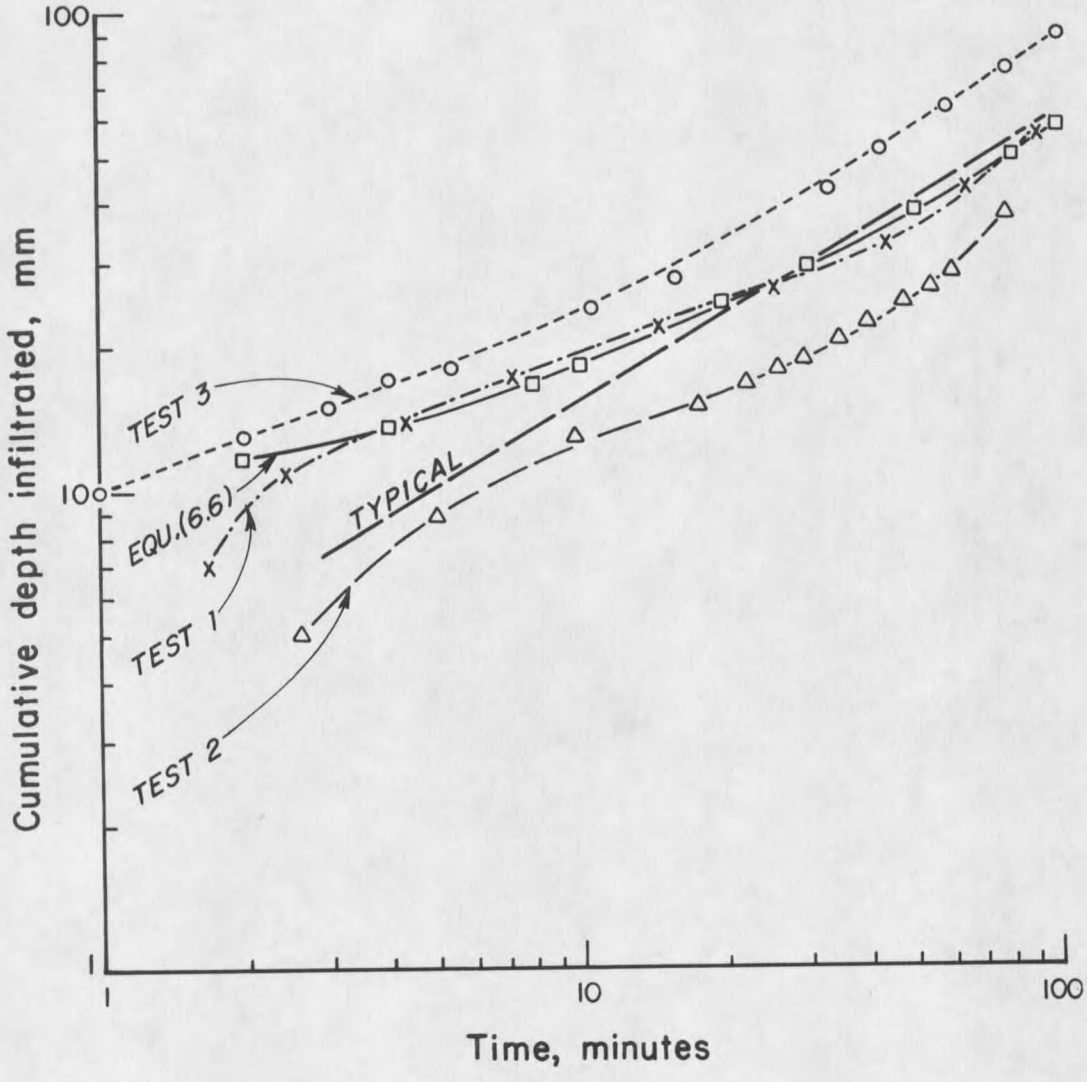


Figure 22. Cumulative cylinder infiltration curves from a bare silty loam soil.

the experiment usually fall along a slight curved line. Since the constant c rectifies this slight deviation from the linear log-log relationship, Eq. (6.1) is considered more comprehensive than the Kostiakov equation (Eq. (2.2)).

The infiltration rate at any time t is obtained by differentiating Eq. (6.1) as follows:

$$dF/dt = a\ t^{b-1} \qquad (6.2)$$

Table 9. Sample data of cylinder infiltrometer (Test 1).

Elapsed time min : sec	Difference min : sec	Cumulative infiltration (mm)	Difference (mm)	Average rate (mm/hr)
00:00	–	–	–	–
1:40	1:40	7	7	252
2:25	2:25	11	4	99.3
4:20	2:40	14	3	67.5
7:12	2:52	17	3	62.8
14:30	7:18	22	5	41.
20:28	5:58	24	2	20.1
26:30	6:02	27	3	29.8
40:20	13:50	33	6	26.0
51:30	11:10	38	5	26.8
64:30	13:	44	6	27.7
77:30	13:	50	6	27.7
91:30	16:	56	6	22.5
107:30	16:	62	6	22.5

The functional relationship between F and t is best represented by Eq. (6.1). The values of the constants a, b and c may be determined by the method of averages using the mathematical procedure suggested by Davis (1943) for developing the empirical equations. From the logarithmic form of Eq. (6.1)

$$\text{Log}(F - c) = \text{Log } a + b \text{ Log } t$$

It is evident that Log (F - c) vs. Log t is a linear relationship. The first step is to plot F vs. t. A smooth curve is then drawn corresponding to the points. Near the extremities of the curve points t_1 F_1 and t_2 F_2 are selected. The geometric mean of the points is then taken to obtain t_3. F_3 is then read corresponding to t_3.

Since the three points lie on the curve

$$F_1 - c = a\ t_1^{\,b}$$

$$F_2 - c = a\ t_2^{\,b}$$

and

$$F_3 - c = a\ t_3^{\,b}$$

and since

$$t_3 = (t_1\ t_2)^{0.5}$$

then

$$a\ t_3^{\,b} = (a\ t_1^{\,b}\ a\ t_2^{\,b})^{0.5}$$

or

$$F_3 - c = [(F_1 - c)(F_2 - c)]^{0.5}$$

from which

$$c = \frac{F_1\ F_2 - F_3^{\,2}}{F_1 + F_2 - 2\ F_3} \qquad (6.3)$$

From the plot of F against t (Fig. 21)

For t_1= 4.33 min, F_1 = 14 mm, and

For t_2= 107.5 min, F_2 = 62 mm.

The rectifying value is found from the relation

$$t_3 = (t_1\ t_2)^{0.5}$$

$$= (4.33 \times 107.5)^{0.5} = 21.57 \text{ min}$$

The corresponding value of F_3 as determined from Fig. 21 is 26 mm. The value of the constant c is obtained from Eq. (6.3) as follows:

$$c = [14(62) - (26)^2] / [14 + 62 - 2(26)] = 8.0 \text{ mm}$$

The c value of 8 is subtracted from each value of F in Table 9. The logarithms of (F - 8) and t are taken. The variables are related by the expression

$$F - 8 = a\ t^b$$

the logarithmic form of which is

$$\text{Log } (F - 8) = \text{Log } a + b \text{ Log } t \qquad (6.5)$$

Substituting the data on average infiltration F and elapsed time t presented in Table 9 into Eq. (6.5) yields the following Equations:

$$\begin{aligned}
0.4771 &= \text{Log } a + 0.3832\ b \\
0.7781 &= \text{Log } a + 0.6364\ b \\
0.9542 &= \text{Log } a + 0.8573\ b \\
1.1461 &= \text{Log } a + 1.1613\ b \\
1.2041 &= \text{Log } a + 1.3117\ b \\
1.2787 &= \text{Log } a + 1.3117\ b \\
\\
1.3979 &= \text{Log } a + 1.6056\ b \\
1.4771 &= \text{Log } a + 1.7118\ b \\
1.5563 &= \text{Log } a + 1.8095\ b \\
1.6232 &= \text{Log } a + 1.8893\ b \\
1.6812 &= \text{Log } a + 1.9614\ b \\
1.7323 &= \text{Log } a + 2.0314\ b
\end{aligned}$$

Adding the first six Equations and the last six,

$$5.8383 = 6 \text{ Log } a + 5.6616\ b \qquad (i)$$

$$1.578 = 6 \text{ Log } a + 11.009\ b \qquad (ii)$$

Dividing Eq. (i) and Eq. (ii) by 6,

$$0.9730 = \text{Log } a + 0.9436\ b \qquad (iii)$$

$$1.578 = \text{Log } a + 1.8348\ b$$

Which yield, on subtraction,

$$0.6049 = 0.8912\ b$$

or

$$b = 0.6788$$

Substituting for b in Eq. (iii)

$$\text{Log } a = 0.9730 - 0.9436\ (0.6788)$$

or

$$a = 2.1504$$

so the general equation for the cumulative infiltration depth is as follows,

$$F = 2.15\ t^{0.6788} + 8 \qquad (6.6)$$

Equation (6.6) was developed using the data obtained from the cylinder infiltrometer Test (1) which lies between Test (2) and Test (3) as shown in Fig. 22. Equation (6.6) is plotted in Fig. 22.

Analysis

Cumulative Intake Curves

Cumulative intake curves are plotted in Fig. 22 from data obtained from three cylinders. The slope of the consistent portion of the lines neglecting the effect of rapid initial intake was used to draw a straight line typical of all tests. This is shown as a dashed line in Figs. 22 and 23. Later the adjusted line (Fig. 23), using the procedure described below, was drawn and was used for the evaluation process because it shows an average intake rate for the whole field and

therefore is more representative than the data from any one of the three cylinders. Averaging the data from all three cylinders to plot only one line would produce a misleading curve because it would not indicate the range of conditions that actually exist.

Adjusted Cumulative Intake

Adjusted cumulative intake is developed for continuous irrigation as shown in Fig. 24. At each station on the total strip (actual and extrapolated portions) the opportunity time (time that water was on the ground), T_o was noted by measuring the time interval between the advance and recession curves (Fig. 24). The corresponding depth infiltrated, D was taken from the typical cumulative intake curve in Fig. 23 and tabulated in Table 10 for the same stations. The average depth for each 10m, D / 10 meters, was determined and entered as shown in Table 10. Thus, the average depth infiltrated for the entire strip was found to be approximately 53 mm as indicated. The general procedure followed in this analysis was developed by Merriam and Keller (1978).

To check the correctness of the location at which the "typical" curve was drawn, the actual average depth of water applied was computed by using the relationship mm = L/min x min /(m x m). The border spacing is 5 m and the strip width is 3 m, but the effective wetted width was measured experimentally to be 2.2 m. For the wetted strip length of 80 meters the depth applied for the application time of 121 minutes is:

$$D = \frac{67.7 \text{ L/min} \times 121 \text{ min}}{2.2 \text{ m} \times 80 \text{ m}} = 46 \text{ mm}$$

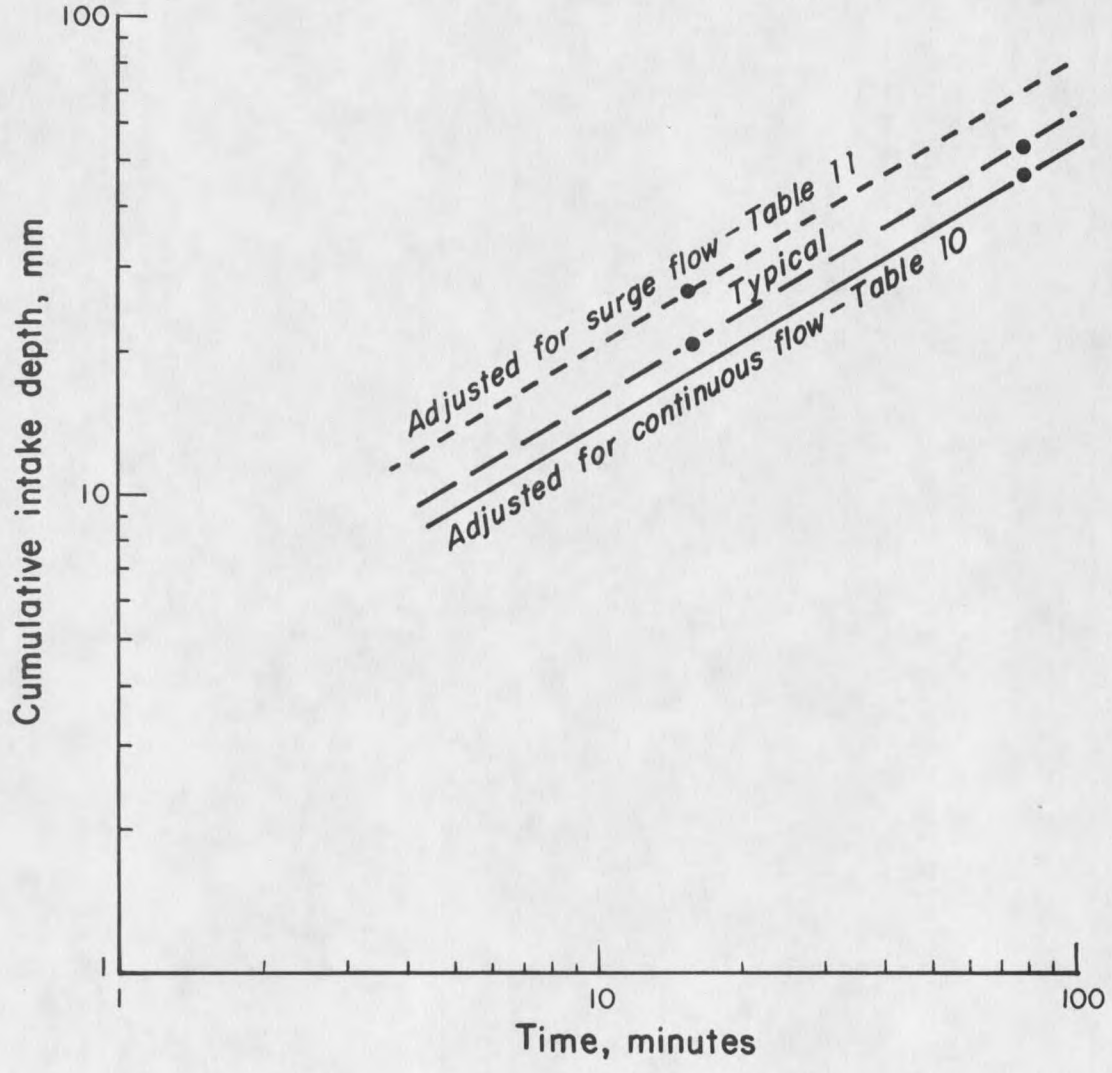


Figure 23. Cumulative cylinder infiltration curves with typical and adjusted intake.

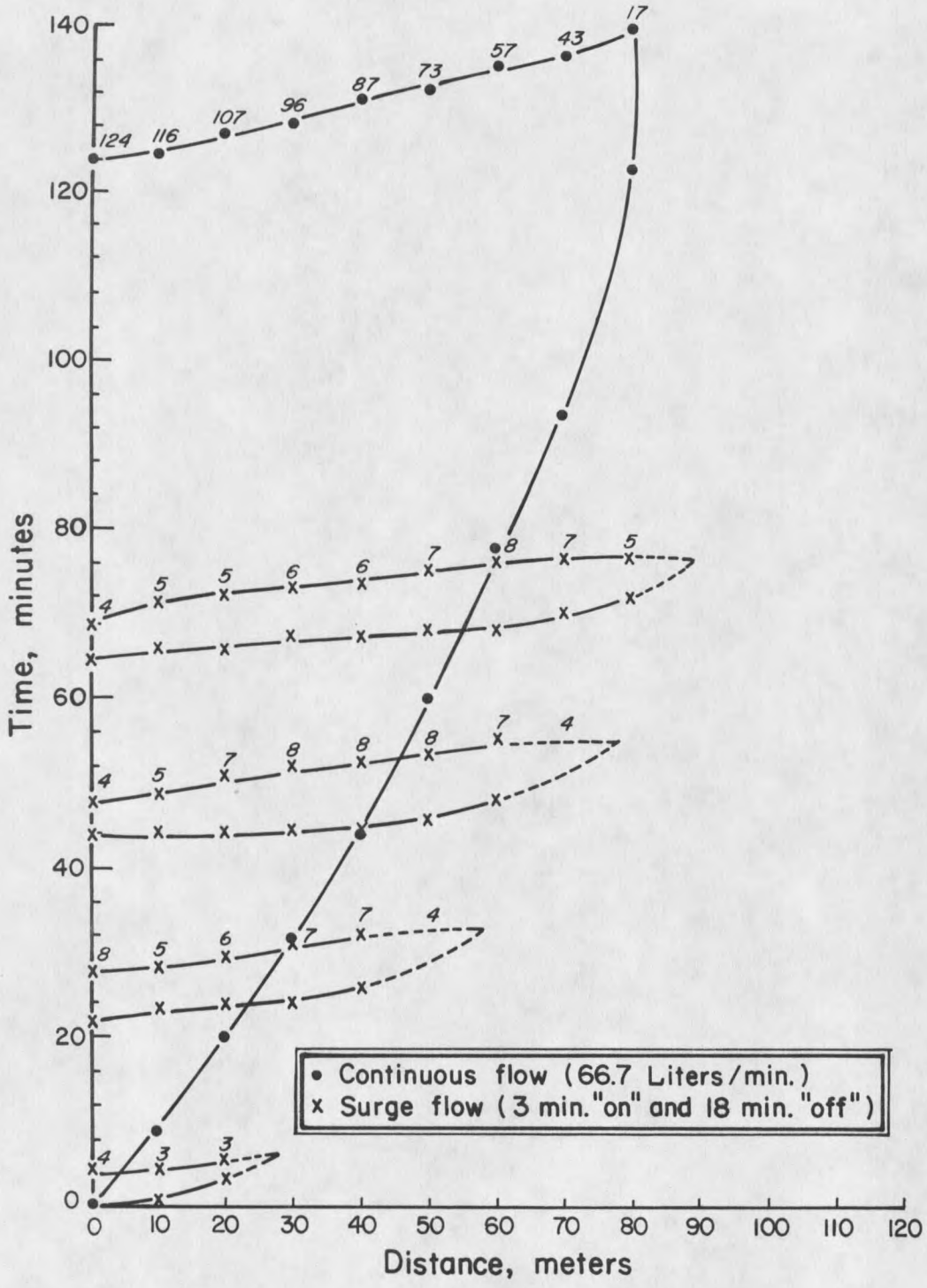


Figure 24. Advance-recession curves for surge flow and continuous flow for field test No. 1.

The "adjusted" line (Fig. 23) was drawn parallel to the "typical" line through this depth of 46 mm at 78 min, the time of which the typical line has an average depth of 53 mm.

As a check, and since the values would be used later, the adjusted depths at each station, the average depths between stations, and the average depth for the whole length were computed again using the adjusted curve (Table 10), and found to be 46 mm. This adequately checks the 46 mm computed depth of inflow and indicates that the adjusted curve on Fig. 23 is reasonably correct.

The adjusted depths of infiltration along the strip are plotted on Fig. 25.

Table 10. Depth infiltrated based on opportunity times from Fig. 24 for continuous flow treatment and depths infiltrated taken from the "typical" line in Fig. 23.

Items	Station-meters x 10								
	0	1	2	3	4	5	6	7	8
T_o	124	116	107	96	87	73	57	43	17
	Typical Intake Curve Data								
Depth-mm	70	68	64	60	57	51	44	37	21
Av. Depth		69	66	62	59	54	48	41	29
Av. Depth	on 80 meters = 428 / 8 = 53 mm								
	Adjusted Intake Curve Data								
Depth-mm	62	60	56	52	50	45	38	32	19
Av. Depth		61	58	54	51	47	41	35	25
Adj. Depth	on 80 meters = 372 / 8 = 46 mm								

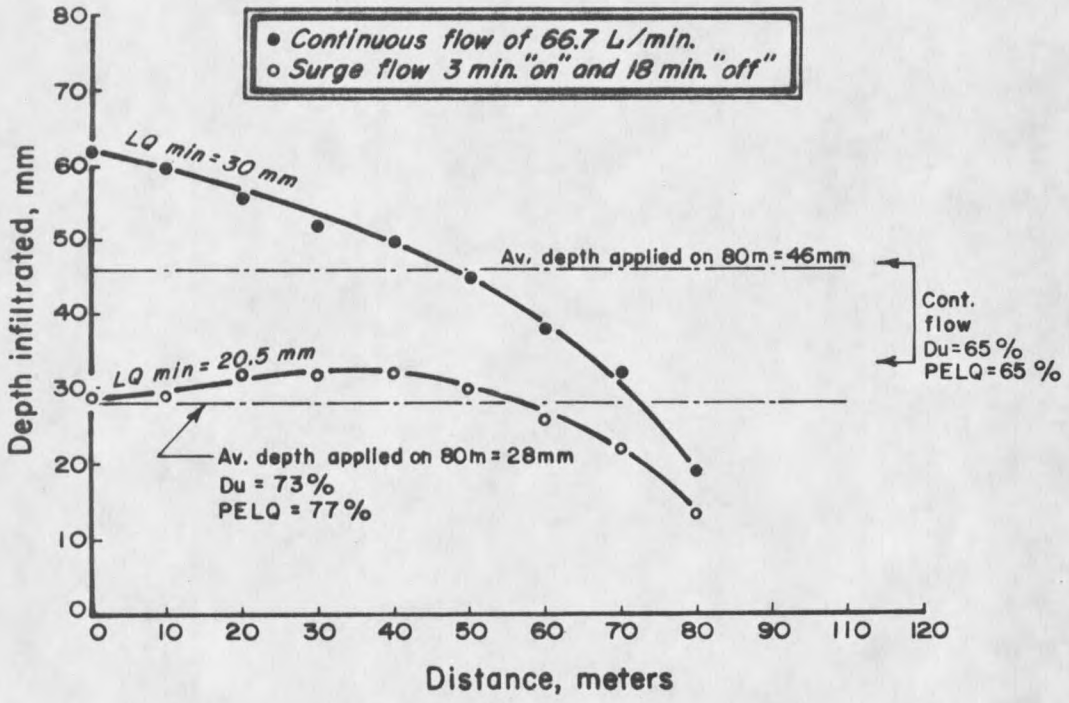


Figure 25. Adjusted depth infiltrated along the irrigated border-strip.

Surge flow involves a cycled application of water such that a complete irrigation may consist of 2-4 individual pulses. Figure 24 illustrates the typical behavior of a surged border system as compared to continuous irrigation by tracing the advance and recession trajectories of individual surges.

In order to compare the water distribution in surge flow with continuous flow a conservative method of analysis was followed to calculate the infiltrated depth based only on the opportunity time. This procedure neglected any effect of surface seal on the infiltration function due to the intermittent irrigation.

Adjusted cumulative intake is developed as shown in Fig. 24 at each station on the total strip (actual and extrapolated portions). This was done by adding the opportunity time, T_o from each surge, which was noted by measuring the time interval between the advance and recession curves. The corresponding depth infiltrated, D, was then taken from the typical cumulative intake curve in Fig. 23 and tabulated in Table 11 for the same stations.

Table 11. Depth infiltrated based on opportunity times, T_o from Fig. 24 for surge flow treatment and depths infiltrated, D, taken from the "typical" line in Fig. 23.

Item	Station-meters x 10									
	0	1	2	3	4	5	6	7	8	9
T_o-min	18	18	21	21	21	19	15	11	5	3
	Typical Intake Curve Data									
Depth-mm	22	22	24	24	24	23	20	17	10	7.5
Av.Depth		22	23	24	24	24	22	19	14	8/2
Av.Depth	on 85 meters = 176/8.5 = 21 mm									
	Adjusted Intake Curve Data									
Depth-mm	29	29	32	32	32	30	26	22	13	10
Av.Depth		29	31	32	32	31	28	24	17	12/2
Av.Depth	on 85 meters = 230/8.5 = 27 mm									

The average depth for each 10 m, D/10 m, was determined and entered as shown in Table 11. Since the end section of the strip was only 5 m long instead of the usual 10 m unit length, its average was determined proportionally to its length (5:10). Thus, the average depth infiltrated for the entire distance (extrapolated) was found to be approximately 21 mm as indicated.

To check the correctness of the location at which the "typical" curve was drawn, the actual average depth of water applied was computed. The border spacing is 5 m and the strip width is 3 m, but the effective wetted width was measured experimentally to be 2.43 m for the wetted strip length of 85 m. Therefore, the depth applied for four surges each 3 min on and 18 min off, i.e., 21 min cycle, is:

$$D = \frac{66.7 \text{ L/min} \times 21 \text{ min (cycle time)} \times 4 \text{ surges}}{2.43 \text{ m} \times 85 \text{ m}} = 27 \text{ mm}$$

The "adjusted" line (Fig. 23) was drawn parallel to the "typical" line through this depth of 27 mm at 16 minutes, the time at which the typical line has an average depth of 21 mm.

The adjusted depths at each station, the average depths between stations, and the average depth for the whole length (extrapolated) were computed again as a check using the "adjusted" curve (Table 11), and was found to be 27 mm. This adequately checks the 27 mm computed depth of inflow and indicates that the "adjusted" curve in Fig. 23 is reasonably correct.

The "adjusted" depths of infiltration along the strip are plotted with the continuous flow in Fig. 25.

The same procedure was followed for each test and the results are shown in Appendix D, Tables 16, 17, 18, 19, 20, 21, 22, 23, 24, 25, 26, and 27. The advance and recession curves were also drawn and shown in Figs. 26, 27, 28, 29, 30, and 31.

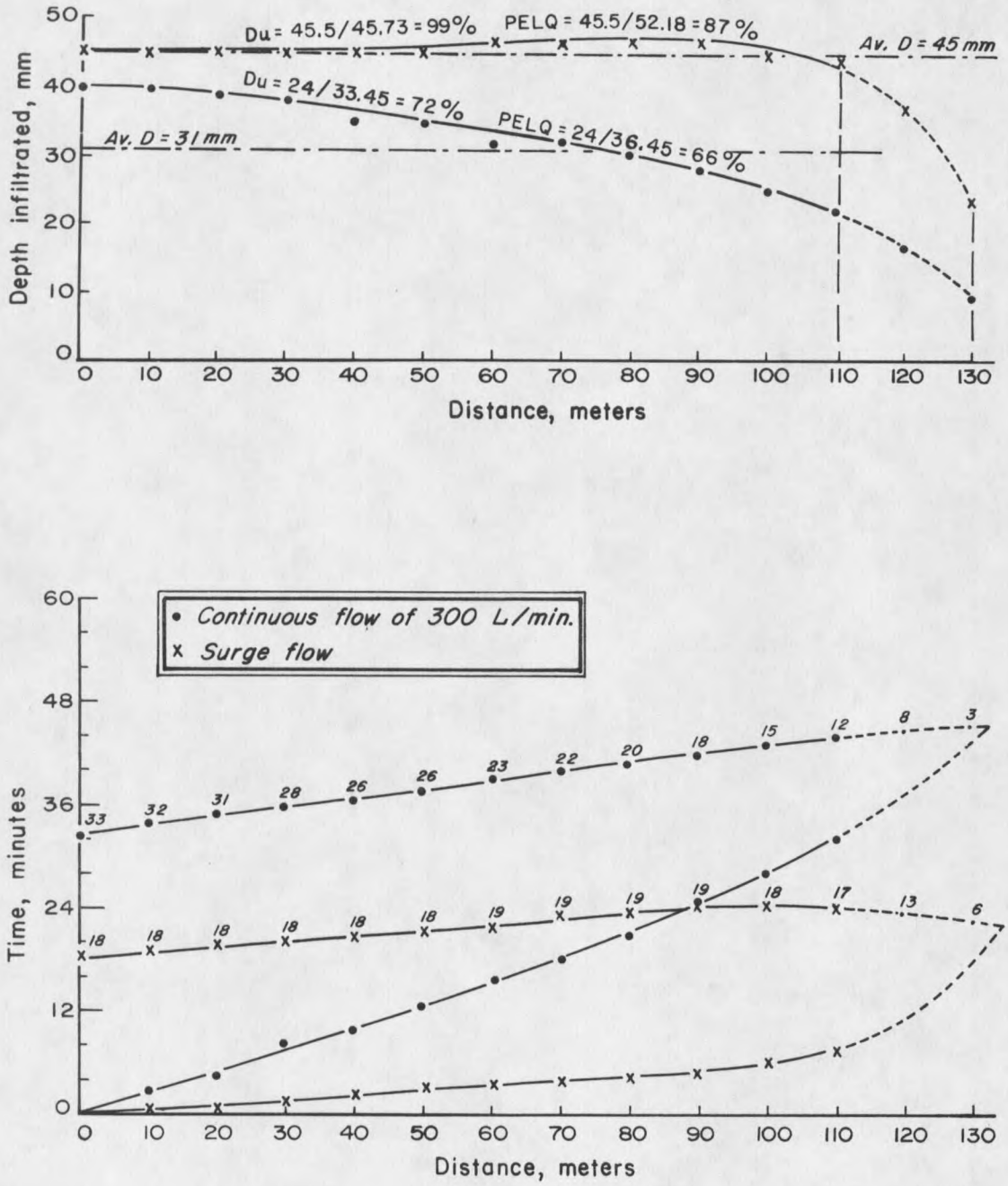


Figure 26. A pilot field test for one surge using a 30 cm gate compared to continuous flow.

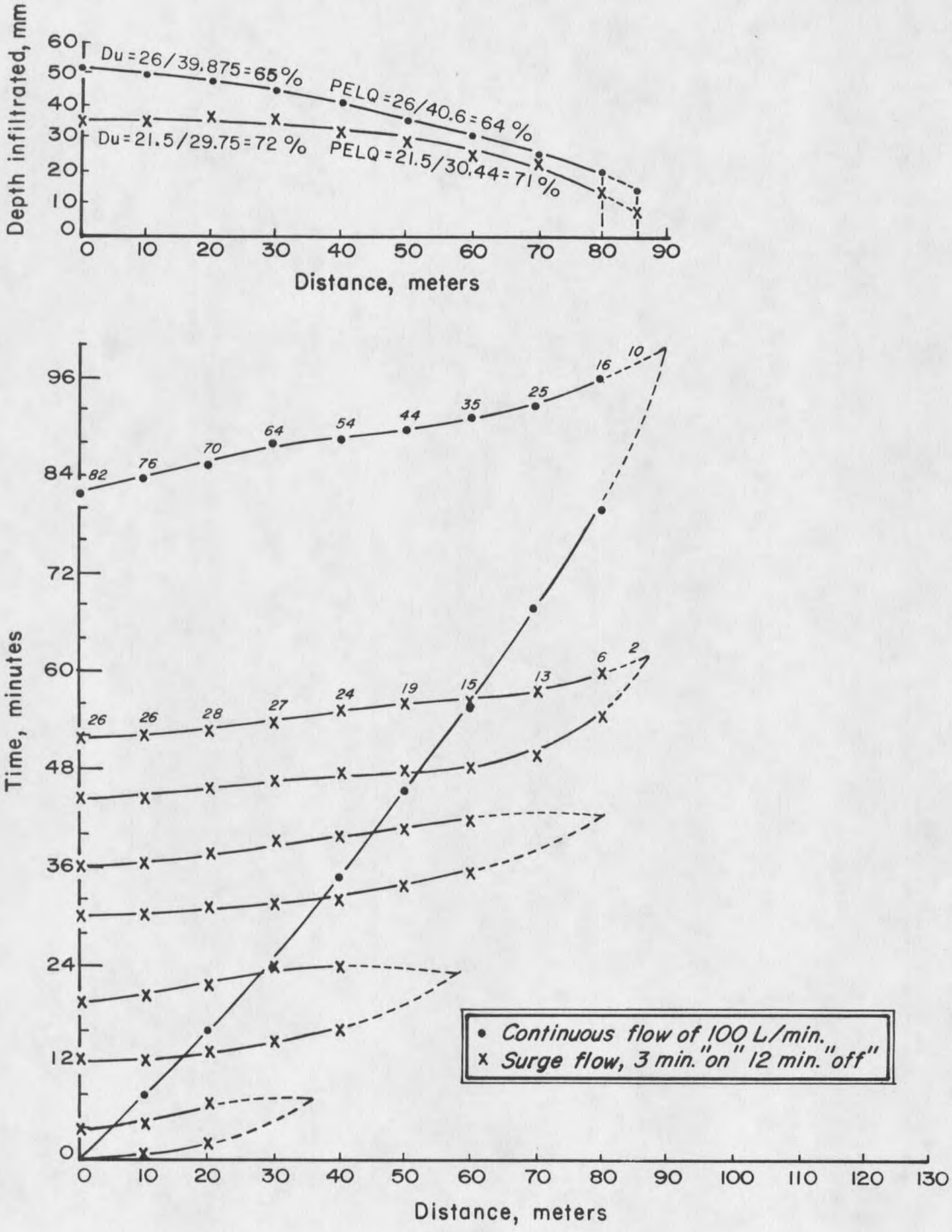


Figure 27. Advance-recession curves for surge flow and continuous flow for field test No. 2.

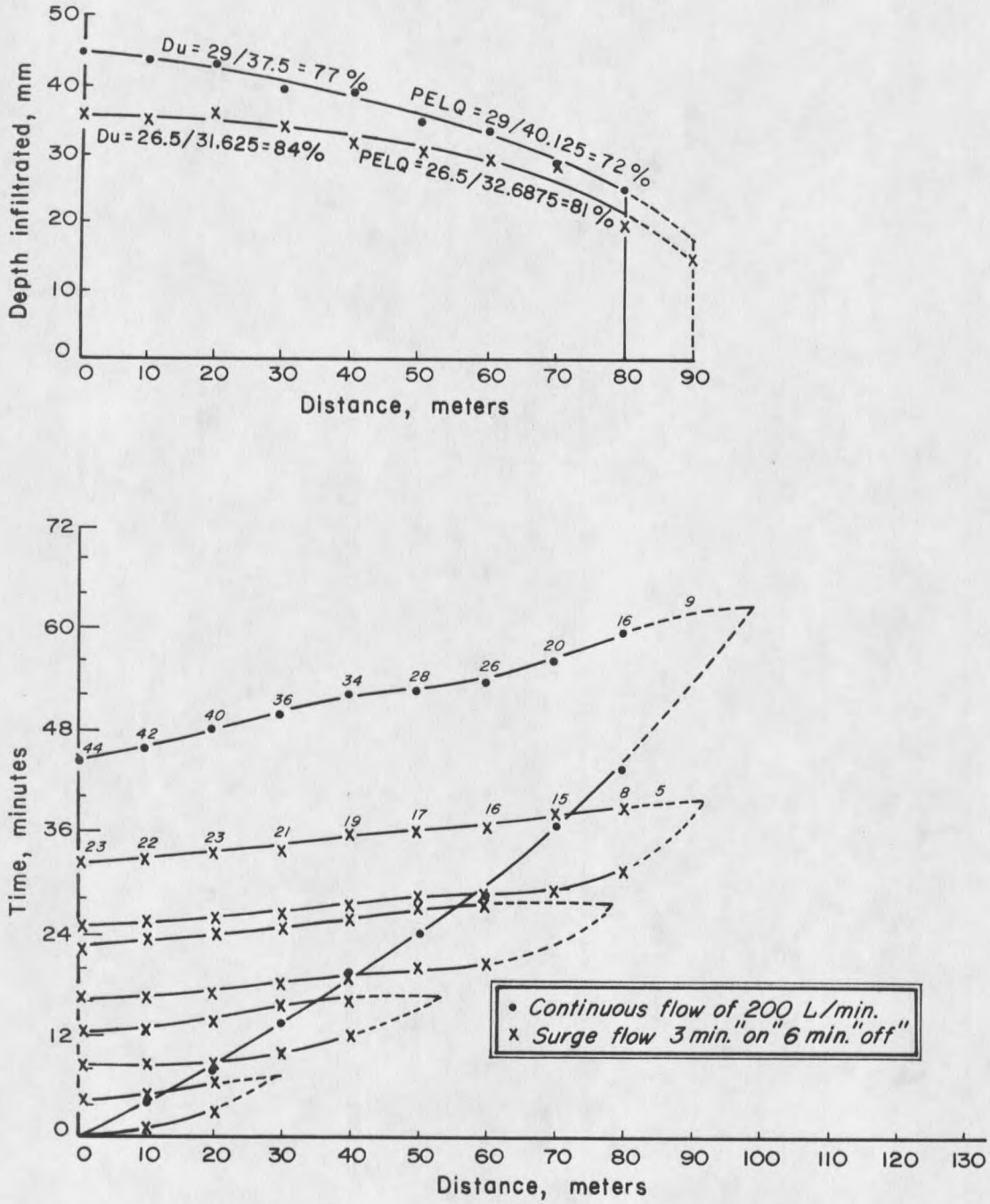


Figure 28. Advance-recession curves for surge flow and continuous flow for field test No. 3.

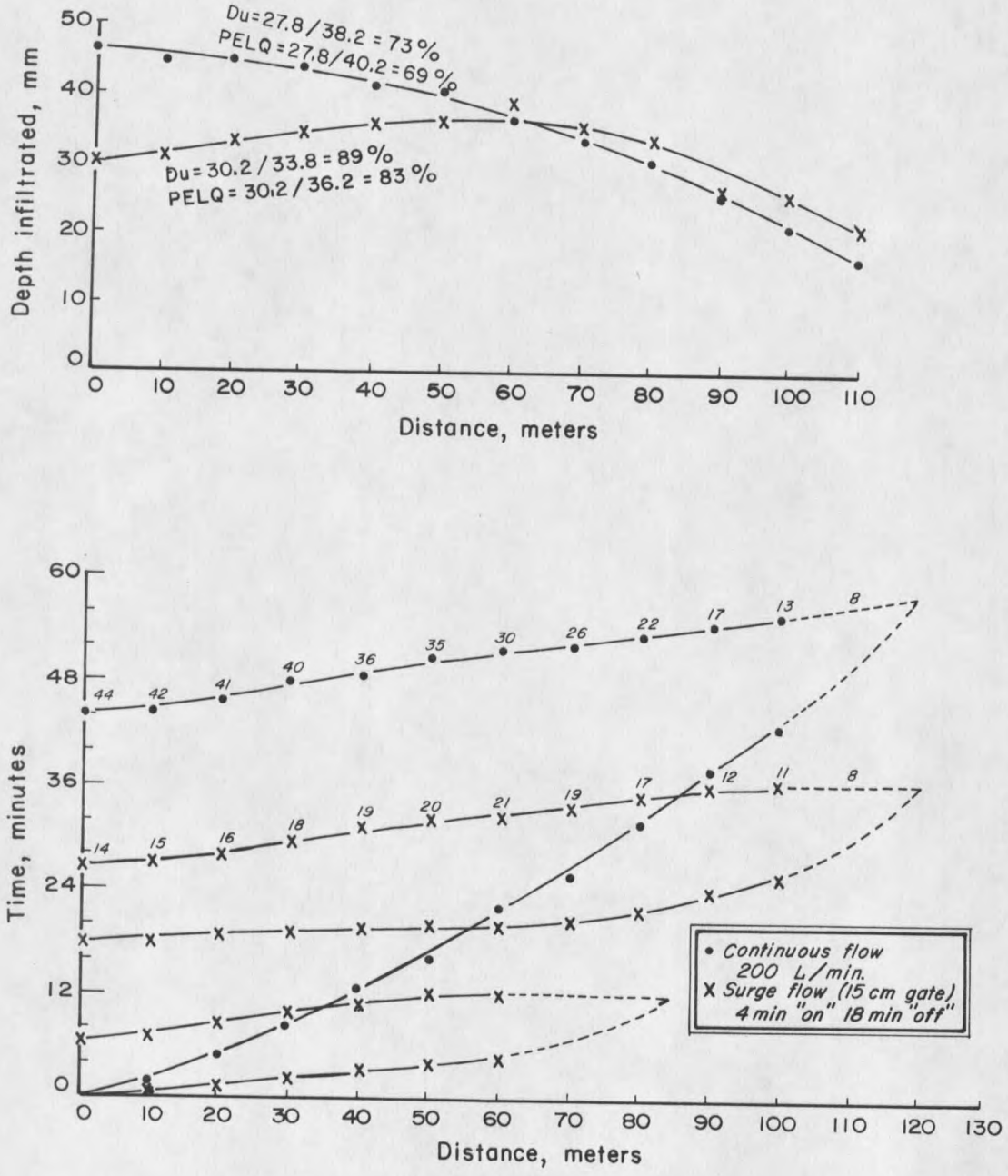


Figure 29. Advance-recession curves for surge flow using a 15 cm gate and continuous flow for field test No. 4.

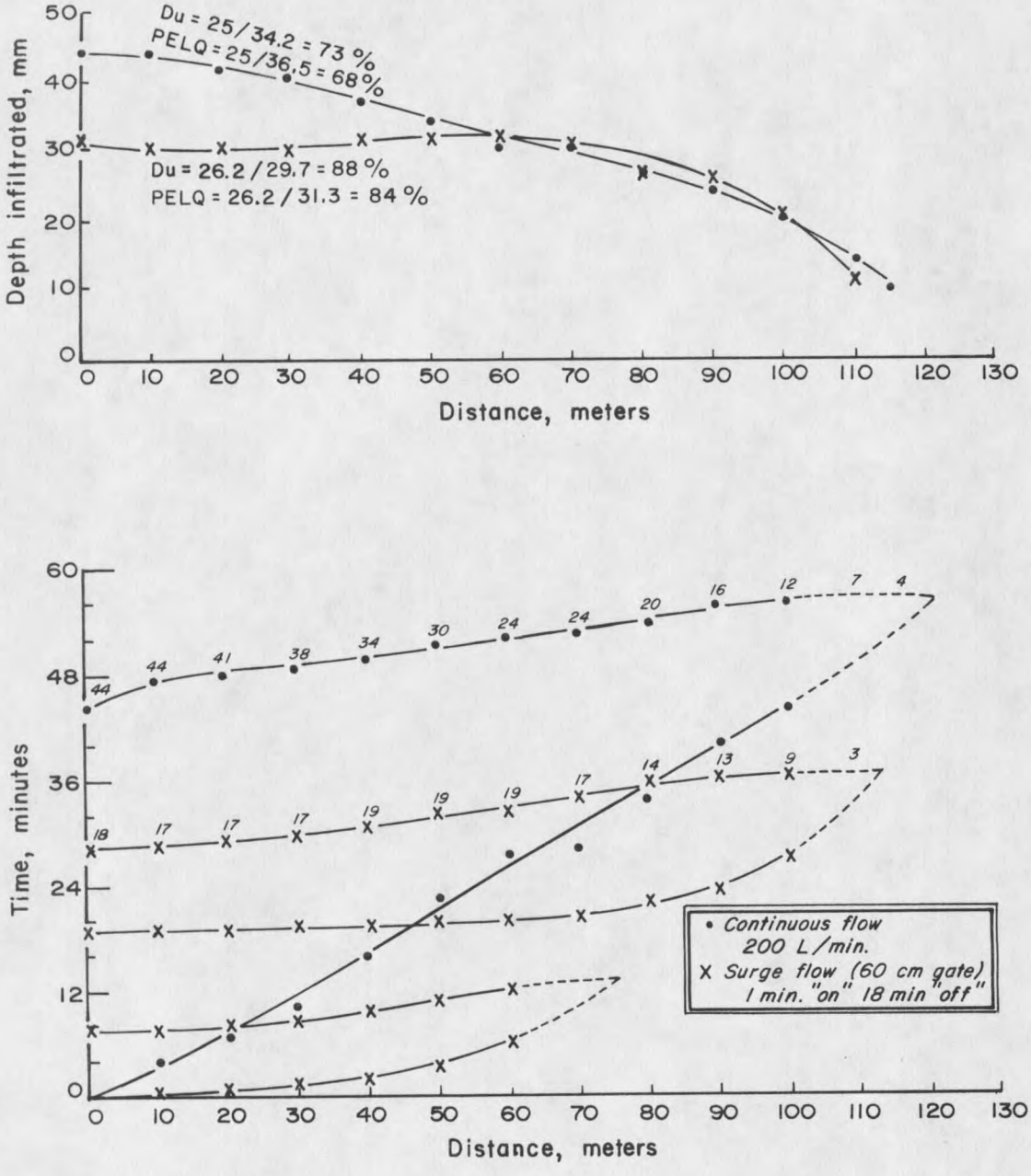


Figure 30. Advance-recession curves for surge flow using a 60 cm gate and continuous flow for field test No. 5.

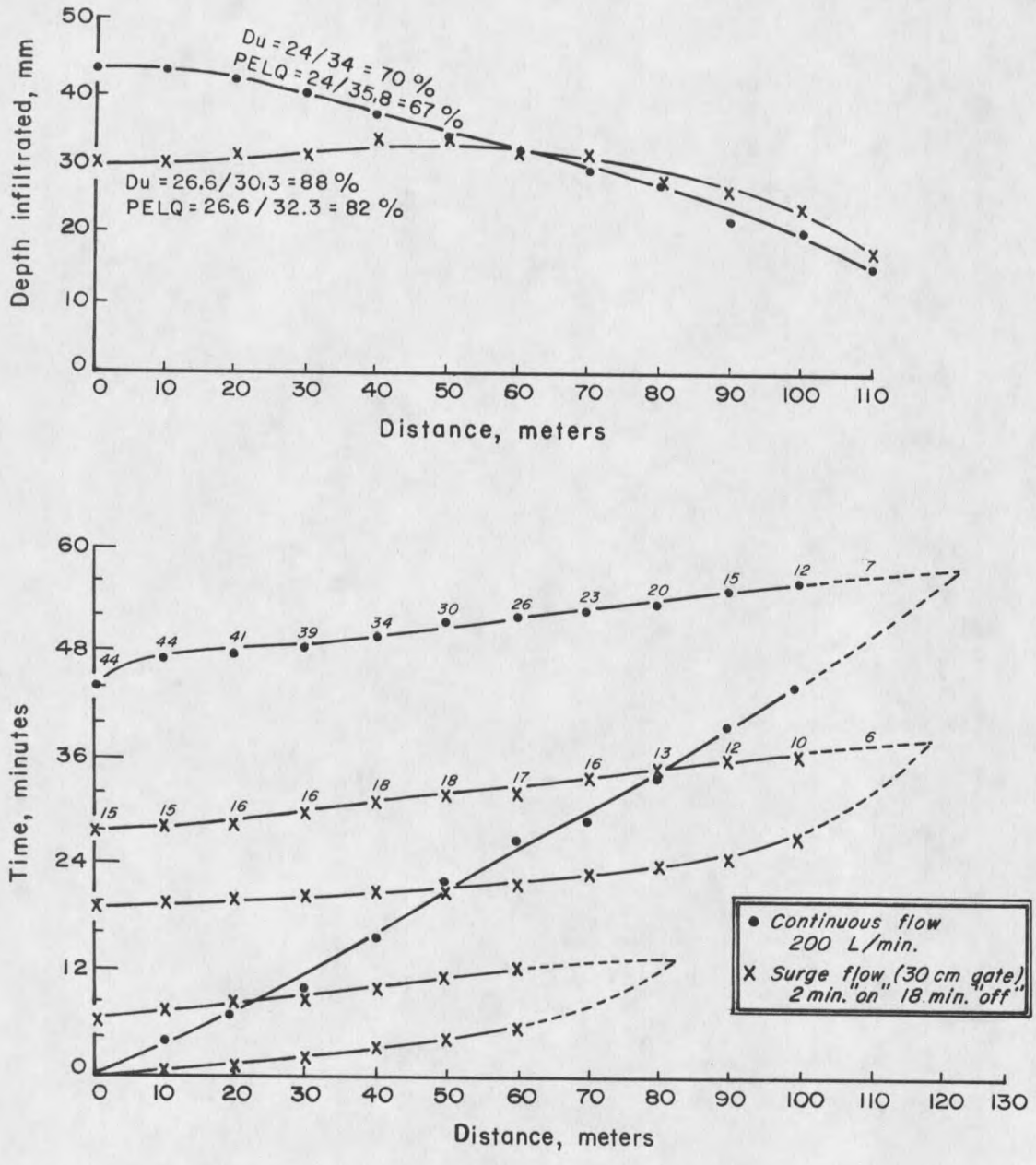


Figure 31. Advance-recession curves for surge flow using a 30 cm gate and continuous flow for field test No. 6.

Performance Parameters

The yield versus water relationship for any crop is a complicated, time-dependent function of the quantity of water made available to the plant. If the irrigation system provides a uniform distribution of water, then each plant in a field should receive an identical amount of water. For this reason, not only the average application, but also the spatial distribution of that application, is important.

In order to interpret measurements and make comparisons between systems a common basis is necessary. This basis is provided by the performance parameters distribution uniformity (DU) and potential application efficiency (PELQ). Both of the efficiencies involve a low quarter (LQ) concept developed by the USDA, Soil Conservation Service, and recommended as the standard for comparing alternative conditions.

Distribution Uniformity

The DU is the average depth infiltrated over the low quarter of the area divided by the average depth infiltrated over the actual strip length. The DU describes how uniformly the water was distributed along the strip for the condition tested. A high percentage would indicate that the advance and recession curves are parallel but would not tell whether the irrigation was adequate. For this percentage, which concerns only the infiltrated water, runoff is not pertinent. The average infiltration for the 80 m was found to be 46 mm from the computations as tabulated in Table 10 or graphically from Fig. 25, for continuous flow irrigation.

Minimum depth can be defined as the average depth over the quarter of the area receiving the least infiltration. For continuous irrigation the average depth was 30 mm over the 20 m length of strip. This is shown graphically on Fig. 25. The DU can be calculated as follows:

$$DU = (30/46) \times 100 = 65\%$$

In case of surge flow the average infiltration for the 80 m distance was found to be 28 mm (224 mm/8 stations) from the computations as tabulated in Table 11 or graphically from Fig. 25. The average depth of the lowest one-quarter (20.5 mm) for the least 20 m in this test is shown graphically on Fig. 25. The DU can be calculated as follows:

$$DU = (20.5/28) \times 100 = 73\ \%$$

The preceding procedure was followed to calculate the distribution uniformity for each test and the results are shown in Figs. 25, 26, 27, 28, 29, 30, and 31.

Potential Application Efficiency

The soil moisture deficit (SMD) is expressed numerically as a depth of water indicating the dryness of the root zone at the time of measurement. This depth is identical to the depth of water to be replaced in the root zone by irrigation under normal management.

The SMD was checked by taking soil samples to a depth of 60 cm. The average SMD was found to be 11.5 cm. Since satisfying the SMD for a certain crop was not the objective of this study, the potential

application efficiency was considered instead of the application efficiency.

The potential application efficiency (PELQ) indicates a measure of system performance attainable under reasonably good management when the desired irrigation is being applied. It is the ratio of the minimum low quarter depth infiltrated when it just equals the management allowed deficit (MAD) or SMD to the average depth applied. For the continuous irrigation Fig. 25 shows that the LQ minimum was 30 mm for the least 20 m, the average depth on the 80 m long field, including the portion that was runoff (in this case there is none)

$$D = 372/8 = 46 \text{ mm}$$

so if MAD equaled the depth over the LQ

$$PELQ = (30/46) \times 100 = 65\%$$

For surge flow the LQ was 20.5 mm, calculated from Fig. 25. From Table 11 the average depth on the 80 m run, including the portion that was runoff, is 28.75 mm (230 mm/8 stations), so if MAD equaled the minimum LQ

$$PELQ = (20.5/28.75) \times 100 = 71\%$$

The PELQ was calculated for each test and appears on the adjusted infiltrated depth along the border in Figs. 25, 26, 27, 28, 29, 30, and 31.

Surge flow irrigation has a PELQ higher than continuous irrigation under the same inflow, which indicates that surge flow uses either less water to achieve the same efficiency or uses the same amount of water at a higher efficiency. The higher efficiency of surge flow can be attributed to the rapid advance of the water front. In addition, the DU and PELQ were calculated neglecting any effect of intermittent irrigation on infiltration. If the effect of intermittent infiltration were considered, the DU and PELQ for surge flow should be increased drastically.

Advance Rate

The advance rate is one of the most important parameters in the success of surface irrigation. When the advance time is short the water distribution efficiency is high. It can be seen from Figs. 24, 25, 26, 27, 28, 29, 30, and 31 that the surge flow treatment cuts the advance time drastically. In this study the reasons for achieving this rapid advance can be attributed to the following:

1. The accumulation of a small inflow to produce a large outflow. The direct effect of this accumulation is to increase the advance rate. The effect of stream size is shown in Fig. 32.
2. The surface seal due to intermittent wetting. The surface aggregates which collapse and slake down during wetting may form a slick layer of dispersed mud, which clogs the surface macropores (the interaggregate cavities which serve as the

principal avenues for the infiltration of water) and thus tend to inhibit the infiltration of water into the soil. Such a layer is often called a surface seal. The first surge advances over dry soil. The next surge advances first over a wet soil (wet advance), then over a dry soil (dry advance). The infiltration during the wet advance is cut drastically by the effect of surface seal. It was found in this study that as a result of intermittent wetting advance distance for the second surge was about 60% more than the first surge (Figs. 24, 26, 27, 28, 29, 30, and 31).

3. The surface hydraulic roughness of the wet advance is less than the surface hydraulic roughness of the dry advance. Therefore the second surge ran faster over the smooth wet surface. It appears that the infiltration and hydraulic roughness interact to give this rapid advance of the next surge.

The quantitative reduction in infiltration rate and hydraulic roughness due to intermittent application are not known. To describe how the hydraulic roughness and the infiltration interact with the other variables to increase the rate of advance, a simple equation can be developed and then validated.

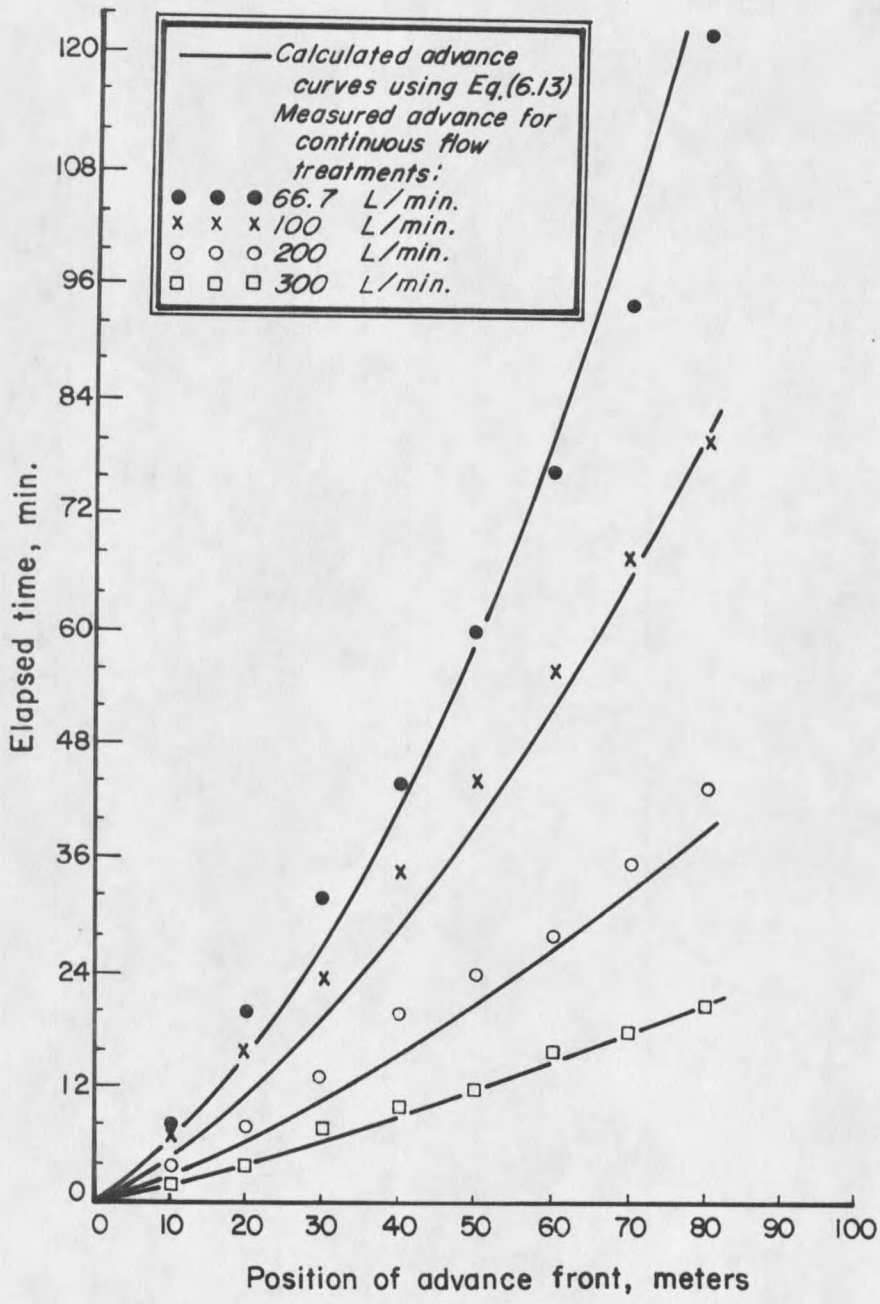


Figure 32. Comparison of the calculated position of the water front to the observed position for the continuous flow irrigation using different stream size.

Equations representing the flow are more useful if they pertain to a border strip of unit width. On a unit width border strip, the volume of water run onto the strip is equal to 60 $Q_u T_a$ cubic meter. The volume run onto the strip is equal to the volume of intake ($F_a L_t$) plus the volume of water in temporary surface storage ($y_a L_t$). From this relationship a rate of advance equation can be developed.

$$60\ Q_u\ T_a = F_a\ L_t + y_a\ L_t \tag{6.7}$$

where:

Q_u = Irrigation stream per meter of strip width (cubic meter per second)

T_a = Time of application (minutes)

F_a = Average depth of intake (meter)

L_t = Length of advance (meter)

y_a = Average depth of flow (meter)

$$L_t = \frac{60\ Q_u\ T_t}{F_a + y_a} \tag{6.8}$$

Equation (6.8) is valid when the time of application (T_a) equals or exceeds the advance time (T_t). If the water is turned off before the advancing front has reached the end of the border strip, the actual rate of advance may be slightly slower than indicated. In this case T_a has to be substituted for T_t, otherwise the following conditions must be used:

If $T_a > T_t$ Eq. (6.8) is valid

If $T_a < T_t$ substitute $T_a = T_t$ in Eq. (6.8)

The average depth of intake (F_a) can be calculated easily for a linear advance function. Similarly, the average depth of flow (d_a), or the average depth of surface storage, can be calculated most readily for a condition of flow over an impervious surface. The rate of advance is curvilinear rather than linear. Therefore, the average depth of intake is underestimated. On the other hand, the average depth of surface storage is correspondingly overestimated. The indicated surface storage depth is greater than the actual surface storage depth because part of the water infiltrates into the soil during advance. Since the two terms are combined, the errors involved are compensating and, therefore, have little effect on the overall results.

The general equation for accumulated intake of water into the soil was developed experimentally (Eq.(6.6)). Therefore, when the advance is assumed to vary linearly with time, the average depth of water that infiltrates the soil in the time (T_t) required for the advancing front to reach a point L_t from the head of the border strip can be obtained by integrating Eq. (6.1) between the limits of T_t and zero and then dividing by T_t. Thus,

$$\int_0^{T_t} F\, dt = \int_0^{T_t} (a\, t^b + c)\, dt$$

$$(F_a\, t)_0^{T_t} = \left(a \frac{T^{b+1}}{b+1} + c\, t\right)_0^{T_t}$$

$$F_a\, T_t = \frac{a\, T_t^{b+1}}{b+1} + c\, T_t$$

$$F_a = \frac{a}{b+1} T^b_t + c \qquad (6.9)$$

Another method of determining the average depth of intake (F_a) is to consider that the intake relationship with time is parabolic. Therefore, the average intake can be calculated as follows:

$$F_a \quad T_t = \frac{2}{3} \quad F_{max} \quad T_t$$

$$F_a \quad T_t = \frac{2}{3} \quad (a \; T_t^b + c) \; T_t$$

$$F_a = 0.67 \; (a \; T_t^b + c) \qquad (6.10)$$

The maximum and average depth of water on an impervious border strip at any time during the advance period can be computed on a quasirational basis using the Manning equation:

$$Q = \frac{1}{n} A \; R^{2/3} \; S_o^{1/2}$$

where

A = Cross sectional area of flow (square meter).

n = Roughness coefficient in Manning's equation.

Q = Irrigation stream for a border strip (cubic meter per second).

R = Hydraulic radius.

S_o = Slope of border strip or irrigation slope (meter per meter).

For a wide rectangular channel R = y, and considering a unit-width strip, A = y.

$$y_n = \frac{Q_u^{.6} \; n^{.6}}{S_o^{.3}} \tag{6.11}$$

The normal depth (y_n) is the maximum depth that occurs at the head of the border strip for a given flow, irrigation slope, and given hydraulic roughness (n). Assuming that the advance wave over the surface has an elliptical shape, the average depth of surface storage can be obtained as follows:

$$y_a \cdot L = (\pi/4) \; y_n \cdot L$$

$$y_a = 0.785 \; y_n \tag{6.12}$$

If T_t is considered to be equal to T_a and Eqs. (6.9) and (6.12) are combined with Eq. (6.8), the length of advance (L_t) can be related to the time of advance (T_t) for a given soil having intake parameters (a), (b), and (c); a given stream size (Q_u); and a given roughness coefficient (n) as follows:

$$L_t = \frac{60 \; Q_u \; T_t}{\frac{1}{1000} \left[\frac{a}{1+b} T_t^b + c\right] + 0.785 \frac{Q_u^{.6} \; n^{.6}}{s_o^{.3}}} \tag{6.13}$$

Formula Validation

The best way to validate the formula (Eq. (6.13)) before using it, is to compare the results of using Eq. (6.13) with the result of a well known formula which has already been validated and verified. An accepted formula was derived by Philip and Ferrel (1964) using as a basis a formula originally proposed by Lewis and Milne (1934).

The following field conditions were given by Michael (1978) in a field test of a border strip irrigation in a wheat field, the following observations were made:

$$Q_u = 1600 \text{ cm}^3/\text{min/cm},$$

$$y_a = 8 \text{ cm}.$$

$$F = 0.84\ t^{.55} + 0.63$$

Michael determined the distance advanced by the water front 54 min after the start of irrigation to be 65.34 m, using Eq. (2.13).

Using the same data in predicting the water front advance by Eq. (6.13);

$$L = \frac{1600 \times 54}{[.84/(1 + .55)](54)^{.55} + .63 + 8} = 6404 \text{ cm}$$

Percentage error = [(65.34 - 64.04)/65.34] x 100 = 2%

If the subsurface shape factor equals 0.67 which corresponds to the parabolic shape as developed in Eq.(6.10), the following answer can be obtained

$$L = \frac{1600 \times 54}{.67[\ .84\ (54)^{.55} + .63] + 8} = 6414 \text{ cm}$$

Percentage error = [(65.34-64.14)/65.34] x 100 = 1.8%

Another field test was outlined by Michael (1978).

The field test was in a border strip at a pre-sowing irrigation on a sandy loam soil

$$Q_u = 2880 \text{ cm}^3/\text{min/cm}$$

$$y_a = 2.345 \text{ cm}$$

$$F = 2.7\ t^{.49} + 0.142$$

Michael determined the distance advanced by the water front 26 min after the start of irrigation to be 66.17 m using Eq. (2.14).

Using the same data in predicting the water front advance by Eq. (6.13)

$$L = \frac{2880 \times 26}{[2.7/(1 + .49)](26)^{.49} + .142 + 2.345} = 6550.8 \text{ cm}$$

$$\text{Percentage error} = [(66.17 - 65.51)/66.17] \times 100 = 1\%$$

Using 0.67 as a shape factor

$$L = \frac{2880 \times 26}{.67[\ 2.7\ (26)^{.49} + .142] + 2.345} = 6586.57 \text{ cm}$$

$$\text{Percentage error} = [(66.17 - 65.865)/66.17] \times 100 = .5\%$$

It can be seen that the parabolic shape factor gives less deviation than the more sophisticated formula. Using the linear integration of the intake depth to obtain the average depth (Eq.(6.10)) gives a close approximation of the answer obtained using the parabolic shape factor. It can also be noticed that the average water depth was given by field measurements, and was not calculated by Michael (1978). Difficulties which are normally encountered in estimating the Manning (n), and the shape factor for surface storage were excluded.

The results of using the formula in predicting the advance curves in continuous irrigation are shown in Fig. 32 with the observed data obtained from using four different stream sizes. The Manning (n) was estimated to be 0.1 for the field which was not planted, but weedy. The formula cannot be used for surge irrigation except for the first surge, because the equation for predicting the infiltration under surge flow is not available.

In the first set of experiments the effect of varying the "off time" was tested. The gate size, basin size, and "on time" were held constant. To obtain a variable "off time" the inflow to the basin was changed.

Figure 33 shows the effect of "off time" on the advance rate. For the first surge there is no effect, but for the next surge the effect becomes clear. For example the 6 min-off shows the fastest advance, the 12 min-off is the next fastest, and the 18 min-off the slowest. This result may be explained as follows. In the first surge there was no difference between the treatments. After that the difference due to the off time starts to be pronounced. In the 6 min-off cycle air was still entrapped in the soil and the surface seal was more pronounced than with the longer "off time."

In the second set of experiments the effect of varying the "on-time" was tested by varying the gate size and keeping the basin size, inflow rate, and "off-time" constant, the effect of varying "on-time" on the first and second surge are shown in Fig. 34 and Fig. 35, respectively.

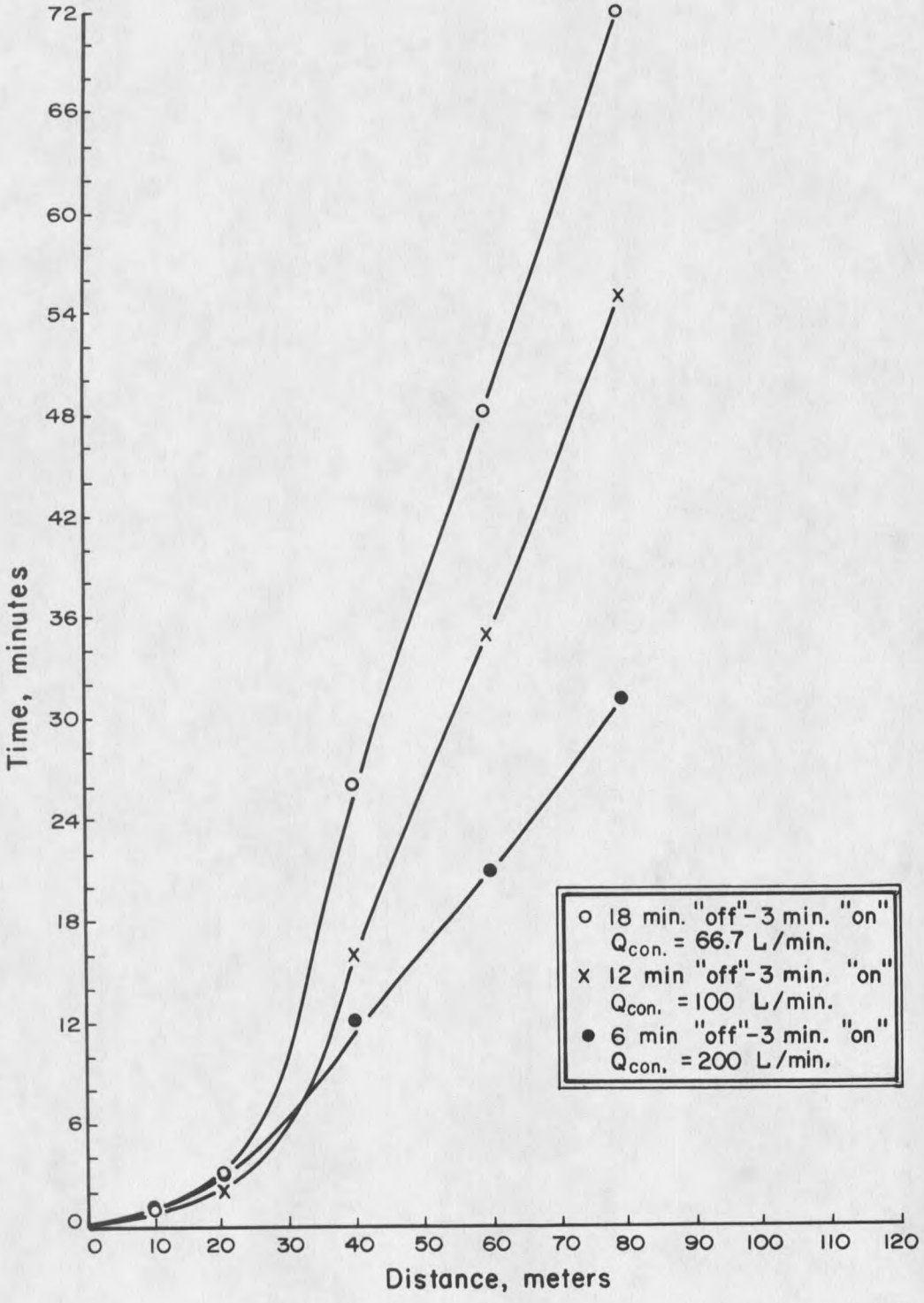


Figure 33. The effect of off-time on the advance rate.

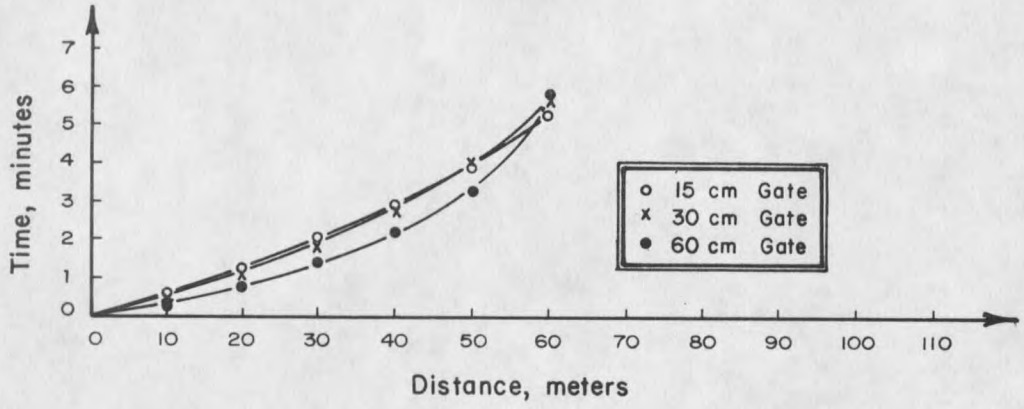


Figure 34. The effect of gate size on the advance rate of the first surge.

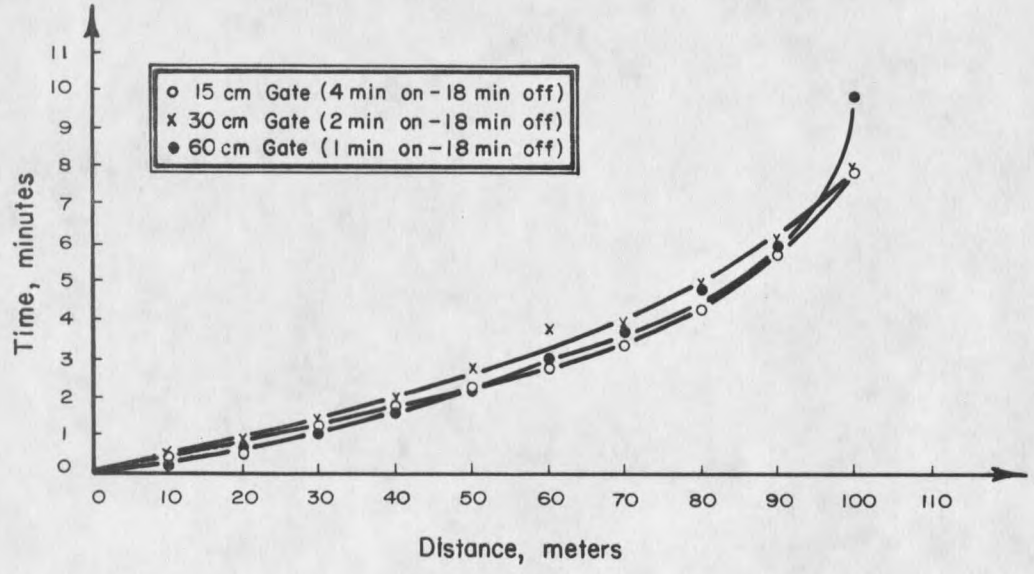


Figure 35. The effect of gate size on the advance rate of the second surge.

It can be seen that using the 60 cm gate produced the fastest advance in the first surge. This was caused by a large flow rate initially released by the large gate (Fig. 34). After 50 m of advance (Fig. 35) the 15 cm gate shows the fastest advance. Equation (6.8) may introduce a logical explanation for this phenomenon by noting that the numerator is a volume equal to the instantaneous inflow multiplied by the cycle time. The instantaneous inflow to the basin was constant in all cases, but the "on-time" was 1, 2, and 4 min for the 60, 30, and 15 cm gate size, respectively. The "off-time" was 18 min for all treatments. Consequently, the cycle time was 19, 20, and 22 min for the 60, 30, and 15 cm gate size. Therefore, the released volume per cycle for the 15 cm gate size was large enough to catch up after 50 m of advance distance due to the higher surge volume.

CHAPTER 7

SUMMARY AND CONCLUSIONS

Surge flow irrigation requires turning the water on and off during the irrigation. To accomplish surge flow a small continuous inflow can be accumulated in a head ditch or a reservoir, then released. Two ways to apply this concept to border irrigation were investigated, a dosing siphon and an automatic drop gate. The dosing siphon constructed of 15 cm PVC pipe worked successfully. The dosing siphon required a minimum head of about 25 cm. The discharge equation was experimentally determined ($Q = 1918.52\ A_p\ H^{.66}$ L/s). The discharge equation fit the experimental data with 6.9% probable error. With the 15 cm dosing siphon and 60 cm available maximum head the average discharge is 22 L/s (340 gpm). This discharge would irrigate a border strip approximately 10x100 m which is practical in some situations. Large dosing siphons were not tested because of material and construction restraints.

The need for an automatic device that functions under any head available and which could be made in virtually any size led to the development of the automatic drop gate. The gate opens automatically when the water level on the upstream side of the gate rises to a predetermined level and remains open during the discharge phase until the water surface drops to a lower predetermined level. The gate then returns automatically to its normally closed position by action of a counter balance weight. The discharge equation was determined

experimentally ($Q = 1632.28\ L\ H^{1.4}$ L/s). The discharge equation fit the experimental data with 9.8% probable error. Considering an average size gate of 60 cm width with 30 cm available head, the average discharge is 102 L/s (1631 gpm). This discharge would irrigate a border strip about 25x200 m which is practical in many situations.

The design of the gate was based on having the closing head equal 0.2 of the opening head (H). In order for the gate to close as intended, the inflow rate must be less than the outflow corresponding to the head of 0.2 H over the gate ($Q < 1632.28\ L\ (0.2H)^{1.4}$).

A mathematical model based on the differential storage equation was developed to simulate the emptying and refilling time of the reservoir or head ditch where flows are accumulated and to give the required frequency ratio for surge flow irrigation. The trapezoidal rule was used to obtain a general solution for the storage outflow function. The model was verified by comparing it to a special analytical solution of the storage outflow function. For validation purposes the results obtained from the laboratory tests were compared to the results obtained from the mathematical model. The maximum error for determining the cycle time was found to be about 2.5%.

Field experiments were conducted to evaluate surge flow border irrigation systems using the automatic drop gate and to compare the surge flow systems with conventional continuous flow. For surge flow experiments, basins of 4.5 m by 3.0 m were constructed at the head of the border strips. The basins accumulated the inflow from the supply pipe for a period of time (off-time), then released the accumulated water (on-time) using the automatic drop gate. The drop gate was built

in three sizes 15, 30, and 60 cm. The developed mathematical model was used to calculate the cycle time required when using a specific drop gate size. The inflow to the basin was measured volumetrically. The same inflow was used for continuous and surge treatments in order to evaluate various surge flow rates and cycle times as compared to continuous flow border irrigation.

The advance and recession curves for each test were obtained. A general cumulative infiltrated depth equation was developed using cylinder infiltrometer data. In order to compare the water distribution in surge flow with continuous flow a conservative method of analysis was followed to calculate the infiltrated depth based only on opportunity time. This procedure neglected the effect of surface seal on the infiltration function due to the intermittent irrigation. In order to interpret measurements and make comparisons between systems the distribution uniformity (DU) and the potentail application efficiency (PELQ) were determined for each test. The surge flow treatments showed a higher DU which indicates that the depth of water infiltrated was more uniform than the continuous flow. Surge flow irrigation also had a higher PELQ than continuous irrigation under the same inflow, which indicates that surge flow used less water to achieve the same efficiency or used the same amount of water at a higher efficiency. The higher efficiency of surge flow can be attributed to the rapid advance of the water front. In this study the reasons for achieving this rapid advance can be attributed to the following:

1. The accumulation of a small inflow to produce a large outflow.
2. The surface seal due to the intermittent wetting.

3. The surface hydraulic roughness of the wet advance is less than the surface hydraulic roughness of the dry advance.

An equation was developed, then validated, to describe how the hydraulic roughness and the infiltration interact with the other variables in border irrigation to increase the rate of advance.

The effect of on-time and off-time on the advance rate was tested. The 6 min off-time showed an advance faster than the 18 min off-time. The 60 cm gate (19 min cycle time) produced the fastest advance during the first surge. After 50 m of advance the 15 cm gate (22 min cycle time) showed the fastest advance due to the higher surge volume.

The dosing siphon can be used by the farmer where a minimum head of about 25 cm can be maintained, a small inflow is common, and small borders are used. The drop gate can be built in any size up to about 75 cm and used by the farmer under any head available where a small inflow exists.

The concept of accumulating a small inflow to produce a large flow using the automatic drop gate showed a substantial improvement of both DU and PELQ in border irrigation under the conditions tested. This study is a first attempt to apply surge flow to border irrigation. Additional studies under varying conditions of slope, border size, soil type, inflow rate, cycle time and cycle ratio will be necessary to verify the adaptability of surge flow border irrigation in other situations.

BIBLIOGRAPHY

BIBLIOGRAPHY

Bassett, D. L. and D. W. Fatzsimmons, 1976. Simulating Overland Flow in Border Irrigation. Trans. of the ASAE 19(4):674-680.

Bishop, A. A., W. R. Walker, N. L. Allen, G. J. Poole, 1981. Furrow Advance Rates under Surge Flow Systems. J. Irrig. and Drain. Div., ASCE, 107(IR3):257-264.

Bondurant, J. A., and A. S. Humpherys, 1962. Surface Irrigation through Automatic Control. Agr. Eng. 43(1):20, 21, 35.

Calder, G. G. and L. H. Weston, 1966. Automatic System of Farm Irrigation. New Zealand J. Agr. 112(2):19, 21, 23.

Chow, Ven Te, 1959. Open Channel Hydraulics. McGraw-Hill Book Company, NY. 680 p.

Coolidge, P. S., W. R. Walker, and A. A. Bishop, 1982. Advance and Runoff-Surge Flow Furrow Irrigation. J. Irrig. and Drain. Div., ASCE, 108(IR1):35-41. March.

Davis, D.S., 1943. Empirical Equations and Nomography. McGraw Hill Book Company, NY. 200 p.

Eilliott, R. E. and W. R. Walker, 1982. Field Evaluation of Furrow Infiltration and Advance Functions. Trans. ASAE, 25(2):396-400.

Evans, R. G., 1977. Improved Semiautomatic Gates for Cut-Back Surface Irrigation Systems. Trans. of the ASAE 20(1):105-108, 112.

Garton, J. E., 1966. Designing An automatic Cut-Back Furrow Irrigation System. Oklahoma Agr. Exp. Sta. Bull. B-651. 20 p.

Green, W. H., Ampt, G. A., 1911. Studies on Soil Physics: I. Flow of Air and Water through Soils. J. Agr. Sci. 4, 1-24.

Hiase, H. R., E. G. Kruse, and N. A. Dimick, 1965. Pneumatic Valves Automation of Irrigation Systems. Agr. Res. Serv. US Dept. Agr. ARS 41-104.

Haise, H. R., E. G. Kruse, M. L. Payne and H. R. Duke, 1980. Automation of Surface Irrigation: 15 years of USDA Research and Development at Fort Collins, Colorado. U. S. Dept. of Agr., Production Research Report No. 179, 60 p.

Hall, W. A., 1956. Estimating Irrigation Border Flow. Agr. Eng. 37:263-265.

Hart, W. E., D. L. Bassett and T. Strelkoff, 1968. Surface Irrigation Hydraulics-Kinematics. Proc. ASCE, Irrig. and Drain. Div. J. 94(IR-4):419-440.

Hart, W. E. and J. Borrelli, 1970. Mechanized Surface Irrigation Systems for Rolling Lands. Univ. of Calif. Water Resour. Ctr. Contr. 133:93.

Hart, W. E. and J. Borrelli, 1972. Distribution Channels with Multiple Outlets. Proc. ASCE, J. of the Irrig. and Drain. Div. 98(IR2):267-274.

Hazen, T. E., 1974. Dosing Siphon. U. S. Pat. 3, 797, 513. March 19.

Hazen, T. E., 1975A. Dosing Siphon. U. S. Pat. 3, 874, 402. April 1.

Hazen, T. E., 1975B. Dosing Siphon. U. S. Pat. 3, 881, 506. May 6.

Henderson, F. M., 1966. Open Channel Flow. Macmillan, NY., 522 p.

Hillel, D., 1971. Soil and Water: Physical Principles and processes. Academic Press, NY.

Horton, R. E., 1940. An approach toward A physical Interpretation of Infiltration-Capacity. Soil Sci. Soc. Am. Proc. 5, 399-417.

Holtan, H. N., 1961. A concept for Infiltration Estimates in Watershed Engineering. U. S. Dept. Agr., Agr. Res. Service Publ. 41-51.

Humpherys, A. S., 1969. Mechanical Structures for Farm Irrigation. Proc. ASCE, J. of The Irrig. and Drain. Div. 95(IR4):463-479.

Humpherys, A. S., 1971. Automatic Furrow Irrigation Systems. Trans. of the ASAE 14(3):466-470.

Katopodes, N. D. and T. Strelkoff, 1977. Hydrodynamics of Border Irrigation-Complete Model. Proc. ASCE, Irrig. and Drain. Div. J., 103(IR-3):309-324.

Kostiakov, A. N., 1932. On the Dynamics of the Coefficient of Water-Percolation in Soils and on the Necessity of Studying it from A dynamic Point of View for Purposes of Amelioration. Trans. Com. Int. Soc. Soil Sci., 6th, Moscow Part A, 17-21.

Kinberlin, L., 1966. Automatic Basin Systems Reduce Irrigation Water and Labor Needs. Soil Cons. 32(2):39-40.

Levin, I., P. C. Van Rooyen and F. C. Van Rooyen, 1979. The Effect of Discharge Rate and Intermittent Water Application by Point-Source Irrigation on the Soil Moisture Distribution Pattern. J. Soil Sci. Amer., 43(1):8-16. January.

Lewis, M. R. and Milne, W. F., 1938. Analysis of Border Irrigation. Agr. Eng., Vol. 19, pp. 267-272.

Lorimor, J. C., 1973. Semiautomatic Gates for Surface Irrigation. Colo. State Univ. Exp. Sta. Progr. Rpt. PR73-77.

Markel, J. A., 1981. Managing Livestock Wastes. AVI Publishing Company Inc., Westport, Connecticut.

Merriam, J. L. and J. Keller, 1978. Farm Irrigation System Evaluation: A guide for Management. 3rd ed., Utah State Univ., Logan, 285 p.

Michael, A. M., 1968. Evaluation of Hydraulic Characteristics Influencing Border Irrigation Design. Ph. D. thesis, Dept. of Agr. Eng., Indian Institute of Technology Kharagpure. 420 p.

Michael, A. M., 1978. Irrigation Theory and Practice. Vikas Publishing House PVT LTD. 801 p.

Nicolaescu, I. and E. G. Kruse, 1971. Automatic Cutback Furrow Irrigation System Design. Proc. ASCE, J. of the Irrig. and Drain. Div. 97(IR3):343-353.

Philip, J. R., 1957. The Theory of Infiltration: 4. Sorptivity and Algebraic Infiltration Equations. Soil Sci. 84, 257-264.

Philip, J. R. and Farrel, D. A., 1964. General Solution of the Infiltration-Advance Problem in Irrigation Hydraulics. J. of Geophysical Research, Vol. 69, No. 4, pp. 621-631.

Podmore, T. H. and H. R. Duke, 1982. Field Evaluation of Surge Irrigation. ASAE Summer Paper No. 82-2102, Madison, WI, 15 p.

Podmore, T. H., H. R. Duke, and F. T. Izuno, 1983. Implementation of Surge Irrigation. ASAE Summer Meeting Paper No. 83-2018, Bozeman, MT, 19 p.

Richards, L. A., 1952. Report of the Subcommittee on Permeability and Infiltration, Committee on Terminology, Soil Sci. Soc. Am. Proc. 16, 85-88.

Smith, R. E., 1972. Border Irrigation Advance and Ephemeral Flood Waves. Proc. ASCE, Irrig. and Drain. Div. J. 98(IR-2):289-307.

Stoker, R., 1978. Simple Efficient Automatic Irrigation. Irrig. Age. 12(6):76-77.

Strelkoff, T., 1969. One Dimensional Equations of Open Channel Flow. Proc. Am. Soc. Civ. Eng., Hydr. Div. J. 95(HY-3):861-876.

Strelkoff, T., 1970. Numerical Solution of the Saint-Venant Equations. Proc. Am. Soc. Civ. Eng., Hydr. Div. J. 96(HY-1):223-252.

Strelkoff, T. and N. D. Katopodes, 1977. Border Irrigation Hydraulics With Zero Inertia. Proc. ASCE, Irrig. and Drain. Div. J. 103(IR-3):325-342.

Stringham, G. E. and J. Keller, 1979. Surge Flow for Automatic Irrigation. Proc. Irrig. and Drain. Specialty Conference, ASCE. Albuquerque, NM, pp. 132-142.

Taylor, A. R., 1965. Notable Advance in Automatic Irrigation. New Zealand J. of Agr. 111(4):67-69, 71.

U. S. Soil Conservation Service, 1974. Border Irrigation. Chp. 4., sect. 15, Nat. Engineering Handbook.

Walker, W. R. and T. S. Lee, 1981. Kinematic Wave Approximation of Surged Furrow Advance. ASAE Winter Meeting Paper No. 81-2544, Chicago, Ill, 25 p.

Walker, W. R., H. Malano, and J. A. Replogle, 1982. Reduction in Infiltrarion Rates due to Intermittent Wetting. ASAE Summer Meeting Paper No. 82-2029, Madison, WI, 14 p.

APPENDICES

APPENDIX A

LEAST SQUARES METHOD CALCULATIONS

Table 12. Probable error calculation for using the broad crested weir equation.

No.	Q (L/s)	log Q	H (m)	log H	e_i	e_i^2
1	36.420	1.561	0.1539	-0.8127	0.0411	0.00169
2	24.384	1.387	0.1319	-0.8797	-.0324	0.00105
3	16.284	1.212	0.0862	-1.0645	0.0697	0.00486
4	20.759	1.317	0.1207	-0.9183	-.0445	0.00198
5	44.236	1.646	0.1777	-0.7503	0.0324	0.00105
6	16.510	1.218	0.0863	-1.0640	0.0750	0.00562
7	25.970	1.415	0.1319	-0.8797	-.0043	0.00002
8	46.020	1.663	0.1893	-0.7228	0.0082	0.00006
9	15.350	1.186	0.0835	-1.0783	0.0644	0.00415
10	31.860	1.503	0.1377	-0.8611	0.0556	0.00309
11	54.516	1.737	0.2005	-0.6978	0.0448	0.00201

s = 0.05334, E(%) = 13%

Table 13. Least squares method calculations for dosing siphon empirical discharge equation.

No.	Q (L/s)	log Q	H (m)	log H	log Q log H	$(\log H)^2$
1	21.580	1.334	0.4267	-.3698	-.4934	0.1368
2	20.645	1.315	0.3706	-.4311	-.5669	0.1858
3	14.670	1.167	0.2545	-.5943	-.6935	0.3532
4	28.094	1.449	0.7684	-.1144	-.1657	0.0131
5	26.111	1.417	0.6236	-.2051	-.2906	0.0421
6	30.303	1.482	0.7303	-.1365	-.2023	0.0186
7	20.844	1.319	0.3892	-.4098	-.5405	0.1679
8	18.748	1.273	0.3283	-.4837	-.6157	0.2340
9	9.431	0.975	0.1426	-.8458	-.8247	0.7155
10	17.813	1.251	0.3810	-.4191	-.5242	0.1756
11	19.088	1.281	0.4115	-.3856	-.4940	0.1487

a = 36.35, r = 0.66

Table 14. Probable error calculations for the dosing siphon empirical equation.

No.	Q (L/s)	log Q	H (m)	log H	e_i	e_i^2
1	21.580	1.334	0.4267	-.3698	0.0175	0.00031
2	20.645	1.315	0.3706	-.4311	0.0389	0.00152
3	14.670	1.167	0.2545	-.5943	-.0013	0.00000
4	28.094	1.449	0.7684	-.1144	-.0360	0.00130
5	26.111	1.417	0.6236	-.2051	-.0082	0.00007
6	30.303	1.482	0.7303	-.1365	0.0115	0.00013
7	20.844	1.319	0.3892	-.4098	0.0288	0.00083
8	18.748	1.273	0.3283	-.4837	0.0316	0.00100
9	9.431	0.975	0.1426	-.8459	-.0273	0.00074
10	17.813	1.251	0.3810	-.4191	-.0330	0.00109
11	19.088	1.281	0.4115	-.3856	-.0250	0.00063

s = 0.02911, E(%) = 6.9%

Table 15. Probable error calculations for the dosing siphon using the orifice equation.

No.	Q (L/s)	log Q	H (m)	log H	e_i	e_i^2
1	21.580	1.334	0.4267	-.3698	0.0119	0.00014
2	20.645	1.315	0.3706	-.4311	0.0235	0.00055
3	14.670	1.167	0.2545	-.5943	-.0428	0.00183
4	28.094	1.449	0.7684	-.1144	-.0007	0.00000
5	26.111	1.417	0.6236	-.2051	0.0125	0.00016
6	30.303	1.482	0.7303	-.1365	0.0433	0.00187
7	20.844	1.319	0.3892	-.4098	0.0169	0.00028
8	18.748	1.273	0.3283	-.4837	0.0078	0.00006
9	17.813	1.251	0.3810	-.4191	-.0464	0.00215
10	19.088	1.281	0.4115	-.3856	-.0331	0.00109

s = 0.03195, E(%) = 7.6%

APPENDIX B

PRINT-OUT OF THE COMPUTER PROGRAM

```
5   PRINT
10  PRINT            MODELING SURGE FLOW
11  PRINT          ***************************
12  DIM Y(300)
13  DIM TF(300)
15  PI=3.141593
20  PRINT
30  PRINT IS THE RESERVOIR RECTANGULAR(1),TRAPEZOIDAL(2),PARABOLIC(3)
40  INPUT S
50  REM S IS TYPE OF RESERVOIR
60  ON S GOTO 80,200,250
80  PRINT FOR RECTANGULAR CROSS SECTION INPUT DIMENSIONS
90  Z=0
100 REM Z=SIDE SLOPE ON RESERVOIR
110 PRINT WHAT IS BOTTOM WIDTH,FEET
120 INPUT B
130 PRINT WHAT IS THE MAXIMUM DEPTH,FEET
140 INPUT D
150 PRINT WHAT IS BOTTOM SLOPE,0.---
160 INPUT SO
170 PRINT WHAT IS RESERVOIR LENGTH,FEET
180 INPUT L
190 IF S=1 THEN 310
195 IF S=3 THEN 300
200 PRINT FOR TRAPEZOIDAL CROSS SECTION INPUT DIMENSIONS
210 PRINT WHAT IS THE SIDE SLOPE,HORIZONTAL COMP.---
220 INPUT Z
230 S=1
240 GOTO 100
250 PRINT FOR PARABOLIC CROSS SECTION INPUT DIMENSIONS
260 PRINT WHAT IS RESERVOIR TOP WIDTH,FEET
270 INPUT X8
280 X8=X8/2
290 GOTO 130
300 CP=D/X8**2
310 PRINT WHICH CONTROL DEVICE,DROP GATE(1),DOSING SIPHON(2)
320 INPUT AC
330 IF AC=2 THEN 450
340 PRINT INPUT DROP GATE DIMENSIONS
350 PRINT WHAT IS GATE WIDTH,FEET
360 INPUT W9
370 PRINT WHAT IS GATE COEFFICIENT OF DISCHARGE
380 INPUT C9
390 E=C9*W9
400 R=3/2
405 PRINT WHAT IS THE GATE BOTTOM DEPTH
406 INPUT HO
410 GOTO 520
450 PRINT INPUT DOSING SIPHON DIMENSIONS
460 PRINT WHAT IS SIPHON DIAMETER,INCHES
470 INPUT D8
```

```
480 PRINT WHAT IS FLOW COEFFICIENT
490 INPUT C9
500 E=(C9*PI*D8**2/4)/144
510 R=1/2
520 PRINT WHAT IS THE MINIMUM WATER DEPTH,FEET
530 INPUT H8
540 IF AC=1 THEN 590
550 PRINT DISTANCE FROM BOTTOM TO SIPHON OUTLET,FEET-DOWN IS PLUS
560 INPUT Y
570 C=-Y
576 H3=H8-C
580 GOTO 600
590 C=HO
595 H3=H8-C
600 PRINT WHAT IS THE INFLOW,CFS
610 INPUT PO
620 HB=(1.1*PO/E)**(1/R)
640 IF H3>HB THEN 660
650 H3=HB
660 IF D<=(SO*L) GOTO 730
670 IF H8>=(SO*L) GOTO 800
680 H1=D-C
690 H2=SO*L-C
710 M=3
720 GOTO 830
730 IF D<(SO*L) THEN 750
740 GO TO 760
750 L=D/SO
760 H1=D-C
770 H2=H3
780 M=2
790 GOTO 830
800 H1=D-C
810 H2=H3
820 M=1
830 IF S=3 THEN GOTO 1250
840 ON M GOTO 850,920,1010
850 AO=B*L-Z*SO*L**2+2*Z*C*L
860 A1=2*Z*L
870 A2=0
880 A3=0
881 IN=INT((H1-H2)/.01)
882 FOR KN=1 TO IN
883 TF(KN)=AO/PO*(KN*0.01)+A1/(2.*PO)*((H2+KN*.01)**2-H2**2)
884 NEXT KN
890 TRF=AO/PO*(H1-H2)+A1/(2.*PO)*(H1**2-H2**2)
891 UO=H1
895 UF=H2
896 K=1
897 C=0
900 GOSUB 2000
```

```
905 GOSUB 3200
906 GOSUB 3000
910 STOP
920 AO=B*C/SO+C*Z/SO
930 A1=B/SO+2*C*Z/SO
940 A2=Z/SO
950 A3=0
960 TRF=AO/PO*(H1-H2)+A1/(2*PO)*(H1**2-H2**2)+A2/(3*PO)*(H1**3-H2**3)
961 UO=H1
962 UF=H2
963 K=1
964 C=0
970 GOSUB 2000
980 GOSUB 3200
990 GOSUB 3000
1000 STOP
1010 AO=B*L-Z*SO*L**2+2*Z*C*L
1020 A1=2*Z*L
1030 A2=0
1040 A3=0
1050 TRF1=AO/PO*(H1-H2)+A1/(2*PO)*(H1**2-H2**2)
1051 NI=INT((H1-H2)/.01)
1052 FOR KN=1 TO NI
1053 TF(KN)=AO/PO*(KN*.01)+A1/(2*PO)*((H2+KN*.01)**2-H2**2)
1054 NEXT KN
1060 UO=H1
1070 UF=H2
1080 K=1
1081 A4=0
1082 A5=0
1083 BU=0
1085 C=0
1086 SR=SO
1087 SO=0
1090 GOSUB 2000
1100 TA=T
1105 PRINT
1110 AO=-B*HO/SR-HO*Z/SR
1120 A1=B/SR-2*HO*Z/SR
1130 A2=Z/SR
1140 A3=0
1150 RTF2=AO/PO*(H2-H3)+A1/(2*PO)*(H2**2-H3**2)+A2/(3*PO)*(H2**3-H3**3)
1170 TRF=TRF1+RTF2
1180 IN=INT((H2-H3)/.01)
1181 IN=IN+NI
1182 FOR KN=(NI+1) TO IN
1183 TF(KN)=AO/PO*(KN-NI)*.01+A1/(2*PO)*((H3+(KN-NI)*.01)**2-H3**2)+A2/
(3*PO)*((H3+(KN-NI)*.01)**2-H3**2)
1184 NEXT KN
1190 UF=H3
```

```
1195 PRINT
1200 GOSUB 2000
1210 T=T+TA
1215 PRINT
1220 GOSUB 3200
1230 GOSUB 3000
1240 STOP
1250 ON M GOTO 1260,1410,1560
1260 BU=4./(3*SO*SQR(CP))
1270 AO=0
1280 A1=0
1290 A2=0
1300 A4=1
1310 A3=1
1320 A5=1
1330 TRF=2/(5*PO)*((H1+C)**2.5-(H2+C)**2.5-(H1+C-SO*L)**2.5+(H2+C-SO*L)
**2.5)
1335 TRF=TRF*BU
1340 UO=H1
1350 UF=H2
1360 K=1
1370 GOSUB 2000
1380 GOSUB 3200
1390 GOSUB 3000
1400 STOP
1410 BU=4/(3*SO*SQR(CP))
1420 AO=0
1430 A1=0
1440 A2=0
1450 A3=1
1460 A4=1
1470 A5=0
1480 TRF=2/(5*PO)*((H1+C)**2.5-(H2+C)**2.5)
1485 TRF=TRF*BU
1490 UO=H1
1500 UF=H2
1510 K=1
1520 GOSUB 2000
1530 GOSUB 3200
1540 GOSUB 3000
1550 STOP
1560 BU=4/(3*SO*SQR(CP))
1570 AO=0
1580 A1=0
1590 A2=0
1595 A3=1
1610 A4=1
1620 A5=1
1630 TRF1=2/(5*PO)*((H1+C)**2.5-(H2+C)**2.5-(H1+C-SO*L)**2.5+(H2+C-
SO*L)**2.5)
1640 UO=H1
```

```
1650 UF=H2
1660 K=1
1670 GOSUB 2000
1680 T=TA
1690 AO=0
1700 A1=0
1710 A2=0
1720 A3=1
1730 A4=1
1740 A5=0
1745 SO=0
1750 TRF2=2/(5*PO)*((H2+C)**2.5-(H3+C)**2.5)
1760 TRF=TRF1+TRF2
1770 TRF=TRF*BU
1780 UF=H3
1790 GOSUB 2000
1800 T=T+TA
1810 GOSUB 3200
1820 GOSUB 3000
1830 STOP
2000 REM SUBROUTINE TRAPEZOIDAL RULE
2010 DEF FNA(X)=(AO+A1*X+A2*X**2+A3*(A4*BU*(X+C)**1.5-A5*BU*(X+C-
SO*L)**1.5))/(E*X**R-PO)
2020 H=.01
2030 MM=INT((UO-UF)/H)
2035 MM=MM-K+1
2040 FOR LL=1 TO MM
2050 IF K=1 THEN 2070
2060 GOTO 2090
2070 SUM=(FNA(UO)+FNA(UO-H))/2
2080 GOTO 2100
2090 SUM=SUM+(FNA(UO-(K-1)*H)+FNA(UO-K*H))/2
2100 Y(K)=H*SUM-(FNA(UO)-FNA(UO-K*H))*H**2/12
2110 K=K+1
2120 NEXT LL
2130 T=Y(K-1)
2140 N=K-1
2150 RETURN
3000 REM SUBROUTINE GRAPHICAL OUTPUT
3010 PRINT GRAPHICAL OUTPUT,Y AXIS IS THE TIME RATIO AND ,X AXIS IS THE
WATER SURFACE ELEV.,FEET
3015 PRINT
3016 PRINT TAB(3)  X  TAB(9)  Y
3017  PRINT TAB(1) H1 TAB(7)  0.0
3020 PRINT TAB(15)  *
3030 FOR J=16 TO 72
3040 PRINT TAB(J)  .
3050 NEXT J
3060 FOR K=2 TO N STEP 5
3070 J=INT(57*Y(K)/Y(N)) +14
```

```
3075 IF J>15 THEN 3080
3076 J=15
3080 EL=H1-(K-1)*.01
3081 PRINT TAB(1) EL TAB(7) Y(K)
3085 PRINT TAB(15)  .  TAB(J)  *
3090 NEXT K
3091 IN=INT((H2-H1)/.01)
3092 FOR KN=1 TO IN STEP 5
3093 EL= H1+KN*.01
3094 J=INT(57*TF(KN)/TF(IN))
3095 TRF=TF(KN)+Y(N)
3096 PRINT TAB(1) EL TAB(7) TRF
3097 PRINT TAB(15)  .  TAB(J)  *
3098 NEXT KN
3100 RETURN
3200 REM SUBROUTINE FOR PRINTING TIME RATIO
3210  PRINT
3220 PRINT        ****************************************
3230 PRINT
3240 PRINT      EMPTYING TIME = ,T, SEC.
3250 PRINT      REFILL TIME = ,TRF, SEC.
3260 PRINT
3270 RETURN
3290 END
```

APPENDIX C

COMPUTER OUTPUT

```
          MODELING SURGE FLOW
         ************************

IS THE RESERVOIR RECTANGULAR(1),TRAPEZOIDAL(2),PARABOLIC(3) 1
FOR RECTANGULAR CROSS SECTION INPUT DIMENSIONS
WHAT IS BOTTOM WIDTH,FEET 3.3333
WHAT IS THE MAXIMUM DEPTH,FEET .95
WHAT IS BOTTOM SLOPE,0.--- 0
WHAT IS RESERVOIR LENGTH,FEET 8
WHICH CONTROL DEVICE,DROP GATE(1),DOSING SIPHON(2) 2
INPUT DOSING SIPHON DIMENSIONS
WHAT IS SIPHON DIAMETER,INCHES 6.115
WHAT IS FLOW COEFFICIENT 3.0106
WHAT IS THE MINIMUM WATER DEPTH,FEET .25
DISTANCE FROM BOTTOM TO SIPHON OUTLET,FEET-DOWN IS PLUS .75
WHAT IS THE INFLOW,CFS .169312

        ************************************

     EMPTYING TIME =          34.7828       SEC.
     REFILL TIME =            110.249       SEC.

GRAPHICAL OUTPUT,Y AXIS IS THE TIME RATIO AND ,X AXIS IS THE WATER SURFACE ELEV.,FEET

  X      Y
1     0.0     *.....................................................
1.01  1.57499
                .
                 *
1.11  17.3248
                  .
                   *
1.21  33.0747
                    .
                     *
1.31  48.8246
                      .
                       *
1.41  64.5744
                        .
                         *
1.51  80.3243
                          .
                           *
1.61  96.0742
                            .
                             *
1.69  111.097
                              .
                               *
1.59  115.437
                              .
                             *
1.49  119.956
                            .
                           *
1.39  124.678
                          .
                         *
1.29  129.628
                        .
                       *
1.19  134.842
                      .
                     *
1.09  140.361
                    .
                   *
```

Figure 36. Computed cycle time for the dosing siphon using 4.8 L/s inflow rate.

```
          MODELING SURGE FLOW
         ***********************

IS THE RESERVOIR RECTANGULAR(1),TRAPEZOIDAL(2),PARABOLIC(3) 1
FOR RECTANGULAR CROSS SECTION INPUT DIMENSIONS
WHAT IS BOTTOM WIDTH,FEET 3.333
WHAT IS THE MAXIMUM DEPTH,FEET 1.7625
WHAT IS BOTTOM SLOPE,0.--- 0
WHAT IS RESERVOIR LENGTH,FEET 8
WHICH CONTROL DEVICE,DROP GATE(1),DOSING SIPHON(2) 1
INPUT DROP GATE DIMENSIONS
WHAT IS GATE WIDTH,FEET .958333
WHAT IS GATE COEFFICIENT OF DISCHARGE 3.4
WHAT IS THE GATE BOTTOM DEPTH 1
WHAT IS THE MINIMUM WATER DEPTH,FEET 1.2
WHAT IS THE INFLOW,CFS .128205

        ************************************

     EMPTYING TIME =          22.6976       SEC.
     REFILL TIME =            116.988       SEC.

GRAPHICAL OUTPUT,Y AXIS IS THE TIME RATIO AND ,X AXIS IS THE WATER SURFACE ELEV.,FEET

 X     Y
.2   0.0     *.....................................................
.21   2.07979
              .
              *
.31   22.8777
              .        *
.41   43.6757
              .              *
.51   64.4736
              .                    *
.61   85.2716
              .                          *
.71   106.069
              .                                *
.7525
      116.735
              .                                   *
.6525
      118.265
              .                          *
.5525
      120.24 .              *
.4525
      122.935
              .     *
.3525
      126.958
              .  *
.2525
      134.096
              .
              *
```

Figure 37. Computed cycle time for the automatic drop gate using 3.6 L/s inflow rate.

```
          MODELING SURGE FLOW
         **************************

IS THE RESERVOIR RECTANGULAR(1),TRAPEZOIDAL(2),PARABOLIC(3) 1
FOR RECTANGULAR CROSS SECTION INPUT DIMENSIONS
WHAT IS BOTTOM WIDTH,FEET 3.3333
WHAT IS THE MAXIMUM DEPTH,FEET 1.55
WHAT IS BOTTOM SLOPE,0.--- 0
WHAT IS RESERVOIR LENGTH,FEET 8
WHICH CONTROL DEVICE,DROP GATE(1),DOSING SIPHON(2) 2
INPUT DOSING SIPHON DIMENSIONS
WHAT IS SIPHON DIAMETER,INCHES 6.115
WHAT IS FLOW COEFFICIENT 3.0106
WHAT IS THE MINIMUM WATER DEPTH,FEET .25
DISTANCE FROM BOTTOM TO SIPHON OUTLET,FEET-DOWN IS PLUS 1.64583
WHAT IS THE INFLOW,CFS .18107

         ************************************

      EMPTYING TIME =          43.9261       SEC.
      REFILL TIME =            191.453       SEC.

GRAPHICAL OUTPUT,Y AXIS IS THE TIME RATIO AND ,X AXIS IS THE WATER SURFACE ELEV.,FEET

  X      Y
1.89583
     0.0     *.....................................................
1.90583
      1.47271
              .
             *
2.10583
      30.927 .       *
2.30583
      60.3812
              .              *
2.50583
      89.8355
              .                     *
2.70583
      119.29 .                            *
2.90583
      148.744
              .                            *
3.10583
      178.198
              .                                   *
3.18583
      192.036
              .                                     *
2.98583
      197.99 .                                    *
2.78583
      204.192
              .                            *
2.58583
      210.671
              .                     *
2.38583
      217.467
              .              *
2.18583
      224.626
              .       *
```

Figure 38. Computed cycle time for the dosing siphon using 5.1 L/s inflow rate.

APPENDIX D

TYPICAL AND ADJUSTED INTAKE

Table 16. Typical and adjusted intake for continuous flow treatment for a pilot field test.

Item	Station-meters x 10													
	0	1	2	3	4	5	6	7	8	9	10	11	12	13
T_o-min	33	32	31	28	26	26	23	22	20	18	15	12	8	3
Typical Intake curve Data														
D-mm	32	31	30	29	28	28	26	25	23	22	20	17	14	7.2
Av.D	32	31	30	29	28	27	26	24	23	21	19	15	10	
Av.D	on 130 meters = 315/13 = 24 mm													
Adjusted Intake Curve Data														
D-mm	40	40	39	38	35	35	32	32	30	28	25	22	17	9.4
av.D	40	40	39	37	35	34	32	31	29	27	24	20	13	
Adj.D	on 130 meters = 401/13 = 31 mm													

D =(300 L/min x 30 min)/(2.2m x 130 m) = 31 mm

Table 17. Typical and adjusted intake for surge flow treatment for a pilot field test.

Item	Station-meters x 10													
	0	1	2	3	4	5	6	7	8	9	10	11	12	13
T_o-min	18	18	18	18	18	18	19	19	19	19	18	17	13	6
Typical Intake Curve Data														
D-mm	22	22	22	22	22	22	23	23	23	23	22	21	18	11
Av.D	22	22	22	22	22	23	23	23	23	23	21	20	15	
Av.D	on 130 meters = 281/13 = 22 mm													
Adjusted Intake Curve Data														
D-mm	45	45	45	45	45	45	47	47	47	47	45	44	37	23
Av.D	45	45	45	45	45	46	47	47	47	46	45	41	30	
Adj.D	on 130 meters = 574/13 = 45 mm													

D = (300 L/min x 48 min x 1 surge)/(2.43 m x 130 m) = 45 mm

Table 18. Typical and adjusted intake for continuous flow treatment for field test No. 2.

Item	Station-meters x 10									
	0	1	2	3	4	5	6	7	8	9
T_o-min	82	76	70	64	54	44	35	25	16	10
	Typical Intake Curve Data									
Depth-mm	55	53	50	47	43	38	33	27	21	16
Av.Depth		54	52	58	45	41	35	30	24	18/2
AV.Depth	on 85 meters = 348/8.5 = 41 mm									
	Adjusted Intake Curve Data									
Depth-mm	53	50	48	45	41	36	31	26	20	15
Av.Depth		52	49	47	43	39	34	29	23	18/2
Adj.Depth	on 85 meters = 325/8.5 = 39 mm									

D = (100 L/min x 80 min)/(2.43 m x 85 m) = 39 mm

Table 19. Typical and adjusted intake for surge flow treatment for field test No. 2.

Item	Station-meter x 10									
	0	1	2	3	4	5	6	7	8	9
T_o-min	26	26	28	27	24	19	15	13	6	2
	Typical Intake Curve Data									
Depth-mm	28	28	29	28	26	23	20	18	11	7.7
Av.Depth		28	29	29	27	25	21	19	15	9.4/2
Av.Depth	on 85 meters = 197.7/8.5 = 23 mm									
	Adjusted Intake Curve Data									
Depth-mm	35	35	37	36	33	29	25	23	14	7.4
Av.Depth		35	31	37	34	31	27	24	19	11/2
Adj.Depth	on 85 meters = 243.5/8.5 = 29 mm									

D =(100 L/min x 15 min x 4 surges)/(2.43 m x 85 m) = 29 mm

Table 20. Typical and adjusted intake for continuous flow treatment for field test No. 3.

Item	Station-meters x 10									
	0	1	2	3	4	5	6	7	8	9
T_o-min	44	42	40	36	34	28	26	20	16	9
	Typical Intake Curves									
Depth-mm	38	37	36	34	32	29	28	24	20	15
Av.Depth	38	37	35	33	31	28	26	22	18	
Av.Depth	on 90 meters = 268/9 = 30 mm									
	Adjusted Intake Curve Data									
Depth-mm	45	44	43	40	39	35	33	28	25	17
Av.Depth	45	44	42	40	37	34	31	27	21	
Adj.Depth	on 90 meters = 321/9 = 36 mm									

D = (200 L/min x 44 min)/(2.73 m x 90 m) = 36 mm

Table 21. Typical and adjusted intake for surge flow treatment for field test No. 3.

Item	Station-meter x 10									
	0	1	2	3	4	5	6	7	8	9
T_o-min	23	22	23	21	19	17	16	15	8	5
	Typical Intake Curve Data									
Depth-mm	26	25	25	24	23	21	21	20	14	10
Av.Depth	26	26	25	24	22	21	20	17	12/2	
Av.Depth	on 85 meters = 187/8.5 = 22 mm									
	Adjusted Intake Curve Data									
Depth-mm	36	35	36	34	32	30	29	28	19	14
Av.Depth	36	35	35	33	31	30	29	24	17/2	
Adj.Depth	on 85 meters = 261.5/8.5 = 31 mm									

D = (200 L/min x 9 min x 4 surges)/(2.73 m x 85 m) = 31 mm

Table 22. Typical and adjusted intake for continuous flow treatment for field test No. 4.

Item	Station-meters x 10											
	0	1	2	3	4	5	6	7	8	9	10	11
T_o-min	44	42	41	40	36	35	30	26	22	17	13	8
	Typical Intake Curve Data											
Depth-mm	38	37	36	35	33	33	30	28	25	21	18	14
Av.Depth	38	37	36	34	33	32	29	27	23	20	16	
Av.Depth	on 110 meters = 325/11 = 29 mm											
	Adjusted Intake Curve Data											
Depth-mm	47	45	45	44	42	41	37	34	31	26	22	17
Av.Depth	46	45	45	43	42	39	36	33	29	24	20	
Adj.Depth	on 110 meters = 402/11 = 36 mm											

D = (200 L/min x 44 min)/(2.2 m x 110 m) = 36 mm

Table 23. Typical and adjusted intake for surge flow treatment for field test No. 4.

Item	Station-meters x 10											
	0	1	2	3	4	5	6	7	8	9	10	11
T_o-min	14	15	16	18	19	20	21	19	17	12	11	8
	Typical Intake Curve Data											
Depth-mm	19	20	21	22	23	24	24	23	21	17	16	14
Av.Depth	20	20	22	23	24	24	24	22	19	17	15	
Av.Depth	on 110 meters = 230/11 = 21 mm											
	Adjusted Intake Curve Data											
Depth-mm	30	31	33	35	36	37	39	36	34	27	26	21
Av.Depth	31	32	34	36	37	38	38	35	31	27	24	
Adj.Depth	on 110 meters = 362/11 = 33 mm											

D = (200 L/min x 22 min x 2 surges)/(2.43 m x 110 m) = 33 mm

Table 24. Typical and adjusted intake for continuous flow treatment for field test No. 5.

Item	Station-meters x 10												
	0	1	2	3	4	5	6	7	8	9	10	11	12
T_o-min	44	44	41	38	34	30	24	24	20	16	12	7	4
Typical Intake Curve Data													
Depth-mm	38	38	36	35	32	30	26	26	24	21	17	12	9
Av.Depth		38	37	36	34	31	28	26	25	23	19	15	10/2
Av.Depth	on 115 meters = 317/11.5 = 27 mm												
Adjusted Intake Curve Data													
Depth-mm	44	44	42	40	37	34	30	30	27	24	20	14	10
Av.Depth		44	43	41	39	36	32	30	29	26	22	17	12/2
Adj.Depth	on 115 meters = 365/11.5 = 31 mm												

D = (200 L/min x 44 min)/(2.43 m x 115 m) = 31 mm

Table 25. Typical and adjusted intake for surge flow treatment for field test No. 5.

Item	Station-meters x 10											
	0	1	2	3	4	5	6	7	8	9	10	11
T_o-min	18	17	17	17	19	19	19	17	14	13	9	3
Typical Intake Curve Data												
Depth-mm	22	21	21	21	23	23	23	20	19	18	15	7.5
Av.Depth		22	21	21	22	23	23	22	20	19	17	11
Av.Depth	on 110 meters = 221/11 = 20 mm											
Adjusted Intake Curve Data												
Depth-mm	31	30	30	30	32	32	32	30	27	26	21	11
Av.Depth		31	30	30	31	32	32	31	29	27	24	16
Adj.Depth	on 110 meters = 28 mm											

D = (200 L/min x 19 min x 2 surges)/(2.43 m x 110 m) = 28 mm

Table 26. Typical and adjusted intake for continuous flow treatment for field test No. 6.

Item	Station-meters x 10											
	0	1	2	3	4	5	6	7	8	9	10	11
T_o-min	44	44	41	39	34	30	26	23	20	15	12	7
Typical Intake Curve Data												
Depth-mm	38	38	36	35	32	30	28	26	24	20	17	13
Av.Depth		38	37	36	34	31	29	27	25	22	19	15
Av.Depth	on 110 meters = 323/11 = 29 mm											
Adjusted Intake Curve Data												
Depth-mm	43	43	42	40	37	34	32	29	27	22	20	15
Av.Depth		43	43	41	39	36	33	31	28	25	21	18
Adj. Depth	on 110 meters = 358/11 = 33 mm											

D = (200 L/min x 44 min)/(2.43 m x 110 m) = 33 mm

Table 27. Typical and adjusted intake for surge flow treatment for field test No. 6.

Item	Station-meters x 10											
	0	1	2	3	4	5	6	7	8	9	10	11
T_o-min	15	15	16	16	18	18	17	16	13	12	10	6
Typical Intake Curve Data												
Depth-mm	20	20	21	21	22	22	22	21	18	17	15	11
Av.Depth		20	21	21	22	22	22	22	20	18	16	13
Av.Depth	on 110 meters = 217/11 = 20 mm											
Adjusted Intake Curve Data												
Depth-mm	30	30	31	31	33	33	32	31	27	26	23	17
Av.Depth		30	31	31	32	33	33	32	29	27	25	20
Adj.Depth	on 110 meters = 323/11 = 30 mm											

D = (200 L/min x 20 min x 2 surges)/(2.43 m x 110 m) = 30 mm

OCT 10 1983

OCT 19 1983

MONTANA STATE UNIVERSITY LIBRARIES
3 1762 10005654 6

D378
Is5 Ismail, S. M.
cop.2 Implementation and
evaluation of surge flow...

DATE	ISSUED TO
	Doug Baker [redacted]
	SEP 11 1985
	OCT [illegible]

D378
Is5
cop.2